UNIVERSITÀ DEGLI STUDI DI TRIESTE

UNIVERSITÀ DEGLI STUDI DI TRIESTE

XXXIV CICLO DEL DOTTORATO DI RICERCA IN

BIOMEDICINA MOLECOLARE

ROLE OF ACYLATED GHRELIN IN ADIPOSE TISSUE METABOLISM AND INVESTIGATION OF ITS INTERACTION WITH O-GlcNAc TRANSFERASE

Settore scientifico-disciplinare: MED/09

DOTTORANDO
FERAS KHARRAT

COORDINATORE
PROF. GERMANA MERONI

SUPERVISORE DI TESI
PROF. ROCCO BARAZZONI

ANNO ACCADEMICO 2020/2021

Contents:

Abstract:

Adipose tissue is an endocrine organ that plays, besides its pivotal role in energy storage, a principal role in the whole-body metabolic homeostasis. Acylated ghrelin exerts major effects on intermediate metabolism and energy homeostasis. While the effects of acylated ghrelin in metabolic tissues like liver and skeletal muscle are at least in part known, those are still to be discovered and largely unknown. This study aimed at investigating the role of acylated ghrelin in adipose tissue metabolism, and identifying possible mediators for the acylated ghrelin effect. We reported in this study that sustained acylated ghrelin treatment lowers insulin sensitivity in the visceral adipose tissue in vivo, in both physiological conditions and in a rodent model of inflammation and wasting by surgically induced-CKD, and in vitro in 3T3L1 differentiated adipocytes. In parallel with lowering insulin sensitivity, AG treatment lowered the mitochondrial function in physiological conditions without altering the redox state and cytokine profile, while in systemic inflammation conditions, AG selectively improved the proinflammatory cytokine profile by lowering TNFα levels without exerting significant effects on redox state and mitochondrial function.

O-GlcNAcylation is a non-canonical glycolisation post-translational dynamic modification (PTM) that resulted in the attachment of O-linked N-acetylglucosamine (O-GlcNAc) moieties to Ser and Thr residues of cellular proteins. O-GlcNAc transferase, OGT, is the enzyme that adds O-GlcNAc to the targets. We reported in our study that OGT levels in the visceral adipose tissue are upregulated by AG treatment in vivo, both healthy and systemic inflamed rats, not in vitro suggesting that OGT upregulation upon AG treatment is regulated by non-adipose tissue mechanism. In the last part of the study, we reported in vitro using 3T3L1 and human differentiated adipocytes that OGT alters the adipocytes sensitivity to the AG treatment, and AG administration to OGT-silenced adipocytes in starvation conditions improved the insulin sensitivity of the adipocytes suggesting potential therapeutic effect for metabolic syndrome still needs to be validated in vivo by transgenic mice knocked for OGT expression in the adipose tissue.

Synopsis:

Adipose tissue is a key endocrine organ orchestrating the metabolism in the whole body. Adipose tissue can be classified according to the localization into subcutaneous adipose tissue (SCAT) and visceral adipose tissue (VAT), and functionally can be classified into white adipose tissue (WAT) which stores the energy in fats form, and brown adipose tissue (BAT) responsible mainly for burning the stored energy in the thermogenesis process.

Adipocytes, the main building unit of the adipose tissue, respond to the insulin by accumulating lipids through the lipogenesis and triglyceride synthesis during the postprandial periods, while fasting and starvation conditions decreases the insulin sensitivity of the adipocytes in order to enhance the lipolysis, the mechanism by which the free fatty acids (FFA) are released from the triglycerides hydrolysis in the adipocytes into the circulation to provide energy. Over-lipid load in the adipocytes in over-nutrition and obesogenic conditions is associated with higher levels of the Reactive Oxygen Species (ROS) which leads to increased oxidative stress and mitochondrial dysfunction, which together alter both the metabolic and the endocrine function of the adipose tissue, elevating the levels of the pro-inflammatory adipokines, and affecting negatively the phosphorylation of several components in the insulin signaling pathway leading to diminishing the signal and insulin resistance. Adipose tissue insulin resistance is associated with increased levels of circulating FFA, modulating negatively the glucose tolerance and insulin sensitivity in other tissues, thus it is considered as a direct cause of several metabolic complications including metabolic syndrome MetS and Type2 Diabetes.

Ghrelin, discovered in the stomach in 1999 and identified as the endogenous ligand for the growth hormone secretagogue receptor (GHS-R), is the only known orexigenic hormone exerting major roles in the intermediate metabolism in different organs. Ghrelin levels rise during fasting and peak immediately before the meal indicating its pivotal role in the metabolizing and storing the digested food. Ghrelin peptide, when ~~a~~cylated (AG) has an orexigenic effect and known receptor. While acylated ghrelin effects on metabolic tissues like skeletal muscle and liver are at least in part known, there is still a lot to be discovered and unraveled about the roles that acylated ghrelin exerts in the adipose tissue, and the mechanisms beyond these effects.

In the first part of the study, by using animal models, we aimed at investigating the effect of the acylated ghrelin on the adipose tissue in healthy and systemic inflammatory conditions since the metabolic profile is largely altered by the inflammation.

First, in a 12 weeks healthy Wistar rats model, acylated ghrelin sustained administrating subcutaneously (200ng x2/day) for 4 days was found to lower the insulin signaling in visceral adipose tissue (at AKT ^{S473} and GSK3 α ^{S21}, β ^{S9} levels, TSC2 ^{S939}, mTOR ^{S2448}), in addition to lowering the mitochondrial activities (cytochrome oxidase and citrate synthase) with no effects on the inflammatory cytokines profile (TNF α, IL10, IL1 β) and redox state (oxidized/total glutathione).

Then we aimed to test the effects of AG in a systemic inflammation model. For this aim, we used 5/6 nephrectomy rat model which is known as standard Chronic Kidney Disease model (CKD). Rats develop in less than two weeks from the surgery the general systemic inflammation. Initial CKD was induced by single step 5/6 nephrectomy (Nx) in 12-week-old male Wistarrats, that were then maintained on a standard chow diet. At 36 days, AG was administered subcutaneously 200ng x2/day (Nx-AG) for 4 days and was found to lower the insulin signaling significantly (AKT ^{S473} with very similar trend for GSK3β^{S9}) compared to the nephrecotmized rats received only vehicles (Nx) which were showing significant low insulin sensitivity compared with sham rats (S). However, these significant effects of the acylated ghrelin were not paralleled at the mitochondrial function level (cytochrome oxidase and citrate synthase) and the redox state (oxidized/total glutathione) although these metabolic markers were also significantly lower in nephrectomized rats (both Nx and Nx-AG) compared to sham. Importantly, at cytokine profile, AG lowered TNFα levels compared to Nx group, suggesting the acylated ghrelin potential in reducing the pro-inflammatory cytokine profile.

Results from the both animal studies suggested that the effects of the acylated ghrelin treatment, among mechanisms investigated, could mainly target its effects on the insulin signaling while it might be secondary on the redox state and mitochondrial function.

The next part of the study, therefore, aimed at identifying possible mediators of acylated ghrelin effects on insulin signalling in the adipose tissue.

O-GlcNAcylation is a non-canonical glycolisation post-translational dynamic modification (PTM) resulted in the attachment of *O*-linked *N*-acetylglucosamine (O-GlcNAc) moieties to Ser and Thr residues of cellular proteins: cytoplasmic, nuclear and mitochondrial. It is controlled by two enzymes: *O*-GlcNAc transferase (OGT) which adds the O-GlcNAc to the targeted proteins and *O*-GlcNAcase (OGA) which is catalyzing the removal of O-GlcNAc from the modified proteins. It plays pivotal roles in adjusting the cellular metabolism according to the nutrient flux. Disruption of O-GlcNAcylation homeostasis was reported to be implicated in different pathological conditions in humans like type 2 diabetes and cancer. In white adipose tissue, OGT deletion was reported to

improve the insulin sensitivity and the lipid turnover in high fat diet induced obesity mice model. These findings were similar to other findings reported that deleting the acylated ghrelin receptor in the white adipose tissue improves the insulin sensitivity and inflammatory cytokines profile. So, the hypothesis arisen was to check whether the effects of the ghrelin could at least in part involve OGT. For this aim, at first the levels of OGT in the adipose tissue were investigated in the animal models of the study, and were found to be significantly increased by the acylated ghrelin treatment in both healthy and CKD rats. These results are highly supportive of a link between the acylated ghrelin and the OGT in the adipose tissue which is, for our knowledge, studied for the first time.

The last and most important step was to see if deleting the OGT in the adipose tissue will prevent the effects of the acylated ghrelin in the adipose tissue. For this aim, in vitro siRNA knockdown studies were performed using 3T3L1 cells, well demonstrated murine mouse model for adipocytes differentiation, and primary human visceral preadipocytes which can be induced to complete the differentiation into human adipocytes. Protocols of the differentiation for both models were set and confirmed by Oil red-O staining and measuring the adipocytes markers: adiponectin and Fatty Acid Binding Protein 4 (FABP4) (qPCR, Western Blot).

We first aimed to test the effects of the AG on the insulin sensitivity in the differentiated human and 3T3L1 murine adipocytes. In this regard, different doses of the acylated ghrelin (10, 100, 1000 ng/ml) were applied to the differentiated cells in different conditions in terms of nutrients availability since the physiological levels of the acylated ghrelin is directly affected by the nutritional status. For 3T3L1 experiments, serum percentage in the medium was the changed to induce the different nutritional conditions: normal feeding conditions with normal serum percentage, partial serum starvation with lowered serum percentage, and complete serum starvation. For the human adipocytes experiments, one commercial starvation medium was used with lowered, not complete, nutrients availability.

In 3T3L1, prolonged acylated ghrelin treatment was found to lower the insulin sensitivity (AKT^{S473} ,$GSK3\ \beta^{S9}$) in differentiated adipocytes in normal serum percentage in the medium in all the used doses ranging significant effect to strong tendency in agreement with our in vivo findings. In both starvation conditions, acylated ghrelin treatment for 24 h did not show significant effect on insulin sensitivity (AKT^{S473} ,$GSK3\ \beta^{S9}$). In human adipocytes, nether prolonged acylated ghrelin treatment in normal feeding conditions, nor 24h treatment in starvation conditions show significant effects on insulin sensitivity (AKT^{S473} ,$GSK3\ \beta^{S9}$).

The last step was to test the link between AG and OGT by investigating the effects of AG on the insulin signaling in the adipocytes knocked down for the OGT. In these experiments, only starvation conditions were followed since the levels of both AG and OGT expression , in white adipose tissue, rise in fasting periods. Different concentrations of siRNA human and murine OGT were tested in different settings to optimize the knocking down ratios (qPCR, WB). In 3T3L1 differentiated adipocytes, and in partial starvation conditions, AG treatment further increased the insulin sensitivity at the GSKβ^{S9} level in the cells knocked down for OGT (siOGT AG) compared with acylated ghrelin treatment control (siCON AG) and silenced-OGT control (siOGT). In complete starvation conditions, knocking OGT was found to significantly lower the insulin sensitivity (AKT ^{S473}) in OGT-basal conditions with similar trend in OGT-silenced cells. In human differentiated adipocytes, AG treatment increased the insulin sensitivity (AKT^{S473}) in OGT-silenced cells (siOGT AG) compared with AG treatment control (siCON AG)and OGT-silenced (siOGT) in agreement with the results obtained from 3T3L1 in partial starvation. These results from 3T3L1 and human adipocytes suggest the OGT alters the sensitivity of the cells to the AG treatment, which was seen in the major changes in insulin sensitivity.

Although the OGT silencing results did not indicate the OGT is directly mediating the AG effects in adipose tissue, but they show for the first time the link between the ghrelin system and the O-GlcNacylation system, and hold a potential in the field of drug development for metabolic syndrome and obesity. However further experiments are needed for further elucidation of this link in vivo by using transgenic animal

1. Introduction

1.1. Adipose Tissue

1.1.1. Overview:

Storing energy in lipids form is a pivotal mechanism highly conserved from prokaryotes and unicellular organisms which store the lipids in intracellular organelles, to complex living organisms like mammalians which own specific tissue to store the lipids called adipose tissue (AT). For a long time, adipose tissue has been known only as an energy reserve and thermal insulator due to its major role in energy storage, and in the last two decades of the 20th century, this view started to change with the arising knowledge about adipose tissue secretion function. Today with the numerous discoveries about adipose tissue roles, a wider definition is built and became more accepted by the scientific community. Besides its energy reserve role, adipose tissue is a major endocrine organ that affects whole-body metabolism whose dysfunction plays an important role in the inducement and development of metabolic complications including insulin resistance and metabolic syndrome (Laclaustra et al. 2007), (Gijs H.Goossens 2008).

In mammals, two principal functionally different types of adipose tissue exist, white adipose tissue (WAT) which functions mainly to store the lipids, and brown adipose tissue (BAT) which burns these stored lipids in a mechanism called thermogenesis to provide the necessary energy in demanding periods. (Zwick et al., 2017).

Adipose tissue is built by a unique cellular combination. Adipocytes are the main unit and the primary component of adipose tissue and comprise the major volume part of the adipose tissue. Two distinct types of adipocytes are present in the white and brown adipose tissue, white adipocytes and brown adipocytes in addition to the beige adipocytes present in white adipose tissue and show at basal state the white adipocytes features while can be functionally switched to the brown adipocytes in a mechanism called Adipose Tissue Browning when stimulated to produce the necessary energy by thermogenesis; so they have an adaptive thermogenesis function (Park et al., 2014). Interestingly, these types differ in morphology which is adapted to the type of function. While white adipocytes have large lipid droplets, brown adipocytes have multi-small droplets. White adipocytes have less expression of Uncoupling Protein 1 (UCP1), a unique mitochondrial membranous protein devoted to adaptive thermogenesis, and adrenergic receptors beta and alpha than brown adipocytes which have higher mitochondrial content as well (Marta et al., 2014).

Other types of nonadipocyte cells are present in the cellular combination of adipose tissue, like endothelial, fibroblasts, pericytes, mesenchymal cells, and immune cells like macrophages, lymphocytes, and neutrophils (Martyniak et al., 2017). Immune and endothelial cells in the adipose tissue play major roles in the different adipocytes functions including adipogenesis, lipolysis, and browning to produce heat. This modulatory role of these cells is mediated by the innervation between these cells and the nerve fibers in their local environment (Guilherme et al., 2019). A very recent study revealed an important finding that three types of adipocytes are present in the white adipose tissue, among them one type is known to be responding to insulin stimulation. The same study suggested that the insulin resistance in the white adipose tissue could be related to the differences in the cellular combination between the three types and the lower presence of the sensitive type of cells in the white adipose tissue. (Bäckdahl et al., 2021). Cellular subpopulations in the adipose tissue have been related to disease development, and a recent transcriptomic RNA Seq-based study revealed the differences in the cellular combination in different adipose tissue depots between genders, across ranges of BMI and in different stages of type-2 diabetes (Lenz et al., 2020). The same study identified adipose tissue as a rich source of multipotent stem/stromal cells and reported a high augmentation of immune cell content in epicardial and pericardial adipose tissue compared to subcutaneous and omental depots.

Anatomically, adipose tissue is spread in the body in two main principal types: Subcutaneous Adipose Tissue (SCAT) and Visceral Adipose Tissue (VAT). Both differ at the cellular, physiological, molecular, and clinical sides. Visceral fats are located in the mesentery and omentum and drain to the liver through the portal circulation. Visceral adipose tissue is known to have an endocrine function with a wide secretory profile affecting the energy homeostasis and affected by the metabolic state of the body. Visceral adipose tissue dysfunction attracted more attention and research because of the direct contribution to different metabolic complications including metabolic syndrome and type 2 diabetes. Subcutaneous adipose tissue was reported to be less affected by insulin with a higher percentage of adipocytes among the cellular combinations, and a higher tendency of the preadipocytes toward the differentiation but with smaller adipocytes than those in visceral adipose tissue. The distribution of both visceral and subcutaneous adipose tissue plays a major role in the outcomes of adipose tissue dysfunction. Accumulating the fats subcutaneously was shown to have a better metabolic state than the same process in the visceral adipose tissue. This can be explained by the fact that the visceral adipose tissue contains more

immune and inflammatory cells that can be affected negatively by the overload of the VAT, whereas insulin resistance is induced and initiating further other complications (Ibrahim et al., 2010).

Many studies highlighted the clinical importance of both types. Among the interesting studies is the study in Japan 2021 in which VAT was found to be correlated with type2 diabetes in men and women while SCAT was correlated only in women (Yokokawa et al., 2021). Interestingly there is grown evidence that visceral adipose tissue releases pro-inflammatory factors that boost the inflammatory reaction triggered by the COVID 19 virus (Silverio et al., 2021).

Adipose tissue percentage of the body weight differs according to several factors including age and sex. White adipose tissue comprises from 5 to 50 % of the total body weight, while brown adipose tissue percentage decreases with age (Ibrahim et al., 2010, O'Rourke 2018). Interestingly, fat mass and distribution in the body were used as a predictive tools of the metabolic profile. For example, percent visceral adipose tissue value (PVATV) was reported to be related to the pattern of plasma ghrelin in fasting conditions (Li et al., 2009).

1.1.2. Adipose tissue metabolism:

1.1.2.1. De novo lipogenesis:

De novo lipogenesis (DNL) is a complex and highly regulated process in which circulated carbohydrates are converted into fatty acids used for synthesizing either triglycerides or other lipid molecules. Insulin plays a major role in this mechanism. Fat accumulation is determined by the balance between TG synthesis and breakdown. fatty acids in adipose tissue are derived mainly from two sources: circulating TG and de novo lipogenesis (DNL)(Wong et al., 2010). When energy is excessive in the body, most of the newly synthesized fatty acids are esterified to become TGs for storage. Circulating TGs are originally synthesized in the intestine or liver, and packaged into chylomicrons or very-low-density lipoproteins (VLDL), which mobilize these TG to ATs. In the adipocytes, insulin activates the lipoprotein lipase (LPL) within vascular endothelium in adipocytes which hydrolyzes the TGs into non-esterified fatty acids (NEFA) that enter the adipocytes through fatty acid transporters such as CD36 and fatty acid transport protein-1 (FATP1) (Endemann et al., 1993), (Song et al., 2018). Insulin also stimulates adipocyte glucose uptake, which initiates DNL in the adipocytes, in which glycerol 3-phosphate derived from glucose is used as a backbone for the

fatty acids to be esterified to form the TGs to be stored in lipid droplets. First, glucose derived from dietary carbohydrates undergoes glycolysis and tricarboxylic acid (TCA) cycle to produce citrate in the mitochondria, which is transported to the cytosol and then releases acetyl-CoA by ATP-citrate lyase (ACLY). Second, the resulting acetyl-CoA is converted to malonyl-CoA by acetyl-CoA carboxylases 1 (ACC1). Third, fatty acid synthase (FASN), the key rate-limiting enzyme in DNL, converts malonyl-CoA into palmitate, which is the first fatty acid product in DNL. Finally, palmitate undergoes the elongation and desaturation reactions to generate the complex fatty acids, including stearic acid, palmitoleic acid, and oleic acid (Song et al., 2018). Regulation of the DNL is affected by the type of diet and is subject to further hormonal regulation. For example, a high-fat diet inhibits the DNL in the adipose tissue while high carbohydrates upregulate the DNL (Tang et al., 2016). DNL is inhibited by the glucagon and catecholamine hormones which are released during the high demand of energy in the body (Li et al., 2011).

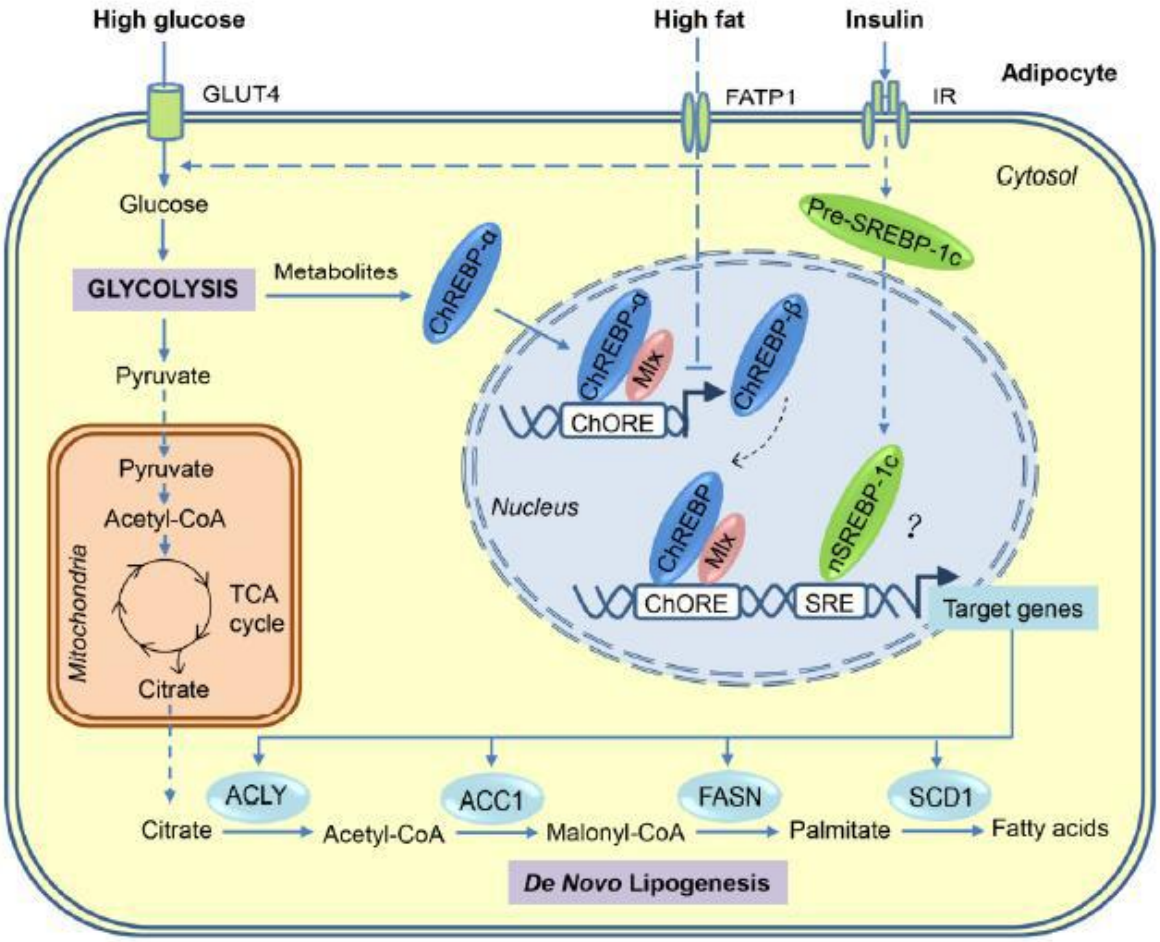

Figure (1). Outlined graph for the de novo lipogenesis in the adipocyte. (Song et al., 2018)

DNL occurs mainly in the liver with lower rates in the adipose tissue. However, adipocytes synthesize by DNL the branched fatty acid esters of hydroxy fatty acids (FAHFAs), which have beneficial metabolic effects, including enhancing insulin-stimulated glucose transport and glucose-stimulated GLP1 and insulin secretion, as well as powerful anti-inflammatory effects (Smith et al., 2016). Notably, under high-calories intake conditions, DNL is enhanced in the skeletal muscle which leads lowers the insulin sensitivity in the skeletal muscle. Inhibiting DNL in skeletal muscle was shown to enhance insulin sensitivity which supports the important role of the DNL in the energy balance in insulin resistance conditions (Funai et al., 2013).

1.1.2.2. Beta Oxidation:

Starvation and prolonged fasting periods enhance the usage of the lipids stored in the adipocytes to produce energy. FFA are released into the circulation by the lipolysis process. In the target cell, FFA is subjected to the oxidation in the mitochondria to produce the ATP after being converted in the cytosol into Acyl-CoA which is transferred to the mitochondria by a cascade of enzymatic activity. In the mitochondria, Acyl-CoA is hydrolyzed to produce Acetyl-CoA which enters the Krebs-cycle to produce the ATP (Saponaro et al., 2015). Interestingly, beta-oxidation was reported to play a major role in the acylation modification of the ghrelin, the major topic of the study, where the long fatty acids from the circulation source are beta-oxidized in the ghrelin producing cells (Ikenoya et al., 2018).

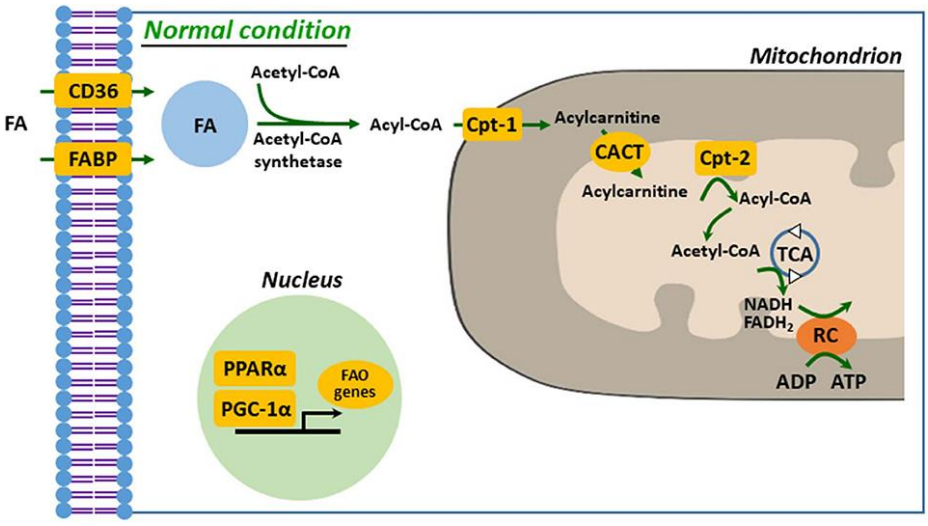

Figure(2). Outlined graph for the beta oxidation mechanism (Jang et al., 2020).

1.1.2.3. Lipolysis:

Lipolysis is the metabolic mechanism in which the triglycerides are subjected to several steps of hydrolysis to release free fatty acids into circulation. Perilipin is an enzyme known to play an important role in lipolysis. One of the major effects of insulin in the adipose tissue is to inhibit lipolysis. Insulin resistance is usually correlated with increased levels of lipolysis.

Due to the major role that ghrelin is playing in GH secretion, it is worth talking about the effects of GH on the lipolysis and insulin signaling in the adipose tissue. GH is known to induce insulin resistance in the adipose tissue and increase the lipolysis rate as well. The effects of the GH in the adipose tissue are mediated by three different enzymes adipose triglyceride lipase (ATGL), hormone-sensitive lipase (HSL), and monoacylglycerol lipase (MGL). Various proteins affect the function of these enzymes. Perilipin is a protein coating the lipid droplets and mitigating the activators of ATGL lowering the lipolysis rate (Sztalryd et al., 2017).

In a study published recently in Nature communications, Violetta et al reported that mice overexpress the perilipin 5 (PLIN5), a protein that coats lipid droplets inside cells, particularly in BAT, maintained significantly lower blood sugar concentrations and higher insulin sensitivity during glucose tolerance tests, compared with mice with normal PLIN5 levels. They also had fewer fatty livers, a condition associated with Type 2 diabetes. Importantly the white adipocytes of these genetically modified mice were smaller and showed a lower level of inflammation (Gallardo-Montejano et al., 2021).

1.1.3. Insulin actions in the adipocytes and its link to whole-body glucose homeostasis:

Undoubtedly, insulin discovery and usage in modern medicine were “one of the miracles” of the history of medicine. Insulin lowers the blood glucose by enhancing the glucose uptake by muscle cells and adipocytes and inhibiting the glucose from the liver. Here we will talk about the insulin action in the adipocytes and its contribution to the whole body metabolism.

The insulin receptor is composed of two extracellular α subunits and two transmembrane β subunits linked together by disulfide bonds. Once insulin is bound to the α subunits, conformational changes in the β subunits are induced leading to the autophosphorylation of several tyrosine residuals, which is recognized by the phosphotyrosine-binding (PTB) domain of the Insulin Receptor Substrate leading to the phosphorylation of key tyrosine residues on IRS proteins, which is recognized by the Src homology 2 (SH2) domain of the p85 regulatory subunit of PI3-kinase (PI3K) which then

phosphorylates phosphatidylinositol (4,5) bisphosphate (PIP2) leading to the formation of PIP3 which activates AKT in combination with the protein kinase 3-phosphoinositide dependent protein kinase-1 (PDK1). AKT is a Protein kinase B (PKB) whose activation leads to the phosphorylation and inactivation of glycogen synthase kinase 3 (GSK3) which is present in two isoforms GSK3 β and GSK3α. Phosphorylation of glycogen synthase (GS) by GSK3 inhibits the glycogen synthesis; thus the inactivation of GSK3 by AKT promotes glucose storage as glycogen. From this point, AKT and GSK3 phosphorylation were used in our study to test insulin sensitivity. Tuberous sclerosis complex protein 2 is a negative regulator of the insulin signaling which is phosphorylated at Ser939 in response to PI3K activation (Manning et al., 2002). The mammalian target of rapamycin (mTOR) is a Ser/Thr protein kinase that plays a major role in the nutrient balance by sensing ATP and amino acid availability. It is phosphorylated at Ser2448 via the PI3 kinase/Akt signaling pathway (Navé et al., 1999), (Peterson et al., 2000). p70 S6 kinase is a mitogen-activated Ser/Thr protein kinase that exerts important roles in cell growth and G1 cell cycle progression. It is phosphorylated at the Thr 421 as a downstream response of PI3K/AKT pathway activation (Pullen et al., 1997), (Dufner et al., 1999). PTEN (phosphatase and tensin homologue deleted on chromosome ten) is a tumor suppressor reported to affect different human cancers. It acts as a negative regulator for the PI3K/AKT signaling pathway upon its phosphorylation at the Ser380 (Vazquez et al., 2000), (Torres et al., 2001).

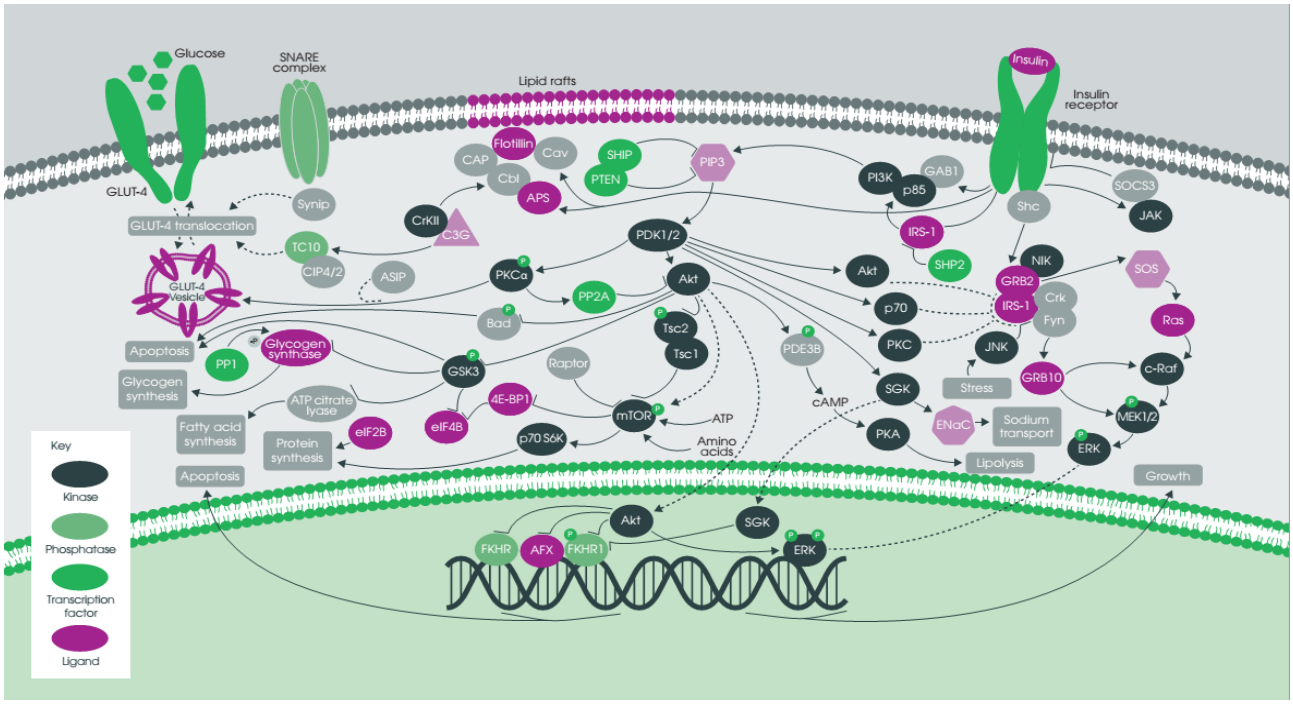

Figure (3). Outlined graph for insulin signaling pathway. (with permission from abcam).

In adipocytes, insulin enhances the glucose uptake by recruiting the GLUT4, which is mostly expressed in adipocytes and skeletal and cardiac cells, to the cellular membrane (Mueckler et al., 2013). Glut4 levels are maintained as long as the insulin levels are upregulated in the periods of fed status, thus enhancing the glucose uptake but they fall when the insulin levels are decreased during fasting periods.

Adipocytes use the taken-up glucose in different ways than muscle cells. Less than 5% of the glucose is conserved as glycogen, and not more than 50% is stored as triglyceride, and a considerable amount of glucose is metabolized into lactate and secreted from cells to function in other tissues as signal molecules or even to serve as fuel. Part of the glucose is oxidized into CO2. (Lagarde et al., 2020), (Flatt et al., 1964).

Insulin enhances the formation of the TGs by increasing the synthesis of glycerol-3-phosphate to which fatty acids can be esterified to synthesize TGs, activating the lipoprotein lipase, an endothelial enzyme degrading circulating TGs that are embedded in VLDLs and chylomicrons, releasing fatty acids and glycerol (Goldberg et al., 2009), increasing the fatty acid uptake in adipocytes by increasing the translocation of fatty acid transporters to the plasma membrane (Stahl et al., 2002), and by the de novo lipogenesis.

Adipocytes' sensitivity to insulin is playing a major role in whole-body glucose homeostasis. Specific deletion of Glut4 in adipocytes was reported to induce peripheral insulin resistance (Abel et al., 2001) while overexpressing the GLUT4 in adipocytes improves the systemic insulin sensitivity even with increased adiposity (Shepherd et al., 1993.), (Yamauchi et al., 2001). Taking into consideration that less than 20% of glucose is disposed of by adipocytes, these findings suggest that the glucose flux into the adipocytes exerts a regulatory role in the whole body's glucose homeostasis, consequently the energy homeostasis. Supporting this hypothesis are the findings from Rab10 adipocytes specific- deletion where the systemic glucose uptake was reduced by 50% which is the same ratio of glucose taken up by adipocytes to be converted and stored as TGs (Vazirani et al., 2016).

Importantly, the anti-lipolytic effect of insulin in the adipose tissue is tightly linked to the gluconeogenesis in the liver. Glycerol and fatty acids released in the lipolysis process initiate gluconeogenesis in the liver (Bergman et al., 2000). Glycerol is a gluconeogenic substrate while fatty acids when converted to acetyl CoA, act as positive allosteric modulators of pyruvate carboxylase, which catalyzes the carboxylation of pyruvate to oxaloacetate, which is the first step of

gluconeogenesis. Notably, this mechanism is altered according to the nutritional state, thus hepatic glucose production is enhanced during the fasting periods when insulin levels are low and glucagon levels are increased, while it is inhibited during fed states when insulin levels are high and glucagon levels are dropped (Perry et al., 2015).

During the DNL pathway, several factors are synthesized, that function in other tissue to regulate metabolism and inflammation. DNL is regulated by the carbohydrate response element-binding protein (ChREBP) which is linked tightly to insulin sensitivity. Downregulating the ChREBP is linked to systemic insulin resistance (Vijayakumar et al., 2017) while its expression in the WAT increases insulin sensitivity even in obesity conditions (Sanchez-Gurmaches et al., 2018).

Branched fatty acid hydroxy fatty acids (FAHFAs) are lipids that resulted during the DNL by the effect of ChREBP. PAHSAs, the palmitic acid esters of hydroxy stearic acids, is a subfamily of FAHFAs that was found to exert anti-diabetic effects, even in type1 diabetes (Syed et al., 2019), and improve the systemic insulin sensitivity by at least in part enhancing the anti-lipolytic effect of the insulin in the adipose tissue (Zhou et al., 2019). Mice knocked out for ChREBP in the adipose tissue developed systemic insulin resistance and administering the 9-PAHSA reverses the insulin resistance, which further supports the role of the adipocytes glucose homeostasis in the whole-body glucose homeostasis (Vijayakumar et al., 2017).

Adipocytes synthesize other lipids that exert signaling roles other than FAHFAs like diacylglycerols (DAGs), acylcarnitines, ceramides, prostaglandins, lysophosphatidic acid, palmitoleate, oxylipins, and N-acyl amino acids, which play different roles enhancing or inhibiting the insulin action in the adipose tissue and other tissues. For example, DAGs were reported to be correlated with insulin resistance in the liver (Ruby et al., 2017), and the circulating ceramides were upregulated in insulin resistants, type2 diabetes patients, and non-alcoholic fatty liver disease (Haus et al., 2009), (Jensen et al., 2019) (Wigger et al., 2017).

Acylcarnitines was found to induce insulin resistance in muscle tissue due to its accumulation in the muscle mitochondria because of the increased levels of beta-oxidation correlated with over-lipid load (Yang et al., 2018).

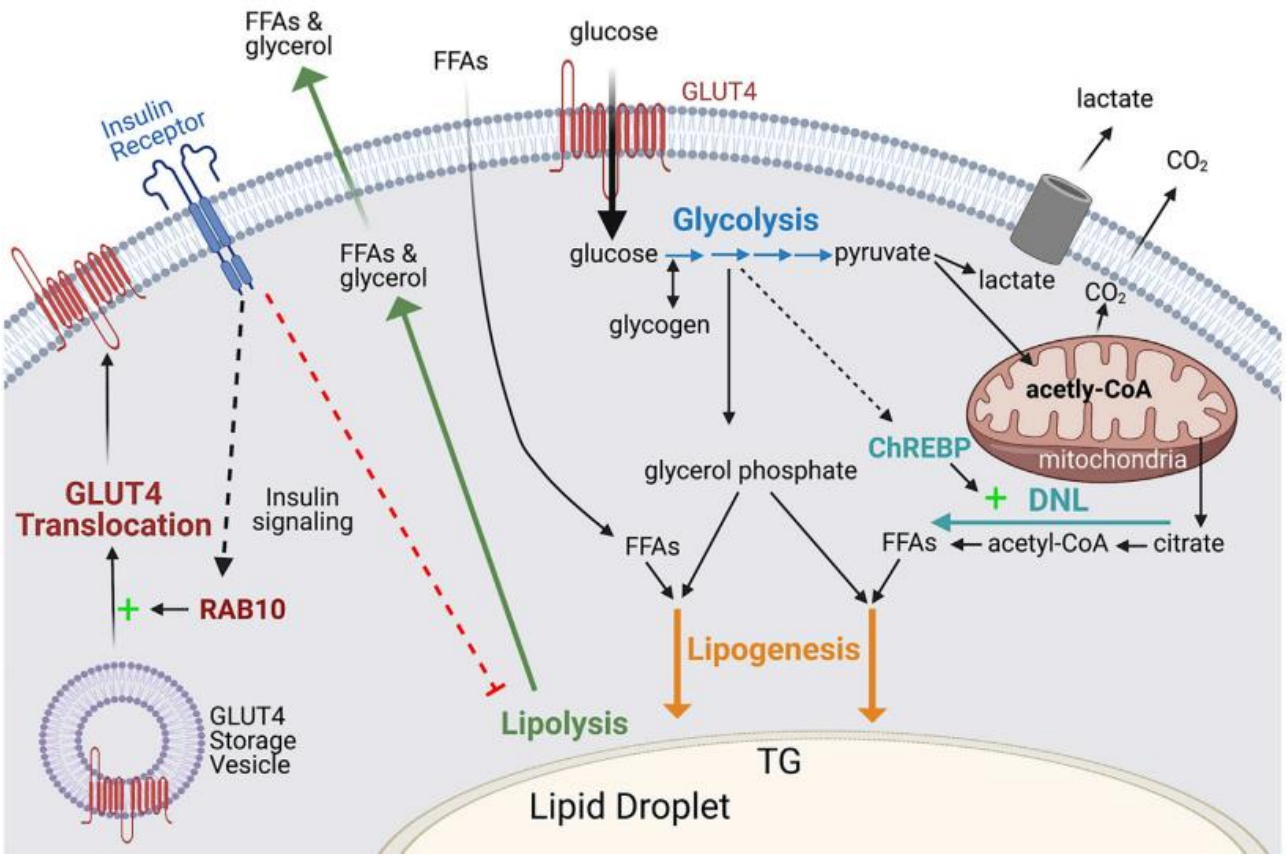

Figure (4). Insulin effects in the adipocyte. (Santoro et al., 2021)

1.1.4. Adipose Tissue Dysfunction:

As adipose tissue is widely involved in metabolic homeostasis, its dysfunction is implicated in metabolic complications including metabolic syndrome with its major confounding, insulin resistance, and in a more developed pathological context, type2 diabetes. In this part, a brief overview of the clinical relevance of the adipose tissue dysfunction will be discussed in addition to the mechanism implicated in adipose tissue dysfunction.

1.1.4.1. Clinical Relevance of Adipose Tissue Dysfunction:

Metabolic syndrome (MetS) is a cluster of conditions that occur together developing atherosclerotic cardiovascular disease, vascular and neurological complications such as a cerebrovascular accident, insulin resistance, and Type2 diabetes mellitus. These conditions are interlinked and share underlying mediators, mechanisms, and pathways. Extra weight and obesity with a sedentary lifestyle are contributing effectively to the pathogenesis of MetS (Swarup et al., 2021), (Huang et al., 2009).

Insulin resistance and obesity are major findings in MetS. Insulin resistance is defined as a subnormal biological response to the normal insulin concentrations which may pertain to biological functions in different tissues. However, from a clinical practice point of view, IR is defined as the state in which a specifically given concentration of insulin is associated with a subnormal glucose response (Moller et al., 1991).

Systemic lipid homeostasis, maintained by white adipocytes which store lipids from the circulation, and brown adipocytes which burn fats in the thermogenesis, is essential in keeping the insulin sensitivity in the whole body, therefore any disruption in the adipocytes function could lead to an alteration in the insulin signaling pathway which contributes to metabolic comorbidities including obesity and metabolic syndrome (Guilherme et al., 2008).

Diabetes mellitus is a group of pathological conditions correlated with the reduced body ability to use and store glucose properly. Type2 diabetes is the most prevalent form of diabetes mellitus characterized by elevated plasma glucose levels because of insulin secretion deficiencies like beta-cell dysfunction and insulin resistance (American Diabetes Association 2018). More than 300 million individuals are expected to develop Type2 Diabetes by 2025 (NCD Risk Factor Collaboration NCD-RisC), so these alarmingly increased numbers create a deep need for extensive research in the mechanisms of insulin resistance and adipose tissue dysfunction to develop drugs serving in this growing area.

1.1.4.2. Mitochondrial dysfunction and oxidative stress in the adipose tissue:

Mitochondria is the major organelle that produces the ATP, but it produces as well the reactive oxygen species ROS as side products. Maintaining the levels of ROS within the normal range is important for cell function. Short-term increase in the ROS concentrations can enhance insulin sensitivity as Kim et al reported in their paper (Loh et al., 2009). Other studies highlighted the role of ROS in the adipocytes differentiation (Tormos et al., 2011) and the thermogenesis in the brown and beige adipose tissue (Chouchani et al., 2017). However, the chronic increase of ROS is not contributing positively to cellular function. Excessive mitochondrial ROS generation by chronic oxidative stress activates various stress pathways such as nuclear factor kappa light chain enhancer of activated B cells (NF-κB), c-Jun N-terminal kinase, and p38 mitogen-activated protein kinase which all trigger the inflammatory response, leading to an increase in the expression of pro-inflammatory cytokines such as interleukin-6 (IL-6), TNF-α, and monocyte chemoattractant protein-

1 (MCP-1) (Bloch-Damti et al., 2005). As a direct result, serine/threonine kinases are activated by these inflammatory cytokines or by ROS directly. The activated serine/threonine kinases alter the phosphorylation profile of the key components involved in the insulin signaling pathways such as insulin receptor (IR) and insulin receptor substrate (IRS), which lead to diminishing the activation of the downstream Src Homology 2 (SH-2) containing signaling molecules and inhibit the IR/IRS interaction (Kim et al., 2006), ultimately inducing the development of insulin resistance and the progression of various metabolic diseases, including type 2 diabetes. Wang et al. reported that higher cellular ROS levels is linked tightly to the impairment of adipocyte function in accordance with glucose intolerance and insulin resistance (Wang et al., 2006). Since the mtDNA lacks the repair mechanisms present in the nucleus, it is highly affected by the ROS increase and this, with other factors, explains the important role of the ROS in inducing mitochondrial dysfunction (Kujoth et al., 2007). Mitochondrial loss of mass and function were reported following the adipose tissue dysfunction in type2 diabetes and this might be in part because of the decrease of mitochondrial DNA (mtDNA) in the adipose tissue in both humans and mice animal models (Wilson-Fritch et al., 2004), (Rong et al., 2007), (Choo et al., 2006). These results are in agreement with other findings that reported the association of the mitochondrial DNA 15497G/A polymorphism with obesity (Okura et al., 2003).

Mitochondrial dynamics, a mitochondrial structural remodeling mechanism which includes fusion and fission, is important for mitochondrial function. Mitochondrial fusion is regulated by GTPase proteins, mitofusin 1 and 2 (MFN1/2) and optic atrophy 1 (OPA1), which are located in the outer and inner mitochondrial membranes, respectively, while dynamin-related protein 1 (DRP1) is regulating the mitochondrial fission (Koshiba et al., 2004), (Elgas et al., 2013). Reshaping the mitochondrial structure is dynamic and sensitive to metabolic signals (Benard et al., 2007). The imbalance between fusion and fission is reported in adipose tissue dysfunction-related diseases including type 2 diabetes. Mechanically, mitochondrial fusion dilutes the ROS levels, thus maintaining the mitochondrial capacity and the mitochondrial biochemical homogeneity, and enhancing the ATP production (Westermann et al., 2010), (Wada et al., 2016), (Liesa et al., 2013), while fission is associated with augmented levels of ROS that lower oxidative phosphorylation and deplete the mtDNA. Inhibiting the expression of MFN2 in mice led to induced insulin resistance and was contributing to mitochondrial dysfunction in obese individuals (Mancini et al., 2019).

Mitophagy is the mechanism enhanced partly by the mitochondrial dynamics, which results in reducing the ROS by removing dysfunctional mitochondria altered by the oxidative stress or the excessive mitochondria accumulated during the adipogenesis (Ashrafi et al., 2013). Mitophagy is triggered by Unc-51 like autophagy activating kinase 1 (ULK1) upon 5'-adenosine monophosphate-activated protein kinase (AMPK) activation or mTORC1 inhibition under cell maturation or nutritional deprivation (Kim et al., 2011). Mitophagy plays important role in the adipocytes differentiation, in which during adipocytes differentiation, mitophagy is enhanced to lower the mitochondrial mass to inhibit the fatty acid oxidation and accumulate more fats in the differentiated adipocytes (Altshuler-Keylin et al., 2017). Mitophagy is the control response for the accumulation of the fats, in which increasing the fats load is associated with lower mitophagy rates to keep the fatty oxidation rates. In this regard, inhibiting the mitophagy selectively in the adipose tissue by ablation of autophagy-related gene 7 (Atg7) improved the insulin sensitivity in mice fed with high-fat diet, prevented the weight gain, and lowered WAT mass but increased the BAT mass (Zhang et al., 2009). Thus, the role of mitophagy is subjected to various factors like nutrition and stress, and this leads to controversial results.

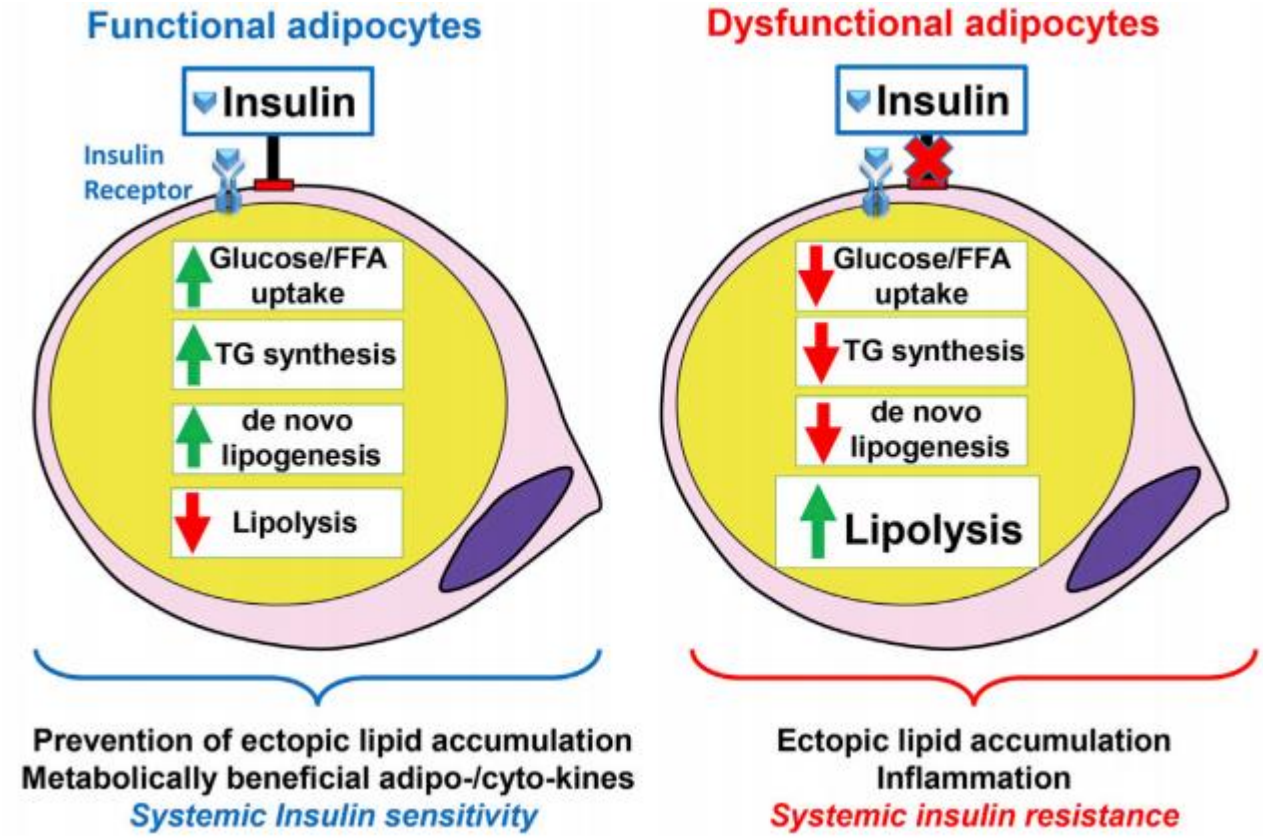

Figure (5). Functional and dysfunctional adipocyte (Santoro et al., 2021)

1.1.4.3. Adipose Tissue Inflammation:

Although it is missing the classical signs of the inflammation, adipose tissue dysfunction correlated with insulin resistance and disruption in the glucose homeostasis is reported as “adipose tissue inflammation”.

Immune and metabolic responses are strongly connected and coregulate each other. Immune cells in the adipose tissue are the main player that defines the function of the adipose tissue in healthy and pathological conditions (Hotamisligil et al., 2017).

Adipose tissue insulin resistance is directly affected by the M1 macrophage phenotype; cytokines released by these dysfunctional macrophages promote insulin resistance in other metabolic tissues as well including skeletal muscles and the liver (Chmelar et al., 2013), (Chung et al., 2018). In particular, inflammatory cytokines affect the insulin sensitivity at different levels mainly at the cellular membrane components of the insulin signaling pathway like glucose transporter type 4 which its translocation to the plasma membrane is downregulated by the effects of IL-1β (Jager et al., 2007), in addition to the binding to the insulin receptor directly as lectin galectin-3, which activates macrophage chemotaxis triggering the inflammatory response, was found to disrupt the insulin signaling by blocking the insulin receptor and found to be elevated in obese human and mice (Li et al., 2016). Reduction of Insulin receptor substrate 1 (IRS1) was also reported as an effect of the inflammatory M1 cytokines (Lumeng et al., 2007).

Eosinophils, which are low present in adipose tissue and further decreased in metabolic complications like obesity (Wu et al., 2011), have been reported to secrete cytokines that ameliorate the inflammatory response of the macrophages and even switch their polarization toward M2 response which is known as a protective anti-inflammatory response. Particularly, IL-4 improved insulin sensitivity and lowered weight gain in an obesity-high fat-induced mice model (Chang et al., 2012), and enhanced the thermogenesis function of beige cells, consequently increasing the energy expenditure and glucose tolerance (Lee et al., 2015).

In high-fat diet conditions, neutrophils accumulate in the adipose tissue by the effect of the macrophages (Talukdar et al., 2012). Neutrophils secrete the elastase which is a pro-inflammatory cytotoxic serine protease reported to be increased in adipose tissue in insulin resistance and overnutrition conditions. Deleting the elastase was shown to have positive outputs where it

attenuated the insulin resistance and reduced the macrophage accumulation in the adipose tissue, and increased fatty acid oxidation in the liver. (Mansuy-Aubert et al., 2013). Myeloperoxidase is another pro-inflammatory factor that is released by the neutrophils and found to induce insulin resistance in accordance with obesogenic conditions, and its deletion was found to improve insulin sensitivity and lower adipose tissue inflammation by reducing macrophage infiltration (Wang et al., 2014).

Adipocytes expansion in response to overnutrition leads to inadequate vascularization leading to hypoxia in the adipose tissue, in addition to mechanical stress due to contact with the surrounding matrix and cells. Hypoxia and mechanical stress lead together to increased adipocytes death which is associated with increased pro-inflammatory factors secretion from the macrophages which is known as the M1 macrophage polarization (Lee et al., 2013), (Michailidou et al., 2012), (Halberg et al., 2009), (Hill et al., 2014)**.** The inflammatory activation of adipose tissue macrophages can be driven by lipids deriving from adipocyte lipolysis and death. In this regard, some immune cells must be exerting some protective roles in the initial response to the high fat load, but by the prolonged exposure to the same conditions, these effects are shifted to the pathological impact. For example, the macrophages buffer the FFAs released by the lipolysis to enhance the angiogenesis and extracellular matrix deposition which are together necessary for adipose tissue reshaping in overnutrition conditions (Shapiro et al., 2013), (Cho et al., 2007)**.**

Adipocytes secrete a wide spectrum of different factors called Adipokines that alter the function of other cells including the immune cells (Fasshauer et al., 2015). When hypertrophic, adipocytes contribute significantly to the systemic adipose tissue inflammation by secreting inflammatory cytokines including tumor necrosis factor (TNF), interleukin (IL)-6, monocyte chemoattractant protein 1 (MCP-1), IL-1, and IL-8 which together strengthen the inflammatory response of the adipose tissue. Interestingly the effect of the adipocytes secretion differs based on the location of the adipose tissue depots and the adipocytes type (Pengcheng et al., 2020). Notably, some cytokines are released from nonadipocytes cells like IL6 and show different effects according to their origin (Han et al., 2020).

Leptin is a proinflammatory factor secreted by white adipocytes that induce insulin resistance and increase the inflammatory response in the immune cells, while adiponectin inhibits the leptin-induced insulin resistance and shift the polarization of the macrophages toward M2 anti-inflammatory protective response (Zhao et al., 2005).

Fatty Acid Binding Protein 4, is a 14-15kDa protein that binds the fatty acids and facilitates the transport of long fatty acids to different organelles in the cell. It is secreted by the adipocytes, therefore considered as an adipokine, in addition to macrophages. FABP4 is transcriptionally regulated by insulin indicating the role of the insulin on the adipocytes secretome (Trojnar et al., 2019). Several animal studies reported the contribution of FABP4 to the metabolic complications resulting from the adipocytes dysfunction including type2 diabetes (Hotamisligil et al., 1996), (Furuhashi et al., 2008). The elevated levels of FABP4 were found to be predictive of both metabolic syndrome (Xu et al., 2007) and cardiovascular death (Saito et al., 2021). Inhibiting the FABP4 protein was reported to improve insulin sensitivity therefore might be a therapeutic strategy to treat type2 diabetes (Furuhashi et al., 2007).

Adiponectin is one of the major adipokines reported to affect several tissues including the liver, kidney, bone, brain, blood vessels, and pancreatic beta cells. Adiponectin is considered as the major responsible for the healthy metabolic roles of the adipose tissue, and notably, upregulating the levels of adiponectin was shown to recover the negative consequences of obesity (Kim et al., 2007). T3 is the first hormone reported to be secreted by the brown adipose tissue in the late 1980s (Silva et al., 1985). Several transplantation studies reported the anti-inflammatory secretion profile of the brown adipose tissue and the different responding tissues including the white adipose tissue where the transplanted brown adipocytes were found to increase the levels of the adiponectin (Gunawardana et al., 2015) in addition to the finding that brown adipocytes also secrete the adiponectin (Hui et al., 2015). This potential health effects of the brown adipocytes could be related to its release of Insulin Growth Like Factor 1 (IGLF1) (Gunawardana et al., 2012).

1.1.5. Chronic Kidney Disease and adipose tissue inflammation:

While the adipose tissue inflammation associated with overnutrition and obesity was studied and unraveled extensively, the contribution of other conditions contribute to adipose tissue inflammation was not well appreciated. Interestingly, chronic kidney disease is a risk factor for chronic inflammation in adipose tissue (Xiang et al., 2017), which leads to adipose tissue atrophy (Minakuchi et al., 2016), (Pelletier et al., 2013). Exposure to the uremic serum results in the activation of inflammatory pathways including NFκB and Hypoxia Inducible Factor 1 (HIF1), upregulation of inflammatory cytokines/chemokines, and catabolism with lipolysis, and lactate production. In addition to increasing the polarization of the inflammatory macrophage (Martos-Rus

et al., 2021). Accumulation of lipids around organs leads to organ dysfunction by a direct local mechanism, and in accordance, perirenal adipose tissue (PRAT) has emerged as an independent risk factor for chronic kidney disease (Hammoud et al., 2011). Several metabolic complications in adipose tissue usually correlate with the CKD including the insulin resistance IR which was reported to be developed even in the early CKD stage (Becker et al., 2005), dyslipidemia, and ectopic lipid deposition (Guebre-Egziabher et al., 2013). Interestingly, these pathological features in addition to others like macrophages infiltration in the adipose tissue, elevated pro-inflammatory cytokines are shared with the obesity-induced chronic inflammation in the adipose tissue (Kusminski et al., 2016, Hammond et al., 2010). Visceral adipose tissue mass was reported to be predictive for the Acute Kidney Injury (AKI) which is tightly correlated to the inflammatory status in patients operated for Radical Nephrectomy (Olivero et al., 2021, Murashima et al., 2019). Obesity was reported to contribute greatly in predicting delayed renal function recovery in living kidney donors (Lee et al., 2017), in agreement with other findings that bariatric surgery improves renal function and lowers the risk of CKD (Martin-Taboada et al., 2021).

While mitochondrial CKD alterations were studied and characterized in skeletal muscle because of the direct link between CKD and muscle mass, these alterations are still to be determined in adipose tissue. A recent study studied the adipose tissue profile in the CKD rats, but in this study, no data were reported about the mitochondrial response to the CKD pathology (Xiang et al., 2017). So, our current study included new findings of the adipose tissue mitochondrial reaction to the CKD in the presence and absence of acylated ghrelin treatment.

Thus, the adipose-renal axis shows interlinked effects, and for this aim, we included in our study investigating the acylated ghrelin effect in the adipose tissue of CKD rats. While CKD animal models including 5/6 nephrectomy were used as a muscle wasting model (Gortan Cappellari et al., 2017), and the ghrelin effects on muscle tissue in CKD was in part known (Deboer et al., 2008), (Wang et al., 2009), (Tamaki et al., 2015), (Barazzoni et al., 2010), the effects of CKD on the adipose tissue is increasingly unraveled, so surely investigating the ghrelin system in this regard is with high importance and even novelty.

1.2. Ghrelin:

1.2.1. Definition and Biology:

Ghrelin was discovered in 1999 by Kojima et al by analyzing the stomach hormones (Kojima et al., 1999) to detect the ligand of the Growth Hormone Secretagogue Receptor (GHSR), and was found to have an orexigenic effect in animals (Wren et al., 2000) and humans (Wren et al., 2001). This work was selected among the breakthrough scientific achievements. Today more thousands of papers are published about ghrelin.

Ghrelin is produced by specific endocrine functioning cells located in the gastrointestinal mucosa with most abundance in the upper part of the stomach, the P/D1 cells in humans, and X/A-like cells in rats (Rindi et al., 2002). Epsilon pancreatic cells also produce ghrelin (Andralojc et al., 2009). Ghrelin was also reported to be produced locally in the brain especially in the hypothalamus which explains in part its function as a secretagogue of the growth hormone.

Ghrelin is subjected to the acylation at the Ser3 (or threonine) by the only enzyme known to catalyze the acyl modification of the ghrelin, ghrelin-O-acyl-transferase (GOAT) (Kojima et al., 2016), (Lemarié et al., 2016), (Gutierrez et al., 2008).

Consequently, ghrelin circulates in two forms: acylated form AG and Unacylated form UnAG. For a long time, acylated ghrelin was considered the active form of the ghrelin without roles for the unacylated form. The ratio between the two forms of the ghrelin is controlled by the ghrelin production/release cycle from the ghrelin-producing cells, the expression and abundance of the GOAT, and the deacylation enzymes like carboxylesterases (De Vriese et al., 2004).

Today, this view is completely reversed and unacylated ghrelin was described to play different physiological roles contributing mainly to the energy balance (Gortan Cappellari et al., 2019). Ghrelin is the only known endocrine hormone to have orexigenic effects and signal for stimulating the food intake in contrast to the leptin, released by adipocytes, that induces satiety (Klok et al., 2007).

GOAT was first reported by two different research groups in 2008 (Gutierrez et al., 2008), (Yang et al., 2008). It is expressed by the MBOAT4 gene (Membrane-bound O Acyl Transferase 4), and this expression is subjected to regulation by the energy balance whereas it is increased in the long fasting and weight loss conditions while it does not seem to play crucial roles in the availability of the nutrients (Zhao et al., 2010). Mice lacking the GOAT showed less ability to maintain the glucose levels in prolonged fasting conditions and the metabolic status which is affected by the ghrelin and its counteract, leptin (Yang et al., 2008). As expected it is more expressed where ghrelin is

expressed, in the stomach, and other tissues expressing ghrelin like pancreas and pituitary. It is also expressed in the testis, brain, and spinal cord. A recent study showed that this GOAT can acylate the exogenous UnAG, and this might explain the distribution of the GOAT in tissues that do not express ghrelin but are affected by the unacylated form of the ghrelin (Hopkins et al., 2017). Interestingly, inhibitors of GOAT were found to increase peripheral insulin sensitivity, thus counteracting obesity and type2 diabetes (Khatib et al., 2015). However, this area is still under investigation to unravel the mechanisms of effects.

Ghrelin levels rise before meals and decrease after meal. The kinetics of the ghrelin is subjected to the control of the autonomic nervous system (Koliaki et al., 2010, Broglio et al., 2004, Gagnon et al., 2012) and the amount and type of the diet (Lomenick et al., 2009, Bowen et al., 2006). Glucagon and norepinephrine hormones, known to be upregulated during fasting, were described to affect the ghrelin promoter activity in agreement with studies that reported upregulation of ghrelin levels in the lack of energy conditions, and with other findings that reported a decrease in the ghrelin levels in the overnutrition conditions and obesity (François et al., 2016, Tschöp et al., 2001, Schalla et al., 2018). However, this is related to the total ghrelin level since elevated AG were detected in obese individuals (Barazzoni et al., 2007b).

Ghrelin was reported to be involved in several pathological conditions. Kojima and Kanagawa who discovered the ghrelin in 1999 studied the plasma ghrelin concentrations in renal failure disease (Yoshimoto et al., 2002). Kanagawa et al reported high acylated ghrelin levels in patients with anorexia (Nakai et al., 2003). As effects of ghrelin were unraveled by time, more clinical research based on plasma ghrelin levels was coming to light to enrich our understanding of the role of this hormone. In our group, it was demonstrated that plasma total and unacylated ghrelin predict 5-year changes in insulin resistance (Barazzoni et al., 2016). Plasma ghrelin concentrations were used as a bio-indicator for a lot of diseases mainly to highlight the metabolic state of the individuals because of the wide effects of ghrelin on the metabolism and energy balance in the body. However, it was reported in other pathological conditions that are still linked to the metabolism like severe motor and intellectual disability (SMID) (Zenitani et al., 2021), insulinomas Patients (Wu et al., 2020), functional dyspepsia (Kim et al., 2010), major depressive disorder (Matsuo et al., 2021).

1.2.2. Ghrelin Expression and Structure:

The human Ghrelin gene is located in chromosome 3 in the region 3p25.3. It contains six exons two of them are noncoding and play a regulatory role in the ghrelin expression. Ghrelin is transcribed into Preproghrelin (117 aa) which is further processed into Proghrelin by removing the 23 aa fragment which consists of the signal peptide. Proghrelin is processed by the enzyme at the arginine 28 by Prohormone convertase 1/3 (PC 1/3) PC1/3 to produce the ghrelin and the C-ghrelin which is further processed to give the other ghrelin gene-related 23 aa hormone, Obestatin. Obestatin was reported to have anorexigenic effects contrary to the ghrelin effects, however, this topic needs to be further elucidated (Ruozi et al ., 2017).

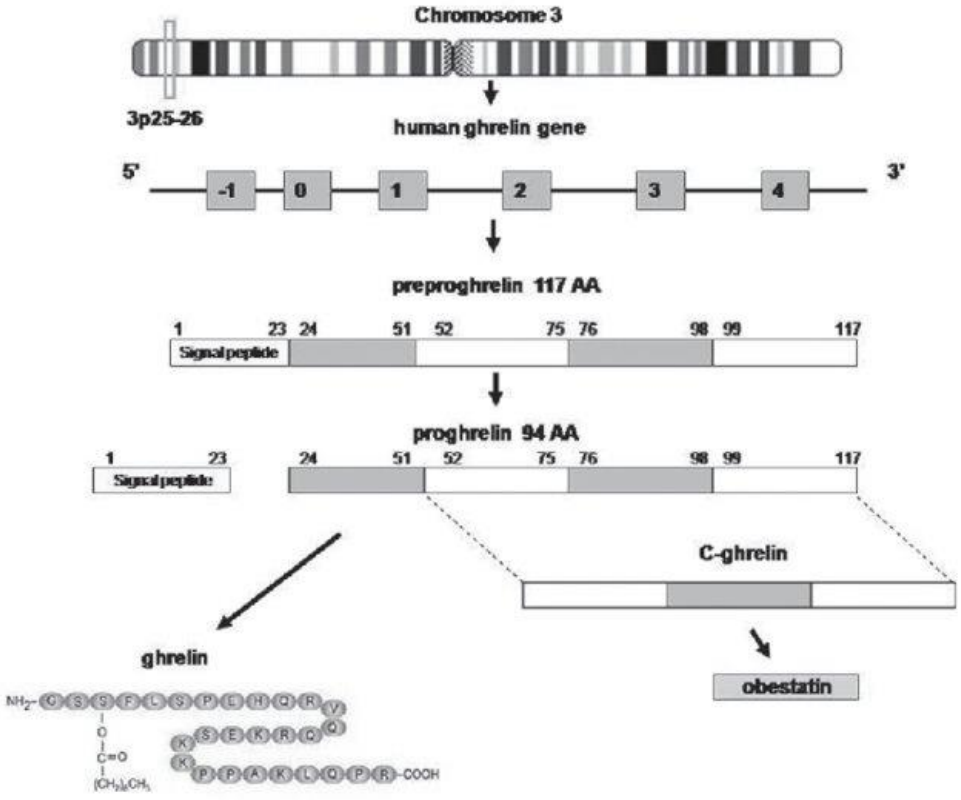

Figure (6). Outlined ghrelin expression (Lim et al., 2012).

Both human and rat ghrelins are 28-amino acid peptides, in which Ser3 is modified by a fatty acid, primarily n-octanoic acid. In rats, the 11th residue is lysine (K) and the 12th is alanine (A).
In rat and mouse stomach, the second type of ghrelin peptide has been detected (des-Gln14-ghrelin) resulting from the usage of CAG codon, which encodes the amino acid Glutamine (Gln), as a splicing site. However, this form is functional like the complete form of the ghrelin and acylated by GOAT at Ser3 (Sato et al., 2012).

Ghrelin amino acid sequence is well conserved in mammalians, especially the first 10 amino acids at the NH2 terminal end which may the importance of this peptide region in the acylation modification at the Ser3. A recent structural biology study based on the cryo-electron methods revealed a unique binding pocket for the octanoyl group which guides the right positioning of the peptide to its receptor and the initial activation of the receptor (Sato et al., 2012).

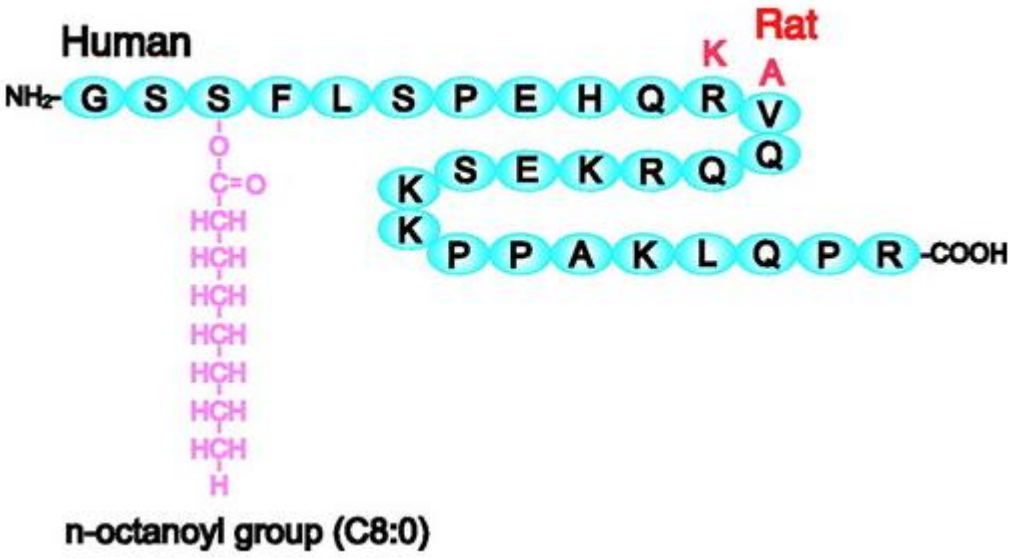

Figure (7). Structures of human and rat ghrelins (Kojima et al., 2005).

1.2.3. Ghrelin Effects on Adipose Tissue Metabolism:

1.2.3.1. Ghrelin and energy balance:

Given the fact of high pre-prandial and low post-prandial acylated ghrelin levels, ghrelin was pointed to play regulatory roles in the energy expenditure. Ghrelin stimulates the appetite consequently it increases the food intake. Together with other findings of its role in the adiposity and the accumulation of fats, acylated ghrelin contributes to weight gain (Tschöp et al., 2000). Ghrelin provides a protective role toward the conditions of starvation and the lack of food. This adaptive role implies accumulating more energy sources like fats in the responsible stores, adipose tissue dots in the body, and reducing the energy expenditure (Mihalache et al., 2016).

This role is supported by several studies. Administration of anti-ghrelin antibodies into laboratory mice increased their energy expenditure (Pradhan et al., 2013). The ablation of the ghrelin receptor increased the energy expenditure by enhancing the thermogenesis in the brown adipose tissue (Sun 2015). In an interesting study, transgenic old mice lacking ghrelin receptor, which is increased by age in adipose tissue, in the white adipose tissue showed lean and insulin-sensitive phenotype with

more energy expenditure (Lin et al., 2016). Acylated ghrelin also lowers energy expenditure by decreasing the activity of the sympathetic nervous system (SNS), and lowering thermogenesis in brown adipose tissue (Yasuda et al., 2003). However, in some pathological conditions of the negative energy balance like anorexia, ghrelin, and acylation levels were found to be high. In these cases, increased ghrelin may reflect an adaptive response with the aim of increasing appetite and preserving energy balance during a poor nutritional state.

1.2.3.2. Ghrelin effects on lipid turnover:

Adipose tissue lipolysis is an essential mechanism to provide energy during starvation and prolonged starvation. Triglycerides are hydrolyzed and FFAs are released into the circulation. β-Adrenoceptors, which are expressed in the adipocytes, activation promotes lipolysis of stored triglycerides in both white and brown adipocytes (Collins 2012). Ghrelin effects on the lipolysis were conflicted between the in vivo, in vitro models and human studies. Ghrelin concentrations peak immediately before the meal and directly decrease after the meal indicating the pivotal role of this hormone in the mobilization of the fats obtained from the digested food. Ghrelin facilitates the storage of the lipids in the adipose tissue and inhibits the lipolysis when there is no need for the lipolysis, while its rise and fall are absent in the prolonged starvation when there is a real need for the lipolysis to maintain the biological functions of the organism. These adaptive roles of the ghrelin resulted in conflicting findings of the role of the ghrelin in the lipid metabolism according to the conditions of the study including mainly the nutritional status. Another reason that increases the complexity of this study is the role of ghrelin as an activator of the growth hormone which is known to have lipolytic activity.

Several studies attempted to unravel the role of ghrelin on lipolysis and still, there is much to be discovered in this area. As ghrelin is known to induce the secretion of the Growth Hormone (GH) which is known to induce insulin resistance and lipolysis in the adipose tissue (figure 8), it is expected that ghrelin has lipolytic effects. Interestingly the lipolytic effects of the acylated ghrelin were found to be independent of the GH. The findings reported by (Lauritzen et al., 2020) showed a whole body increase in the lipolysis rates in patients with hypopituitary after infusion of acylated ghrelin independently of GH. These results are in contrast with other results reported blunted lipolysis after administration of isoproterenol (an β_1 and β_2 agonist) in rat adipose tissue cells incubated with ghrelin (Choi et al., 2003). However, this could be due to the difference between humans and rats in response to ghrelin in addition to the difference between in vivo and in vitro outputs. In the same context, ghrelin treatment was reported to increase the levels of the lipogenesis markers in vivo in

rat deficient for GH and wild type rats (Sangiao-Alvarello et al., 2009). Rodrequez et al (Rodríguez et al., 2009) reported that higher acylated ghrelin levels were correlated with elevated accumulation of fat in visceral adipose tissue, and its higher circulating levels in obese individuals could be the reason behind the excessive amount of fats in obesity.

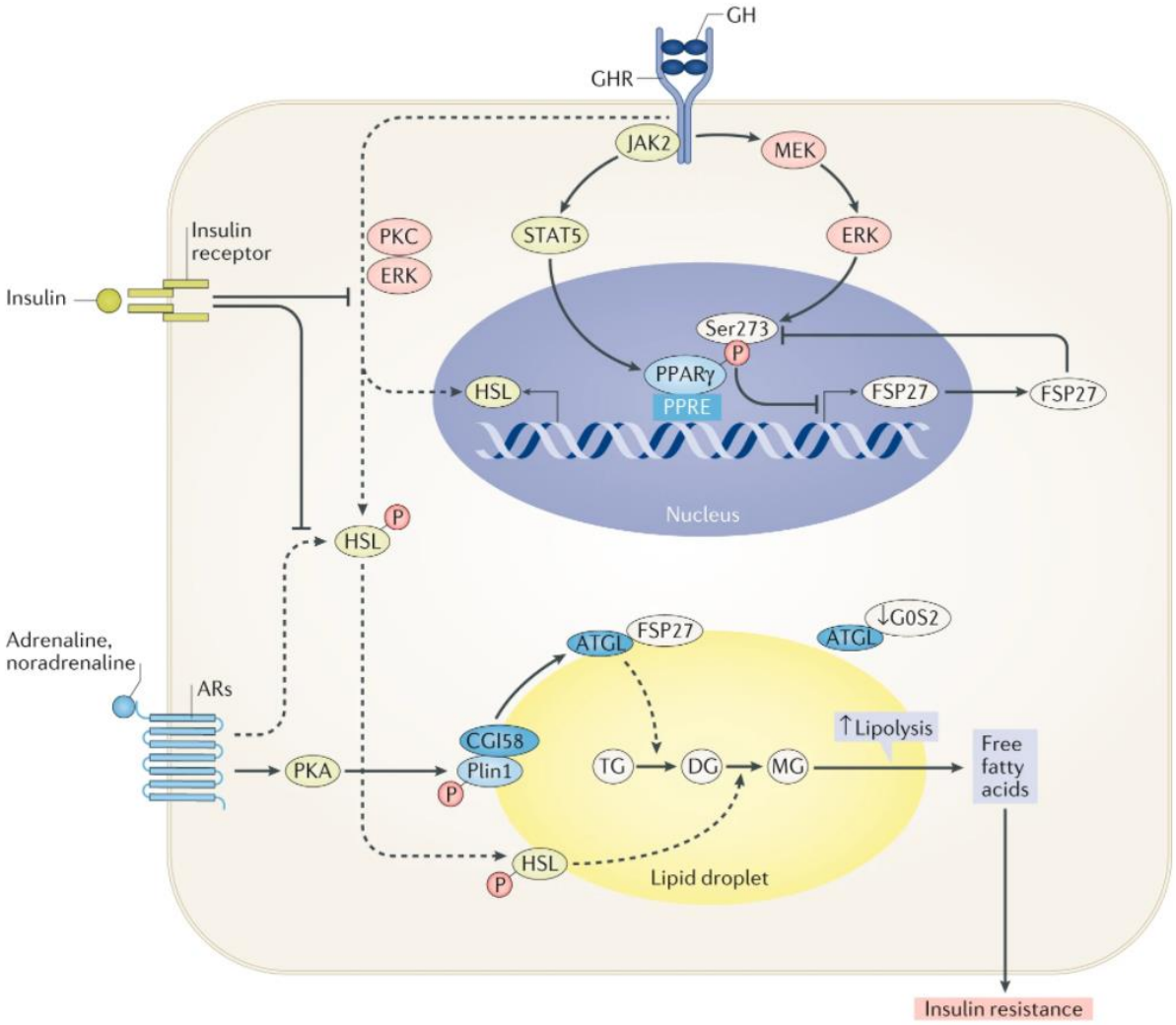

Figure (8). Growth hormone effects on adipose tissue. GH is known to induce insulin resistance and lipolysis in adipose tissue (Kopchick et al., 2020).

1.2.3.3. Ghrelin and Insulin action in adipose tissue:

Insulin signaling in the adipose tissue is a major player of the lipid metabolism in the adipose tissue. Adipocytes respond to the insulin by increasing the glucose uptake and the triglycerides synthesis and inhibiting the lipolysis, thus enhancing the lipid accumulation, while adipose tissue insulin resistance resulting from the over fat load contribute to increasing the lipolysis rates pathologically by elevating the levels of circulating FFA which induce the whole-body insulin resistance leading to

a higher risk of the metabolic complications and type2 diabetes. Hence, the direct link between lipolysis and insulin sensitivity is important to be considered when investigating insulin sensitivity in adipose tissue. In other words, lipolysis can, at least, be studied as an indicator of insulin sensitivity in adipose tissue.

Several studies dissected the link between ghrelin and insulin sensitivity. Early reports after the discovery of the ghrelin reported decreased levels of the total ghrelin in type2 diabetes patients. In our group, acylated ghrelin treatment was shown to modulate positively the insulin sensitivity in the skeletal muscle at the level of AKT phosphorylation (Barazzoni et al., 2017).

It was also demonstrated that the elevated AG levels are associated with HOMA-IR and Body Mass Index (BMI) in patients of MetS which indicated the potential role of the acylated ghrelin in the adiposity and lipid accumulation (Barazzoni et al., 2007b). In an elegant study published in 2017, ghrelin infusion was shown to induce insulin resistance independently of the growth hormone GH, cortisol, and FFA. In that study ghrelin induced peripheral insulin resistance but did not exert consistent regulation of insulin sensitivity in the skeletal muscle. No data from this study were about the insulin sensitivity in the adipose tissue (Vestergaard et al., 2017).

1.2.3.4. Ghrelin as an anti-inflammatory factor:

Ghrelin was reported in many studies to exert anti-inflammatory effects in different tissues. Technically, ghrelin stimulates the anti-inflammatory processes and inhibits pro-inflammatory actions. For example, Regarding the anti-inflammatory effects of ghrelin in adipose tissue, ghrelin treatment was found to protect against apoptosis and correlated by upregulated levels of TNFα and autophagy in primary human visceral adipocytes of patients with type2 diabetes (Rodríguez et al., 2012). Similar findings were reported about the role of acylated ghrelin in patients with obesity and nonalcoholic fatty liver disease (NAFLD) where the acylated ghrelin protected against the apoptosis induced by TNFα (Ezquerro et al., 2019). Ghrelin was also shown to suppress the apoptosis induced by the high glucose/high lipid conditions via inhibiting JNK1/2 and p38 signaling (Liao et al., 2017). These findings are in agreement as mentioned before with the fact the ghrelin is playing anti-inflammatory roles by acting as an endogenous antioxidant and scavenger for the free radicals thus lowering the ROS levels and ameliorating the redox state (Dong et al., 2006), and other findings in other pathological conditions like obstructive sleep apnea (OSA) and coronary heart disease where the plasma ghrelin levels were upregulated with lowered levels of TNFα and IL-6 suggesting a protective role of the ghrelin towards the pro-inflammatory factors correlated with the OSA (Yang

et al., 2003). Moreover, in a rat model of testicular ischemia-reperfusion, ghrelin treatment was shown to have anti-inflammatory effects where it lowered significantly TNFα and IL6 (Taati et al., 2015).

1.2.4. Ghrelin in CKD:

Plasma ghrelin levels were reported to be upregulated in children (Canpolat et al., 2018) and adults (Jarkovská et al., 2005) patients of CKD. These high levels of ghrelin could be explained in part by the low renal degradation of the ghrelin (Mak et al., 2007). Interestingly, these high levels of the ghrelin were correlated with a healthy profile in non-obese, non-diabetic hemodialysis patients, where preserved insulin sensitivity and low whole-body inflammation was reported (Barazzoni et al 2008). Ghrelin administration to the nephrectomized rats lowered the circulating levels of proinflammatory cytokines, and this might be the reason behind the protective role in preserving the muscle mass in the nephrectomized rats (Deboer et al., 2008), which is in agreement with other findings in nephrectomized mice where ghrelin treatment improved the physical decline (Tamaki et al., 2015). Improved mitochondrial function by the ghrelin treatment was reported as well in the CKD rats model and was furtherly correlated by enhanced insulin sensitivity in the high food intake conditions (Barazzoni et al., 2010).

In adipose tissue, the effects of ghrelin in CKD are largely unknown.

1.3. O-GlcNAcylation:

1.3.1. Definition:

O-GlcNAcylation is a non-canonical glycosylation post-translational dynamic modification (PTM) that resulted in the attachment of *O*-linked *N*-acetylglucosamine (O-GlcNAc) moieties to Ser and Thr residues of cellular proteins: cytoplasmic, nuclear, and mitochondrial. It is controlled by two enzymes: *O*-GlcNAc transferase (OGT) which adds the O-GlcNAc to the targeted proteins and *O*-GlcNAcase (OGA) which is catalyzing the removal of O-GlcNAc from the modified proteins. Hexosamine Biosynthetic Pathway (HBP) is the major pathway that generates the donor substrate for O-GlcNAcylation, uridine diphosphate GlcNAc (UDP-GlcNAc) by integrating the metabolism of glucose, fatty acids, and other biomolecules in the cell. Since its discovery in the eighties of the last century, it attracted the attention of scientists especially in the last five years, and several studies were performed to understand this unique type of PTM and its different roles in different biological functions. Today we know more about O-GlcNAcylation and its roles in cellular signaling dynamics,

transcription, epigenetics, and maintaining cellular homeostasis. Disruption of O-GlcNAcylation homeostasis was reported to be implicated in different pathological conditions in humans like diabetes and cancer. O-GlcNacylation was found to regulate gene transcription and proteasomal activities in addition to autophagy. Molecular genetics studies reported the effects of OGT mutations in different pathological conditions like the X-linked intellectual disability. The global O-GlcNacylation levels were also found to change with age (Fülöp et al., 2008). However, most importantly, we know that O-GlcNAcylation represents the cellular response towards both nutrient availability and the various types of stress like heat shock, hypoxia, and deprivation. Its levels are highly affected by these two factors, and confidently it can be said that the O-GlcNAcylation is a nutrient and stress cellular sensor that plays major roles in cellular events including metabolism (Yang et al., 2017, Mueller et al., 2021).

1.3.2. O-GlcNAcylation, unique PTM and homeostasis mechanism:

Differing from other PTMs which are regulated generally by a large number of mediators, the O-GlcNAcylation is regulated by a single couple of enzymes. This mechanism of regulation is beginning to be understood. Different theories were suggested to elucidate this mechanism. The most prevailed theory is that TRPs domains can produce a unique conformation to facilitate the attachment of the moiety to the target protein. Interestingly, O-GlcNacylation was reported to have crosstalks with other PTMs, like ubiquitination where O-GlcNAcylation prevent the target protein degradation by recruitment of deubiquitinases to O-GlcNAcylated proteins (Ruan et al., 2013). Many O-GlcNAc proteins are also phosphorylated and evidence of a degree of interplay between phosphorylation and O-GlcNAcylation has been reported. A lot of proteins that undergo the O-GlcNAcylation are also reported to undergo the phosphorylation, and in this context, there is a lot of evidence about the interplay between the two mechanisms (Hart et al., 2011, Hanover et al., 2012, Comer et al., 2000).

Around 5000 human proteins were found to be O-GlcNAcylated (Wulff-Fuentes et al., 2021). Importantly, once a protein is reported to be O-GlcNAcylated, the second step is to identify the role and the localization of this modified protein. Recently, a human O-GlcNAcome database was established and can be found at this link: www.oglcnac.mcw.edu.

At the atomic level, the O-GlcNAcylation occurs as a β-glycosidic bond between the hydroxyl group of serine or threonine side chains and *N*-acetylglucosamine (GlcNAc). This differs from the protein glycation which occurs by forming the bond between the amino group in the protein and aldehyde group in the sugar, and also differs from polysaccharide chain attached to surface proteins of the

plasma membrane in a non-dynamic process in contrast to O-GlcNAcylation which is a dynamic and reversible process (Zhao et al., 2016).

Homeostasis of O-GlcNacylation:

Since the O-GlcNacylation system is involved in a wide array of cellular functions and processes, it is very important to maintain the levels of the O-GlcNacylation. Studies on the C.elegans model reported that the effects of knocking down both OGT and OGA are similar suggesting a mechanism in which both enzymes are working differentially in a buffering region, an optimal zone, to maintain the O-GlcNAcylation levels in the cell which is necessary to maintain the cellular functional spectrum. Among the suggested mechanisms is that both OGT and OGA regulate the expression of each other, in addition, that both enzymes are subjected for the O-GlcNAcylation which means the autoregulation of the O-GlcNacylation system in the cell.

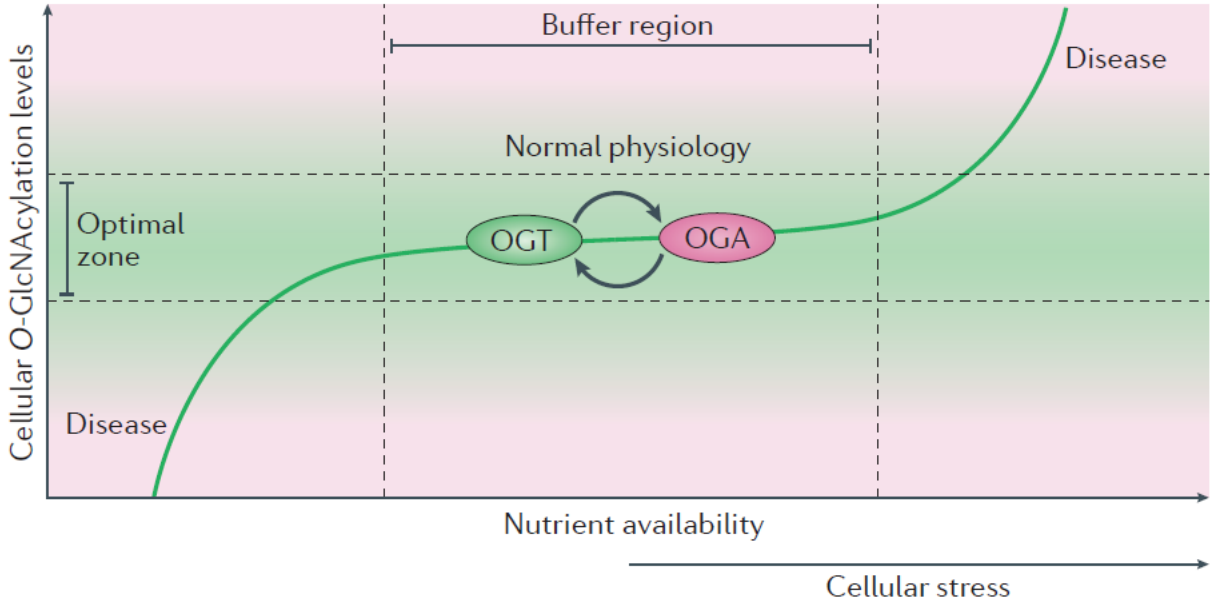

Figure (9). Suggested mechanism for O-GlcNacylation homeostasis (Yang et al., 2017).

1.3.3. OGT Expression, Isoforms, and Functional Studies:

The Human OGT gene is located on chromosome X at the locus Xq13.1 close to the X-inactivation center (Shafi et al., 2000). Three isoforms are produced from the OGT human gene. The longest is the nucleocytoplasmic OGT (ncOGT) 117kDa which is considered as the canonical isoform and found to be sufficient for the O-GlcNAcylation of mitochondrial proteins (Trapannone et al., 2016). The mitochondrial OGT differs from the ncOGT 103 kDa in the first 50 amino acids at the N-terminus end of the protein which forms the MTS (Mitochondrial Target Sequence) for the mOGT. The last isoform

is the cytosolic short OGT (sOGT) 75kDa which is the shortest form. All the three sequences have an identical catalytic part which includes two domains CDI and CDII and differs one from another by the number of tetratricopeptide repeats. While little is known about sOGT, ncOGT and mOGT were studied mostly in the literature. The ncOGT isoform is mainly localized in the nucleus with the ability to shuttle toward the cytoplasm and the cellular membrane in response to different stimuli signals. The nuclear localization of the ncOGT is mediated by three amino acids in the OGT sequence acting as localization signal, and the O-GlcNAcylation of the TPR domain of OGT. The mitochondrial OGT isoform exerts important roles in a wide spectrum of mitochondrial functions and even biogenesis. Notably, mOGT is detectable mostly in vito (Lazarus et al., 2006), and ncOGT was reported to be sufficient to maintain the the O-GlcNAc mitochondrial proteome (Trapannone et al., 2016). In our study, ncOGT was the isoform corresponding to the OGT detected from the white adipose tissue of the animals of the study, while mOGT was the isoform corresponding to the OGT in 3T3L1 cellular experiments. Uniquely, in the muscle tissue of the healthy rats, sOGT was the isoform corresponding to OGT.

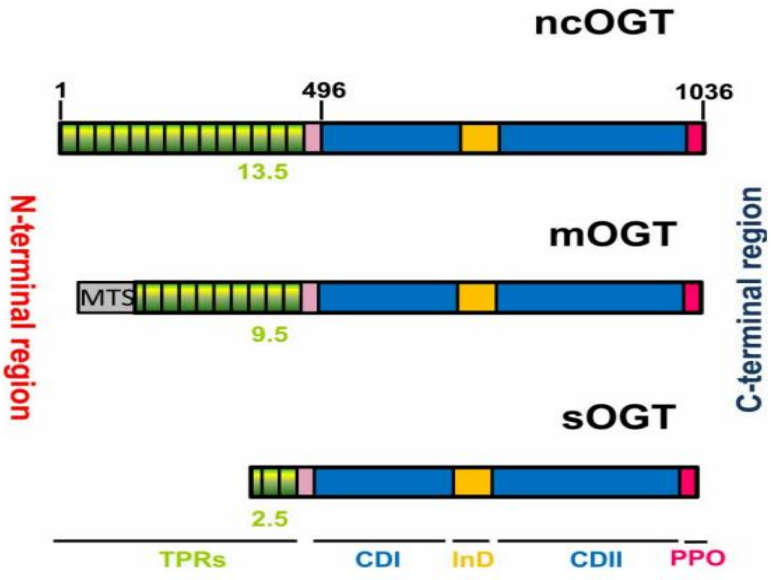

Figure (10). OGT isoforms. TPRs, tetratricopeptide repeats; CD, catalytic domain; InD, intervening domain; PPO, PIP-binding activity of OGT; MTS, mitochondrial targeting sequence. (Aquino-Gil et al., 2017).

Functional Studies of OGT:

Several studies reported the effects of deleting the OGT in different organs, which in general leads to pathological output with few exceptions reported in skeletal muscle and adipose tissue. In the heart, deleting OGT was reported to be lethally in neonates and different defects in the mice reaching the adult life (only 12%) (Mu et al., 2020). These results are in contrast with the findings

reported from deleting OGT in skeletal muscle where it leads to lowering the insulin resistance in the high-fat diet mice model (Murata et al., 2018). Intestinal OGT deletion affected the gut microbiome and increased the glucose clearance rate (Zhao et al., 2020).

1.3.4. OGT Cellular Functions:

1.3.4.1. OGT and the cellular stress response:

Many studies evidenced the role of *O*-GlcNAcylation as a stress sensor. The overall increase in the *O*-GlcNAcylation was found to be associated with stress tolerance, in which the cells respond to the stress stimuli and organize the response to enhance the cell survival (Zachara et al., 2004, Butkinaree et al., 2010). For example, in the cardiovascular system, elevating *O*-GlcNAcylation indeed can rise the cell survival rates in presence of acute stress conditions including hypoxia, ischemia, oxidative stress (Ngoh et al., 2010). Further studies demonstrated the protective role of the *O*-GlcNAcylation in different stress stimuli cold and heat shock, oxidative stress, ethanol stress, genotoxic stress, reductive stress, endoplasmic reticulum stress, hypoxia-reoxygenation, osmotic stress, ATP depletion, ischemia-reperfusion injury, and trauma hemorrhage (Liu et al., 2021).

Importantly, O-GlcNAcylation plays a crucial role in protein homeostasis by protecting nascent polypeptides from degradation. Unstructured protein regions, enriched in nascent polypeptides, are usually the main O-GlcNAcylated regions. This is supported by studies reporting that the nascent polypeptides of SP1 and NUP62 are highly O-GlcNAcylated than their mature forms (Zhu et al., 2015). During cellular stress, the unfolded proteins levels are increased which activates the Unfolded Protein Response (UPR) which enhances the HBP pathway leading to more production of the UDP-GlcNAc, the main meioty used by OGT, which leads to nonspecific O-GlcNAcylation of unfolded proteins in the cytoplasm, which protects these proteins from degradation by inhibiting protein ubiquitylation or proteasomal function and facilitate there refolding by chaperones with O-GlcNAc-directed lectin activity (Ruan et al ., 2012, Zhang et al., 2003, Li et al., 2013, Ruan et al., 2013, Guinez et al., 2004, 2006, 2007).

However, deprivation conditions were reported to increase the global levels of the O-GlcNacylation. This is explained by the increased levels of OGT (Taylor et al., 2009).

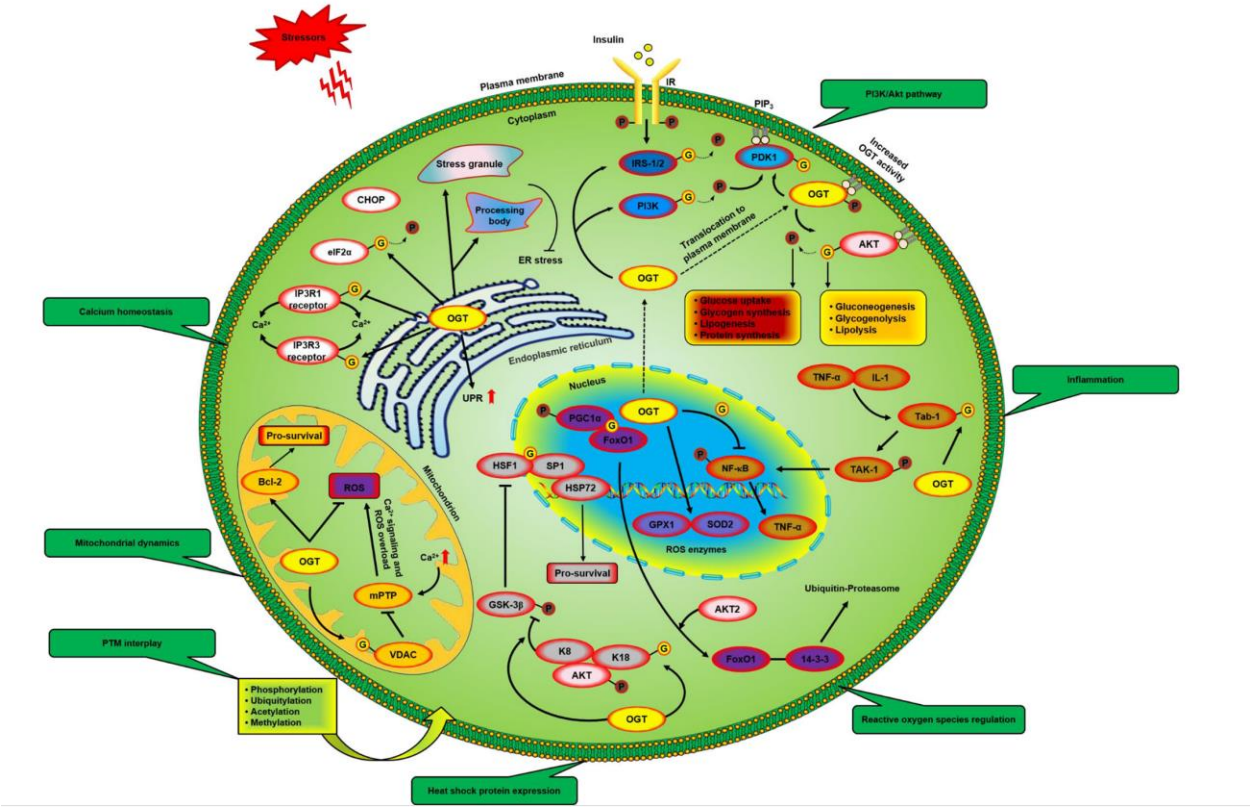

Figure (11). Outlined network for OGT as a stress sensor (Liu et al., 2021)

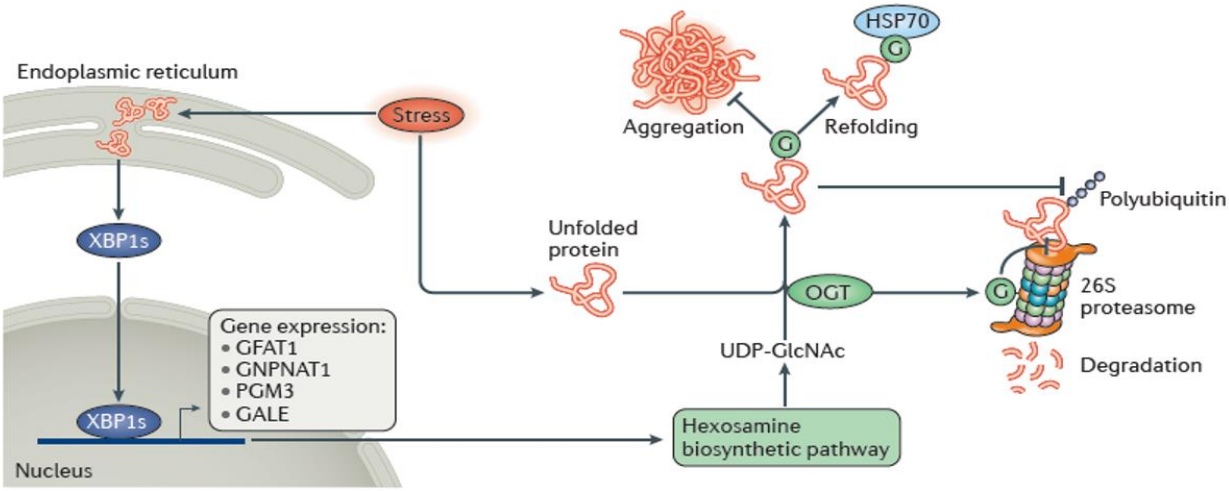

Figure (12). Suggested mechanism for OGT function as a stress sensor in Unfolded Protein Response. (Yang et al., 2017).

1.3.4.2. OGT as a nutrient sensor:

Around 3% of the cellular glucose goes through the hexosamine biosynthesis pathway (HBP) leading to the production of the donor substrate of *O*-GlcNAcylation, uridine diphosphate N-acetylglucosamine (UPD-GlcNAc). This production is affected by a lot of nutrients, carbohydrates, amino acids, fatty acids, and nucleic acids. Therefore, the level of *O*-GlcNAcylation is controlled

directly by the metabolism and the availability of the nutrients. This highlights the role of nutrients in the cellular activities mediated by the *O*-GlcNAcylation modification (Hardivillé et al 2014). *O*-GlcNAcylation was reported to maintain the metabolic homeostasis under differential nutrient-availability conditions by affecting key metabolic pathways including for example insulin-AKT pathway, MAPK pathway, mTOR pathway, AMPK pathway (Hanover et al., 2010).

1.3.5. Role of *O*-GlcNAcylation in metabolic homeostasis:

O-GlcNAcylation is thought to be the bridge from metabolism to chronic diseases (Bond et al., 2013). It plays a pivotal role in adjusting the cellular metabolism according to the nutrient flux aiming at protecting the organ environment homeostasis. For example, in pancreatic beta cells, the disruption of O-GlcNAcylation induces endoplasmic reticulum stress, which results in β-cell failure (Alejandro et al 2015). Additionally, the knockdown of O-GlcNAcylation induces hyperinsulinemia, which suggests a link with the pathogenesis of type 2 diabetes mellitus (Ida et al., 2017).

In the liver, O-GlcNAcylation plays a major role in the regulation of gluconeogenesis by O-GlcNAcylating the peroxisome proliferator-activated receptor-γ coactivator (PGC)-1α which increases its stability and enhances its role in the gluconeogenesis enhanced during the starvation. (Ruan et al., 2012). Additionally, O-GlcNAc regulates FoxO1 activation in response to glucose resulting in the increased expression of the genes involved in the gluconeogenesis response to the starvation and fasting conditions (Housley et al., 2008). Cyclic adenosine monophosphate response element-binding protein (CREB) was also found to be O-GlcNAcylated by OGT which enhances the hepatic gluconeogenesis (Dentin et al., 2008). Importantly, OGT was found to be phosphorylated by calcium/calmodulin-dependent kinase II (CaMKII) in response to glucagon which is released during starvation. CaMKII then recruits OGT to the autophagy-initiating kinase UNC-51-like kinase 1 (ULK1) and enhance the autophagy in the liver to release amino acids and fatty acids for ketogenesis and gluconeogenesis (Yang et al., 2017).

In skeletal muscle, O-GlcNAcylation exerts an important role in controlling the whole body oxidative metabolism by regulating the expression of the IL-15, in which OGT is involved in the repression of IL-15 transcription, and mice knocked out for OGT in skeletal muscle showed increased levels of IL-15 which promotes the endurance, oxidative energy metabolism, and muscle PPARδ, SIRT1, PGC-1α, and PGC-1β expression (Shi et al., 2018).

Most importantly, in the adipose tissue which is a master regulator of the whole body metabolism, O-GlcNAcylation was reported to affect different mechanisms related to the metabolism. In adipose tissue, OGT overexpression was reported to induce the lipid accumulation while its deletion increased the lipolysis and the insulin sensitivity (Yang et al., 2020). These effects were related to the white adipose tissue, while in brown adipose tissue OGT deletion lowers severely the thermogenesis in mice exposed to 4C due to the decreased mitochondrial biogenesis, in which OGT plays important role in the mitochondrial biogenesis by altering PGC-1α, the main regulator of mitochondrial biogenesis (Ohashi et al., 2017). However, more discussion about the OGT in adipose tissue will be in other parts of the thesis.

1.3.6. OGT and inulin sensitivity:

Insulin sensitivity is reduced by the activity of the OGT since it reduces the phosphorylation of the key mediators in the insulin signaling pathway including the AKT, PDK1, PI3K, and IRS1.

Insulin affects OGT at three levels, modulation of OGT expression, subcellular localization, and enzymatic activity. Insulin upregulates the OGT expression by the PI3K-dependent pathway.

Insulin signaling enhances the translocation of OGT from the nucleus to the cytoplasm and the localization of OGT to lipid rafts in the plasma membrane, where it becomes active by tyrosine phosphorylation by the insulin receptor.

Importantly, prolonged insulin stimulation leads to the localization of OGT to the lipid rafts in the plasma membrane. This mechanism is mediated by the PIP3 and leads to the inactivation of several components of the insulin signaling pathway by the O-GlcNacylation.

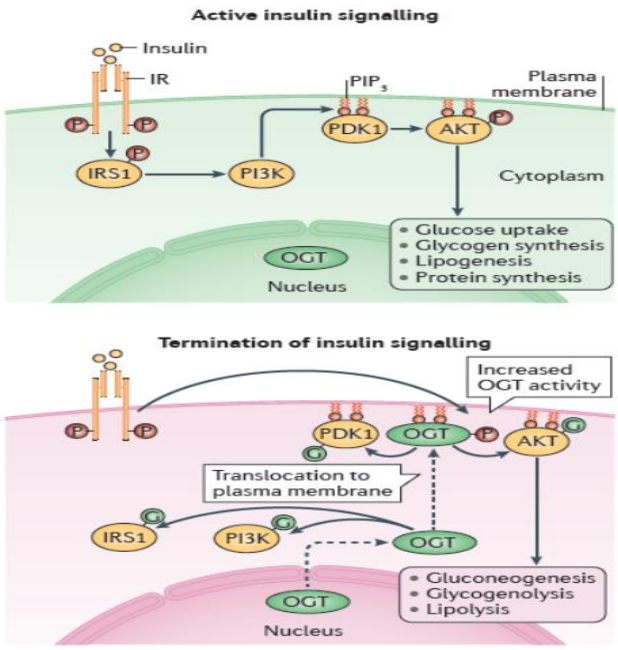

Figure (13). OGT function in response to insulin signaling activation. (Yang et al., 2017)

1.3.7. adipose tissue-brain axis and OGT:

Nutritional regulation of the appetite is of paramount importance in overnutrition-induced obesogenic conditions. Several studies highlighted the role of the brain sensors of appetite homeostasis, for instance, SirT1 in AGRp neurons (Dietrich et al., 2010), hypothalamic mTOR (Cota et al., 2006), and hypothalamic AMP-Kinase (Minokoshi et al., 2004). The connections between the adipose tissue and the brain started to attract more attention in parallel with the increased interest in the adipose tissue endocrine function. Adipocytes secrete a wide spectrum of hormones that play pivotal roles in metabolism and energy homeostasis, and these hormones function in several tissues including the brain. One of the most studied proteins is leptin, the hormone that exerts the opposite effects of ghrelin. Leptin is released from the adipocytes in the white adipose tissue at levels proportional to the body's fat reserves and regulates appetite by controlling the feeling of fullness. It acts contrary to ghrelin. The satiety signals are transported to the brain by tanycytes which are attached to the LepR receptor. The deletion of this receptor led to disruption in the energy homeostasis and increased the percentage of lipids to the muscle mass severely (Duquenne et al., 2021). Interestingly, leptin satiety signals are mediated by the increased levels of OGT in the adipose tissue reported during the meal (Perry et al., 2020). Going the other way, brain to adipose tissue, it was found by crossing Crossing Ogt floxed mice with AgRP-Cre mice that mice knocked out for OGT in Hypothalamus arcuate nucleus had higher rates of thermogenesis in the white adipose tissue correlated with better insulin sensitivity and lower body weight gain in response to the high-fat diet (Ruan et al., 2014). The same study reported that the ghrelin released from the stomach during fasting conditions increases the levels of the OGT in the hypothalamus which leads ultimately to decreased browning rates in the white adipose tissue.

These interesting findings were recently supported by novel findings suggesting a model for the OGT mechanism the mediates the adipose tissue-brain axis. OGT stimulates lipid accumulation and hyperphagia by transcriptional activation of de novo lipid desaturation and accumulation of N-arachidonic ethanolamine (AEA), an endogenous appetite-inducing cannabinoid (CB). CB signals (CB1) are then transferred to the brain to induce hyperphagia.

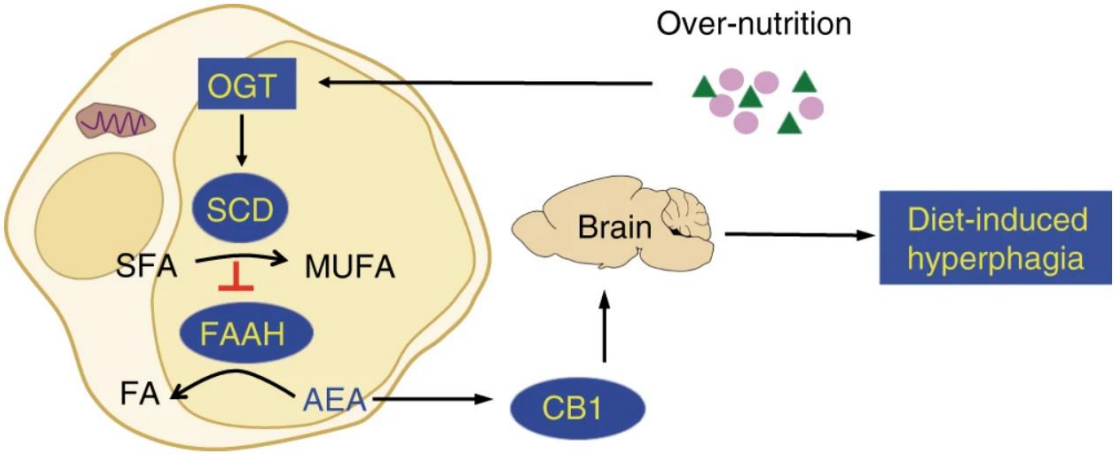

Figure (14). OGT role as a lipid level sensor.(Li et al., 2018)

These findings highlight the role of O-GlcNacylation in response to the metabolic systemic changes including overnutrition, postprandial during which the availability of nutrients, and the fasting conditions.

1.3.8. Targeting OGT as a therapeutic strategy for Obesity:

In several conditions, targeting OGT was holding a beneficial effect, so it is worth addressing this question: what is the safety of targeting the OGT?

What pushes the efforts in the direction of targeting OGT for the treatment of obesity is the fact that it is not interfering with mental health and homeostatic feeding, in addition to being precise. Advanced biophysics tools and high throughput technologies revealed cell-permeable inhibitors for the OGT: APNT and APBT (Wang et al., 2017), OSMI-1 (Ortiz-Meoz et al., 2015), and the only natural product L01 (Liu et al., 2017). Interestingly, experiments performed on cellular and zebrafish models revealed low toxicity of L01 which might be promising. OSMI-1was also tested in several mammalians in vitro cellular models and it showed that it does not affect the cellular surface N- or O-linked glycans. The safety margin of targeting OGT may be, at least in part, explained by the results of Li et al (Li et al., 2018) when they demonstrated that OGT knockdown in the adipose tissue of mice did not alter the baseline food intake when mice were fed on a normal diet, while it significantly reduced high fat diet-induced hyperphagia.

2. Aims of the study

Acylated ghrelin plays major role in the intermediate metabolism and is directly involved in energy homeostasis, hence investigating the metabolic role of AG in the major metabolic tissues is of high importance and demand. While the effects of the acylated ghrelin in the liver and muscle tissue are, at least in part, described, its effects in the adipose tissue are largely unknown. So, we aimed first to study, in particular, the metabolic alterations in the adipose tissue of healthy rats upon sustained administration of acylated ghrelin. We aimed to test the metabolic profile at different mechanisms: insulin sensitivity, mitochondrial function, redox state, and cytokine profile in both physiological conditions and in a rodent model of inflammation and wasting by surgically induced-CKD.

In the second part of the study, we aimed to confirm and further investigate in vitro the findings observed in the animal studies. Insulin signaling among other mechanisms was suggested to be directly targeted by the AG in the adipose tissue, so we aimed to test the effect of acylated ghrelin treatment on the insulin sensitivity in cultured differentiated adipocytes.

The study also aimed at identifying possible mediators for the acylated ghrelin metabolic effects in the adipose tissue. Based on the growing evidence in the literature that reported similar effects of adipose tissue specific-deletion of both OGT and the AG receptor (GHS-R) at improving the insulin sensitivity in the white adipose tissue, we aimed to test whether the effects of the ghrelin could at least in part involve OGT. We aimed first to test the OGT levels in the white adipose tissue of the animals' models of the study. We then aimed to test, in vitro by using cultured adipocytes, whether the effect of AG on OGT in white adipose tissue is locally regulated by adipocyte mechanism.

In the last part of the study, we aimed to test our hypothesis that OGT is involved in the AG network by gene expression silencing methods. We aimed at investigating the AG effect on the insulin sensitivity in OGT-silenced cultured adipocytes in conditions related to the physiological dynamics of both OGT and AG.

3. Materials and Methods

3. 1. Animal Studies:

3.1.1 Sustained Exogenous Acylated Ghrelin Administration for 4-Days in Healthy Rats:

The present animal experiments were performed in the context of a wider study on the effects of ghrelin forms on the metabolism of insulin-sensitive tissues, and the relative protocol previously published (Gortan Cappellari et al., 2016).

The study was approved by the Animal Studies Committee of the University of Trieste, and the animals were housed at the University of Trieste Animal Facility. 12 weeks old male Wistar rats (Harlan-Italy, San Pietro al Natisone, Udine, Italy) were divided into individual cages with free access to water and standard chow (Harlan 2018, 14.2 kJ/g), in a 12 hours' light/dark cycle conditions for one week, then they were randomly divided into two groups (n=8 each group); the control group (Con) received subcutaneous (s.c.) injection of saline solution (NaCl 0.9% weight for volume), and the Acylated Ghrelin treatment group (AG) in which the 200-ng was administered subcutaneously to each rat twice a day for four days. The used dose and period were selected based on previous studies (444 roberta thesis). Bodyweight and food intake measurements were taken daily during the experiment. Rats were killed three hours after the last injection by anesthesia (tiobutabarbital 100mg/kg, tiletamine/zolazepam [1:1] 40 mg/kg i.p.). White adipose tissue was collected surgically from the retroperitoneal adipose tissue and frozen at -80°C for the following analysis, and blood was collected by heart puncture for glucose measurement. The study protocol is outlined in figure 15.

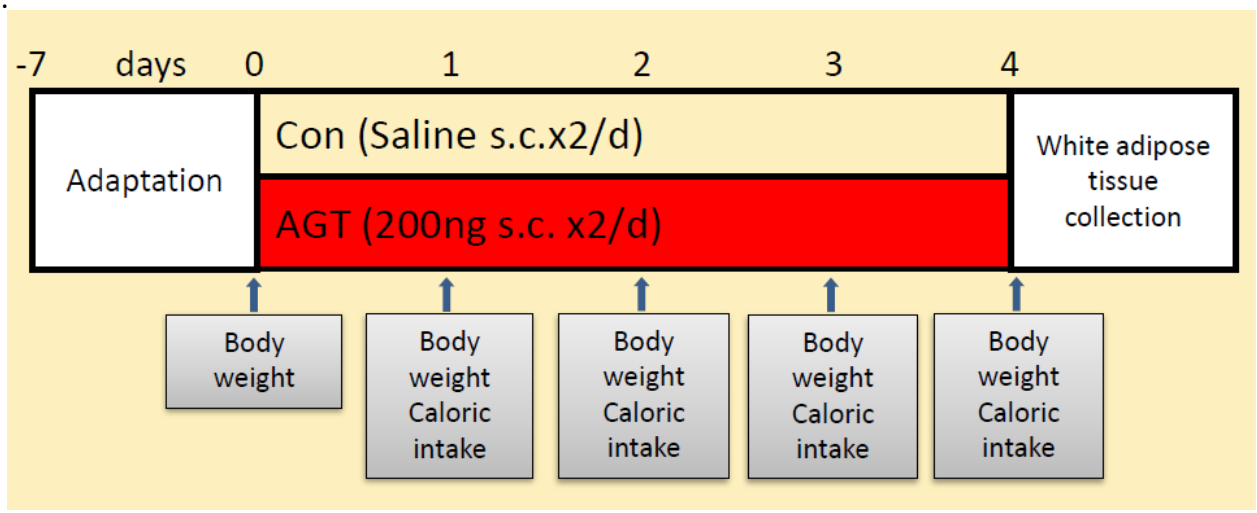

Figure (15). Schematic outline for the study protocol.

3.1.2 Sustained Exogenous Acylated Ghrelin Administration for 4-Days in Uremic 5/6 Nephrectomized Rats:

The present animal experiments were performed in the context of a wider study on the effects of ghrelin forms on the metabolism of insulin-sensitive tissues in CKD, and the relative protocol previously published (Gortan Cappellari et al., 2017).

The study was approved by the Italian Health Ministry Animal Experimentation Authority.

Thirty 12-weeks old male Wistar rats (Harlan-Italy, San Pietro al Natisone, Udine, Italy) were divided into individual cages with free access to water and standard chow (Harlan 2018, 14.2 kJ/g), in a 12 hours' light/dark cycle conditions for one week, then they were assigned randomly to 5/6 nephrectomy (20 rats) or sham surgery (10 rats). Surgery was performed using a single-step laparotomic approach, to reduce animal stress and complications. Surgical procedures were performed in in surgical sterility and anaesthesia (Premedication: dexemetomodin (0,025- 0,05 mg/kg IP, anaesthesia: Zoletil (20-25 mg/kg IP,). Ten days after the surgery, animals were free of any complications or treatment. On day 36, nephrectomized rats were randomly assigned to a 4-day, twice-daily s.c. saline (Nx, n=10), AG (Nx-AG, n=10) while sham rats (S, n=10) were treated with saline as well. Anaesthesia, tissue, and blood collecting and processing were also performed as described in the first study. The study protocol is outlined in figure (16).

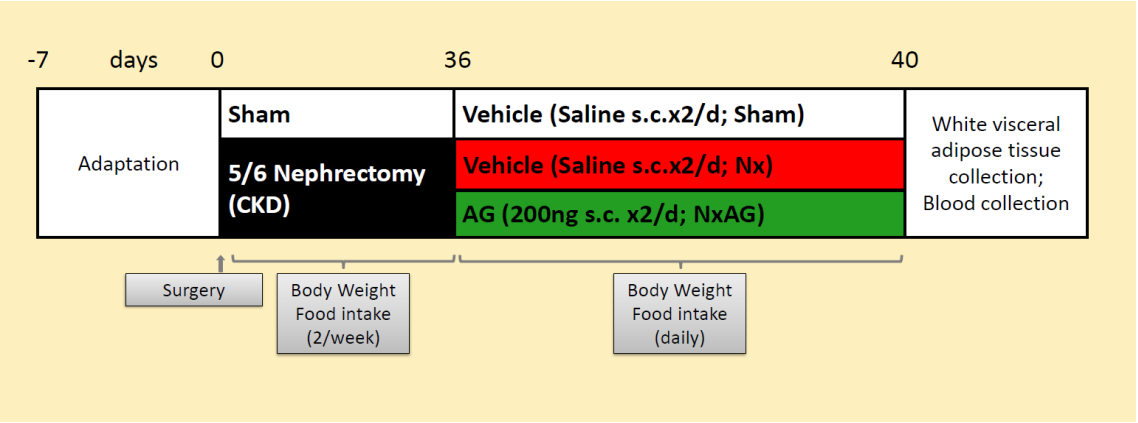

Figure (16). Schematic outline for the study

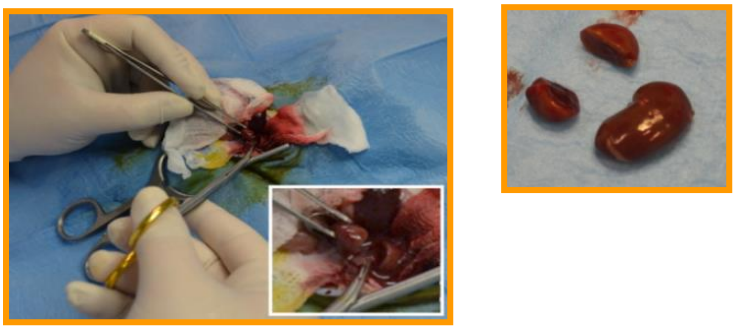

Figure (17). 5/6 single step surgery nephrectomy.

3.2. In vitro models:

For the in vitro experiments, we focused on the effects of AG on the insulin sensitivity in the differentiated adipocytes as the in vivo findings suggested a direct effect of the AG on insulin sensitivity. Since the AG control is tightly linked to the nutritional status, the study aimed to test the AG effect on insulin sensitivity in different nutritional conditions based on the FBS content in the medium. The study included experiments performed in normal FBS10% concentration referred to normal feeding conditions, in addition to reduced FBS concentration referred to partial starvation, and completely serum deprivation referred to complete starvation. Starvation conditions were used in this study since AG is known to increase in fasting conditions. Different doses of the AG were applied (1000; 100; 10 ng/ml) in all the aforementioned conditions. Three independent experiments were run for each condition, duplicated in the siRNA- AG experiments analyzed by ELISA.

3.2.1. 3T3L1 cellular model:

3T3L1 cell line is a murine-derived cell line used in adipose tissue research. The cells are fibroblast shaped like 3T3 murine cells, but under specific conditions, they undergo differentiation into adipocytes-like cells by accumulating the lipids. Functionally, differentiated 3T3L1 adipocytes are also responsive to the hormonal stimulatory effects like insulin (Green et al., 1975).

3T3L1 cells used in the study were received as a kind gift from Dr. Barbara Toffoli, Ph.D.

3.2.1.1 Proliferation:

Cells were received as a vial moved from liquid nitrogen. The vial was thawed at 37 °C and the contents of the vial were moved to prewarmed Proliferation Medium: DMEM High Glucose (Sigma D5796, ST Louis Missouri, USA), Calf bovine serum 10% inactivated at 56 °C for 20 minutes (Sigma 12133C, ST Louis Missouri, USA), Glutamin 2mM (Sigma TMS002C, ST Louis Missouri, USA), Pencellin: Streptomycin 1unit/ml: 0.1mg/ml (Sigma P4333, ST Louis Missouri, USA). Cells were then centrifuged at 1000 RPM for 5 min. The cellular pellet was resuspended in an appropriate volume

of the proliferation medium and plated at 3000 cells/cm^2 in at 0.2-0.25 ml/cm^2. Filtered flasks (Sarstedt 83.3911.002, Nümbrecht, Germany) were used for culturing the cells. Plated flasks were moved to the incubator at 37 °C, 5% CO_2. Cells were kept until they were 60-70% confluent with changing the medium every other day before subculturing.

Subculturing 3T3L1 cells: For the trypsinization, the medium was discarded followed by a brief wash with warmed PBS (Sigma P3813, ST Louis Missouri, USA), then warmed Trypsin-EDTA (Sigma 59428C, ST Louis Missouri, USA) was added in 0.04 ml/cm^2 and the cells were kept in the incubator tell getting the rounded shape, then the cells were collected to 50 ml flask (Starstedt 6255901, Nümbrecht, Germany) containing prewarmed proliferation medium to block the trypsin effect. Cells were then centrifuged, the pellet was resuspended and cells were counted using a hemocytometer (THOMA 0.0025mm2) to be plated as mentioned before.

3.2.1.2. Differentiation:

Cells were plated in proliferating medium and kept until they were confluent with changing the medium every other day. When confluent, cells were kept for 48 hours, then induced for differentiation using the MDI induction medium (methylisobutylxanthine, dexamethasone, insulin). MDI induction medium consisted of the same formula of the proliferation medium with switching to Fetal Bovine Serum FBS(Sigma F7524, ST Louis Missouri, USA) instead of calf bovine serum, in addition to adding the following compounds:

1) 3-isobutyl-1-methylxanthine/IBMX 0.5 mM(Sigma I5879, ST Louis Missouri, USA). The stock was diluted in Dimethyl Sulfoxide DMSO.

2) Dexametasone 1 µM (Sigma D1756 , ST Louis Missouri, USA). The stock was diluted in DMSO.

3) Insulin (Sigma I6634, ST Louis Missouri, USA) diluted in filtered 20mM Acetic Acid. Different final concentrations of the insulin were used to optimize the differentiation protocol (1;2.5; 5; 10 µg/ml). The concentration of 10 µg/ml was selected to proceed with.

Cells were kept in MDI induction medium for 48 h, then moved to the maintenance medium which is IBMX/ Dexametasoe free medium for 8 days changing the medium every other day. Images were taken during the differentiation to monitor the lipid droplets in the cells.

3.2.2. Human Cells:

Human White Preadipocytes HWP were purchased from PromoCell (C-12732, Heidelberg Germany). These cells were collected from visceral adipose tissue origin. Upon plating, they were in passage 2 (P2).

3.2.2.1. Proliferation:

Cells were thawed and plated in filtered flasks 5000 cells/cm2 using Human Preadipocyte Growth Medium (Sigma 811-500, ST Louis Missouri, USA) 0.2ml/cm2. The medium was changed every other day until cells reached 75-80% confluence, then they were sub-cultured. For the trypsinization, the medium was discarded and cells were washed with PBS, then treated by Trypsin-EDTA 1x solution (Sigma T3924, ST Louis Missouri, USA). 5 ml of Trypsin-EDTA solution were added to the T75 flask and directly 4 ml were discarded, and the flask was kept at room temperature for 2-3 minutes until cells were round, then 5 ml of Trypsin Inhibitor (Sigma T6414, ST Louis Missouri, USA) were added and the cells were collected to 50 ml falcon, and centrifuged at 220g for 5 min to pellet the cells. The supernatant was not completely removed to assure not disrupting the cells. Cells were resuspended in an appropriate volume and plated again in 5000 cells/cm2 for normal proliferation, or plated in 25000 cells/cm2 for differentiation.

3.2.2.2. Differentiation:

Cells were plated in multi-well plates in 25000 cells/cm2 using Preadipocyte Growth Medium (1 ml for one well of 24 wells plate). When the cells arrived at more than 90% confluence, the medium was changed to a differentiation medium prepared from the Bulletkit (Lonza PT-8002, Walkersville, Maryland, USA). The kit included both PGMTM-2 Basal Medium (PT-8202) and PGMTM-2 SingleQuotsTM supplements (Lonza PT-9502, Walkersville, Maryland, USA) required for the growth and differentiation into mature adipocytes.

The growth medium was prepared by mixing the entire contents of the FBS, L-glutamine, GA-1000 SingleQuots™ to the bottle of Preadipocyte Basal Medium-2 (The final concentrations of the supplements will be 10%, 2 mM, 30 μg/ml, and 15 ng/ml respectively). The entire contents of the SingleQuots™ of human insulin, dexamethasone, indomethacin, and isobutyl-methylxanthine were dissolved in 100 ml of the Growth Medium and kept in 4 °C as 2x stock for the differentiation medium. The final differentiation medium was prepared by mixing one volume of the stock 2x with the same volume of the growth medium.

The cells were differentiated for 14 days then were processed for further experiments.

Acylated ghrelin treatment was performed in different conditions. In starvation conditions AG was added in different doses for 24h using the Human Adipocytes Starvation medium (Sigma 811S250, ST Louis Missouri, USA). AG was also tested in different doses in nutrient availability conditions using the differentiation medium for 5 days.

3.2.3. siRNA transfection protocol:

3.2.3.1. 3T3L1 Adipocytes:

siRNA transfection was performed on the terminally differentiated adipocytes. The siRNAs used in the work are MISSION esiRNA from Sigma, which are a heterogeneous mixture of siRNA that all target the same mRNA sequence, thus assuring high-specific and effective gene silencing. Mission esiRNA murine OGT (Sigma EMU006701, ST Louis Missouri, USA) , Mission esiRNA murine GAPDH (Sigma EMU156001, ST Louis Missouri, USA) and Universal Negative Control (Sigma SIC001, ST Louis Missouri, USA) were used in the experiments. It was performed in two methods, forward transfection and in suspension transfection. However, the protein yields in the latter method were not high so the rest of the experiments, with ghrelin treatment, were performed in the forward transfection method.

3.2.3.1.1. In suspension transfection:

Different concentrations of siRNAs were used with RNAimax lipofectamine (ThermoFischer 13778150, Waltham, Massachusetts, United States). Both RNAimax and siRNAs were diluted in serum/penstrep-free medium separately, then incubated together for 15 minutes.

Cells were differentiated in T75 flasks. Cells on day10 of the differentiation were trypsinized. Centrifugation of differentiated cells was done for 2min at 80g to avoid the disruption of the lipid droplets in the cells. Cells were then resuspended in serum/penstrep-free medium (Sigma MegaCell m3942, ST Louis Missouri, USA). An appropriate number of cells was mixed with the siRNA/RNAimax and plated (30000 differentiated cells/cm2). Six hours after plating, the medium containing the siRNA/RNAimax was removed and the maintenance medium was added again. RNA was extracted at 48, 96 h after the transfection, and protein was extracted 120 h after the transfection.

3.2.3.1.2. Forward transfection and Acylated Ghrelin Treatment:

Cells were plated and differentiated in multi-well plates (Sarstedt, 833920, 833921, 832922 Nümbrecht, Germany). On day 10 of the differentiation, the maintenance medium was discarded and serum/penstrep-free medium was added in a volume 40% of the maintenance medium (for one well of 24 well plate with usual 500µl volume, 200 µl were added). siRNA and RNAimax were diluted in serum/penstrep-free medium (Sigma m3942, ST Louis Missouri, USA) and mixed in a final volume of 10% of the maintenance medium (for one well of 24 well plate, 50 µl were added), incubated for 15 min then added to the cells to reach 50% of the maintenance medium volume (for one well of 24 well plate, 250 µl were added). Six hours after, the same volume was added of medium (MegaCell

Sigma m3942) containing FBS 20% and Glutamin 4mM, so the final volume of the wells was the same volume of the maintenance medium. The next day, the medium was changed to the reduced FBS medium (Megacell, FBS 3%, Glutamin 2mM, PenStrep) for 24 h, then the acylated ghrelin (Bubendorf, Switzerland) was added for 24h either in the same medium (added fresh) for the partial starvation treatment, or without FBS for the complete serum starvation treatment.

3.2.3.2. siRNA transfection for the human differentiated adipocytes and AG treatment:

Human siRNAs for OGT, GAPDH were purchased from sigma (mission esiRNA EHU082301, EHU146741 respectively, ST Louis Missouri, USA), and the negative siRNA control was the same used in 3T3L1 experiments. The transfection reagent RNAimax, used for murine cells, was used as well for the human cells.

On day 14 of the differentiation, cells were siRNA-transfected to knock down the expression of the OGT in the cells using the forward strategy. Differentiation medium was removed and serum-free medium (Megacell Sigma 3942) was added for 1 h. 100 nM of the siRNA were mixed with the RNAimax in serum/antibiotics free medium then added to the cells for 6 h, then medium with FBS20% was added for 24 h, then cells were starved by human starvation medium (Sigma 811S250, ST Louis Missouri, USA) for 24h before adding the AG in the same fresh starvation medium (Sigma 811S250, ST Louis Missouri, USA) for 24 h.

Protein extraction and RNA extraction were performed as in the 3T3L1 adipocytes.

3.2.4. Gene expression quantification:

3.2.4.1. RNA extraction:

RNA was extracted using TRIgent method. TRIgent solution was got from MRC (TR 118, Ohio, USA). Cells were homogenized in an appropriate volume of TRIgent solution (200 µl for one well of 24 wells plate) at cold 4 °C. Cellular homogenates were then centrifuged at 12000 g for 10 minutes at 4 °C. The supernatant was collected to another tube and kept to stand at room temperature for 5 min, then an appropriate volume of chloroform was added to the tube (40 µl chloroform for 200 µl TRIgent) and shaken vigorously for 15 Sec then kept to stand at room temperature for 15 minutes, then centrifuged at 12000g for 15 min at 4 °C. The colorless upper aqueous phase containing the RNA was collected to a new tube and mixed with an appropriate volume of Isopropanol 100% (the half amount of TRIgent used volume) and kept to stand at room temperature for 10 minutes. Tubes were then centrifuged at 12000 g for 10 min at 4 °C to precipitate the RNA. The supernatant was removed and the RNA pellet was washed vigorously by ethanol 75% (the same volume of TRIgent) then centrifuged at 7500 g for 5 min at 4 °C. Ethanol supernatant was then discarded and RNA pellet

was left to dry under the hood at room temperature, then dissolved in Nuclease free water (Thermo Fischer Scientific AM9920, Waltham, Massachusetts, United States) at 55 °C for 15 min.
RNA concentrations were then measured by the microspectrophotometer Nanodrop (ND1000).

3.2.4.2. Complementary DNA (cDNA) Synthesis:

cDNA or reverse transcription reaction was performed using Taqman Reverse Transcription (Applied Biosystem by Thermo Fischer Scientific N8080234, Waltham, Massachusetts, United States). Equal amounts diluted to the same volume were prepared from the RNA samples and senatured at 65 °C for 5 min. The cDNA reaction was performed using the thermocycler machine: MyCycler Thermal from Biorad. 0.5 µg RNA was reverse-transcribed using 2.5 µM Random Hexamer, 0.5 mM each dNTP and 25 U MultiScribe™ Reverse Transcriptase.

Thermal Cycle program:
25 °C for 10 min
42 °C for 60 min
70 °C for 10 min
4 °C indefinite time

3.2.4.3. Quantitative Real-Time PCR (qPCR)

Taqman method was used in the quantitative PCR. Sets of primers and probes were designed manually using the references sequences stored in the National Centre for Biotechnology Information (NCBI) of the genes of interest, then ordered from Sigma-Aldrich. The sets were checked for their melting temperature and other thermodynamic features using the Idtdna online tool. The cDNA was amplified using 300 nM forward and reverse primers, and a 240 nM dual-labeled probe in Universal Taqman Master Mix (4404437 Applied Biosystem by Thermo Fischer Scientific, Waltham, Massachusetts, United States)

Relative quantity curve was prepared by pooled samples at 1; 1:5; 1:10; 1:20 dilutions.
The qPCR reaction was performed using ABI PRISM 7900HT, and the results were interpolated to the standard curve of dilutions.

Sequences of the primers and probes used in the study:

Human & Murine 18S: (RefSeq: NR_003278.3)

Sense Primer: 5’ CGGCTACCACATCCAAGGAA 3’

Antisense Primer: 5’ GCTGGAATTACCGCGGCT 3’
Antisense dual-labeled probe: 5’ TET- TGCTGGCACCAGACTTGCCCTC- TAMRA 3’

Murine GAPDH: (RefSeq: NM_008084.3)

Sense Primer: 5’ TGTGTCCGTCGTGGATCTGA 3’
Antisense Primer: 5’ CCTGCTTCACCACCTTCTTGA 3’
Sense Dual-Labeled Probe: 5’ TET-CCGCCTGGAGAAACCTGCCAAGTATG-TAMRA 3’

Human GAPDH: (RefSeq: NM_002046.7)
Sense Primer: 5’ GACAGTCAGCCGCATCTTC 3’
Antisense Primer: 5’ ACTCCGACCTTCACCTTCC 3’
Sense Dual-Labeled Probe: 5’ TET- CGCCAGCCGAGCCACATCGC- TAMRA 3’

Murine Adiponectin: (RefSeq: NM_009605.5)

Sense Primer: 5’ AAGGAGATGCAGGTCTTCTTGGT 3’
Antisense primer: 5’ ACACTGAACGCTGAGCGATACA 3’
Sense Dual-Labeled Probe: 5’ 6FAM -TGGCCCTTCAGCTCCTGTCATTCCA- TAMRA 3’

Human Adiponectin: (RefSeq:NM_004797.4)

Sense Primer: 5’ CTGGGAGCTGTTCTACTG 3’
Antisense primer: 5’ CTTGAGTCGTGGTTTCCT 3’
Antisense Dual-Labeled Probe 5’ 6FAM – TCATGACCGGGCAGAGCTAATAG- TAMRA 3’

Murine fatty acid-binding protein 4 (Fabp4): (RefSeq:NM_024406.3)

Sense Primer: 5’ CGACAGGAAGGTGAAGAG 3’
Antisense Primer: 5’ GAAGTCACGCCTTTCATAAC 3’
Anti Sense Dual-Labeled Probe: 5’ 6FAM – GACTTTCCATCCCACTTCTGCACCTG- TAMRA 3’

Human fatty acid-binding protein 4 (FABP4): (RefSeq:NM_001442.2)
Sense Primer: 5’ AGCACCATAACCTTAGATG 3’
Anti-Sense Primer: 5’ GCTCTCTCATAAACTCTC 3’
Anti-Sense Dual-Labeled Probe: 5’ 6FAM –TGACGCATTCCACCACCAGT- TAMRA 3’

Murine OGT: (RefSeq:NM_139144.4)

Sense Primer: 5’ GCCATACGAATTAGTCCTA 3’
Antisense Primer: 5’ CATCCTGCATCTCCTTTA 3’
Sense Dual-Labeled probe: 5’ 6FAM –TCCCATATTGGAATAAGCATCAGCAAA- TAMRA 3’

Human OGT: (RefSeq:NM_181672.3)

Sense primer: 5’ TGGTGACTATGCCAGGAGAG 3’
Antisense Primer: 5’ TTCCAGACTTTGCCACGAAC 3’
Antisense dual-labeled probe: 5’ 6FAM –TGCAGCATCCCAGCTCACTTGC- TAMRA 3’

3.2.5. Oil Red O Staining:

Oil Red O powder (Sigma O0625, ST Louis Missouri, USA) was dissolved in isopropanol 100% in this ratio: 60 mg in 20 ml). The solution was then filtered using Whiteman paper then diluted in mqH2O in the ratio (3vol Oil red O: 2 vol mqH2O) to get the working Oil Red O solution just before being used.

This method was used to stain the lipid droplets within the adipocytes with the red stain as referenced in (Krahmer et al., 2013).

Cells were fixed in 10% neutral formalin (Sigma HT501128, ST Louis Missouri, USA) for 1 hour, then washed by water, then isopropanol 60% was added to the cells for 5 min, then Oil red O working solution was added for 20 minutes with gentle shaking. After the staining, extensive washing with water was applied to remove the extra diet. Multichmper slides (Sigma C6932, ST Louis Missouri, USA) were used for lipid staining in human adipocytes’ experiments. The volumes used for each step were the same volumes used for the cell culture medium.

To measure the Oil Red O staining, isopropanol 100%, which extracts the dye, was added to the cells in half of the volume used for the staining, then this reading was applied in 96 wells plate with the spectrophotometer at 485 nm.

3.3. Protein Analysis:

3.3.1. Protein extraction and measurement of the protein concentration:

Cells were washed briefly with cold PBS (4 °C) and treated with cold Cell Extraction Buffer (FNN 0011, Invitrogen by Thermo Fischer Scientific, Waltham, Massachusetts, United States) added with Phenylmethilsulfonyl fluoride (PMSF 1M) and 4.8% of Protease Inhibitor cocktail (P8340, Sigma-Aldrich, St. Louis, MO, USA), then moved to clean 1.5 ml tubes. Three cycles of brief spin/vortex were applied, followed by ultrasonic homogenization in wet-bath (Branson 3200) at room temperature for 10 min. Homogenates were then kept on ice for 15 min then centrifuged at 13000 RPM at 4 °C (Thermo Scientific SL16R) for 10 min. In the case of differentiated adipocytes, lipids were floating on the top of the tube and cellular organelles and components were precipitated as a

pellet at the bottom of the tube. The supernatant was collected and aliquoted into several autoclaved 1.5 ml tubes and kept at -80 °C.

For the animal adipose tissue samples, pieces were prepared from the visceral white adipose tissue and weighed, then treated with the same cell extraction buffer 10µl/mg, and hand-homogenated for 10 min in ice, rested in ice for 20 min, then centrifuged at the 13000 RPM for 15 min at 4 °C. The lipids were compacted to the top of the tube, while the cellular organelles precipitated at the bottom of the tube, and the clear supernatant was collected to new autoclaved tubes and kept at -80 °C.

Protein concentration was measured using the colorimetric detection method based on bicinchoninic acid (BCA) (Smith et al., 1985).

3.3.2. xMAP Technology:

The word xMAP is derived from Multi-Analyte Profiling for x unknown sample. From the name, it is a multiplex technology applicable for high-throughput detection of different analytes in one sample. The technology can be used for multiplex assays for proteins and nucleic acids. In our study, we used xMAP only for protein measurements. xMAP is an immuno-based technology where the analytes in the sample bind to the antibodies that cover colored magnetic beads. Each bead is coated with a specific antibody to identify the analyte. All the beads are excited by laser light at 635 nm but the fluorescent emission differs specifically allowing accurate identifying of the bead/analyte. To quantify the analyte, a reporter is added to target the molecule of interest that is attached to the antibodies on the bead, then another laser is used to excite the reporter at 532 nm (Fulton et al., 1997).

3.3.3. Western Blot:

Equal amounts of protein samples were run in Sodium Dodecyl Sulfate Polyacrylamide Gel Electrophoresis (SDS PAGE). Protein samples were diluted in PBS to reach the same volume and mixed with 6x Laemmli Loading Buffer LB (TrisBase 480 mM pH 8.8, SDS 7.2%, Glycerol 30%, Bromophenol Blue 0.02%, β-mercaptoethanol 20%) in a ratio (5 vol protein: 1 vol LB) and heated at 95 °C for 5 min. Denatured protein samples were then loaded in stacking gel (Tris 0,15 mM pH 6.8, SDS 0,05%, acrylamide 3.6%, Ammonium Persulfate 0,1%, TEMED 0,1%) to run for 15 min at 80 Volt, 10 mA. Once bands were compacted they passed to Running gel (Tris 0,4 M pH 8,8, SDS 0,05%, acrylamide 12%, Ammonium Persulfate 0,05% TEMED 0,01%) to run at 100 Volt, 15mA for 120 min

in the Running Buffer (TrisBase 0.25M, Glycine 1.92M, SDS 0.1%). A colored ladder was used to detect the molecular weight of the protein bands (ColorBurst C1992 Sigma). After the end of the run, gels were soaked in transfer buffer (TrisBase 0.25M, Glycine 1.92M, Methanol 10%) for 5 min, then placed on wet 0.2 μm nitrocellulose membrane (Amersham 10600080) with plot paper (Biorad) in a sandwich form in a semi-dry transfer system (Biorad). Transfer run was performed in a constant voltage of 17 V for 90 min. After the transfer was completed, The gel was processed for coomassie blue staining; the gel was first soaked in fixing solution (50% methanol, 10 % Glacial Acetic Acid) overnight, then stained by staining solution (0.1% Coomassie Brilliant Blue R-250, 50% methanol, and 10% glacial acetic acid) for 20 min, then destained by destaining buffer (40% methanol and 10% glacial acetic acid) until the background of the gel was fully destained, then stored in storing solution (5% glacial acetic acid) and imaged by densitometer (Biorad GS 700). Images were analyzed using Quantity One image analysis software (Bio-Rad).

The membrane was stained with Ponceau S (Sigma P7170) to check the protein bands' separation and ensure equal amounts of the protein. The stained membrane was imaged and documented. Ponceau S was then washed by PBS and the membrane was incubated in Blocking Buffer (PBS, powder Milk 5%, Tween 0.05%) for 60 min to block the non-specific protein binding sites. Membranes were then probed overnight at 4 °C with the primary antibodies that were diluted in the blocking buffer to the manufacturer's recommended usage dilution. Membranes were then washed extensively using washing buffer (PBS, Tween 0.05%) and probed with the secondary horseradish peroxidase (HRP)-linked antibodies diluted in the blocking buffer to the manufacturer recommended usage dilution. A list of the antibodies used in the study is in table (). The membrane was again washed extensively by washing buffer, then the detection of the protein bands was enhanced by incubating the membrane with the Electrochemical Luminescence solution (LumiGLO Reagent A 95538S, Peroxide Reagent B 39864S, Cell Signalling Beverly, MA, USA) and exposing the membrane to X-ray film in dark, followed by developing the protein signal by soaking the exposed film in developing solution then in fixing solution. The films with the protein bands were imaged by the densitometer (Biorad GS 700). Images were analyzed using Quantity One image analysis software (Bio-Rad).

	Antibody name	**Code**	**Company**
Insulin Signaling	Phospho-AKT (Ser473)	9271	cell signaling
	Phospho-GSK-3β (Ser9)	9336	cell signaling
	AKT	9272	cell signaling

	GSK-3β	9315	cell signaling
	IRS-1	2382	cell signaling
O-GlcNacylation	OGT	HPA030751	Sigma
Adipocytes Differentiation	FABP4	SAB4300636	Sigma
	Adiponectin	2789	cell signaling
Inflammation	TNFα	sc-52746	Santa-Cruz Biotechnology, Dallas, USA
Housekeeping	Beta-actin	A3853	Sigma
	GAPDH	2118	cell signaling
Secondary Antibodies	Anti-Rabbit IgG HPR-linked	7074	cell signaling
	Anti-Mouse IgG HPR-linked	NA931	GE Healthcare Life Sciences, Little Chalfont, USA

Table (1). List of the antibodies used in the study.

3.3.4. Enzyme-Linked Immunosorbent *Assay* (ELISA):

Commercial ELISA kits were used to quantify AKT_{ser473} total/phosphor (85-86046, Invitrogen**);** and $GSK3\beta_{ser21}$ total/phospho (85-86173, Invitrogen) in the insulin signaling pathway.

Following the manufacturer's instructions, 50 µl Adipocytes protein extracts were added to the pre-treated 96 well plate, then 50 µl of the antibody cocktail were added to the wells and incubated for 1 h with moderate shaking 300 rpm. Wells were then washed by the washing buffer provided with the kit, then 100 µl of the detection reagent were added to each test well and incubated for 25 min. The reaction was stopped by adding 100 µl of the stop solution to each well then the plate was read using the spectrophotometer at 450 nm.

3.4. Measuring Redox State: Glutathione:

Acting as a free radical scavenger and inhibitor of lipid peroxidation, GSH is considered a major antioxidant factor in the cell, besides its role in the detoxification of hydrogen peroxide by various glutathione peroxidases. GSH is present in the cell in two forms, reduced GSH and oxidized GSSG, thus the ratio GSH/GSSG is an important indicator for the redox state in the cell and the cellular health. In normal physiological conditions, the reduced form GSH represents around 98% of the

total amount of glutathione. GSH is the most abundant antioxidant in aerobic cells and its concentrations range from micromolar in body fluids to millimolar in tissue.

Rahman et al (Rahman et al., 2006) reported the method for the quantification of glutathione, in both forms. Oxidized glutathione GSSH can give two molecules of reduced GSH in reducing conditions as NADPH with the presence of glutathione reductase (GR). This reaction can be measured by the spectrophotometer by adding the 5,5'-dithiol-bis(2-nitrobenzoic acid) (DTNB) which is converted in the same conditions to the TNB that can be measured at 412 nm. This method can estimate the total glutathione content. GSSH content can be measured by adding 2-vinylpyridine which binds to the reduced glutathione, so only GSSH will contribute to the reaction.

Practically, adipose tissue samples were hand-homogenized for 10 min in 5% metaphosphoric acid (weight/volume; 4µl of solution every mg of tissue) and then centrifuged at 12000g at 4°C for 15 min. The supernatant was collected and frozen at -80 for further analysis. Six volumes of reaction Buffer (Glutathione Reductase 3.33 U/ml Sigma; DTNB 0.84 mM Sigma; KPE Buffer pH=7.5: EDTA 5 mM, KH2PO4 81.5 mM) was prepared and incubated with one volume of the sample in 96 wells plate in dark for 30 Sec, then β-NADPH was added in solution with KPE (β-NADPH 0.8 mM in KPE buffer 0.1 M) and readings were taken every 60 Sec for 15 min. The total amount of glutathione can be measured by interpretation from the standard solutions that have known concentrations of the glutathione content. GSSH was measured in the same method by just incubating the samples for 10 minutes with 4-vinilpiridine diluted 1:10 in KPE Buffer. The reduced form of glutathione was calculated by subtracting the GSSH value from the total glutathione value.

3.5. Measuring Mitochondrial Function:

Mitochondrial function was estimated at the levels of mitochondrial enzymes Citrate Synthase (CS) and Cytochrome C Oxidase (COX). Both were measured according to (Barazzoni et al., 2005).

3.5.1. Mitochondrial Enzymatic Extraction:

Since the protein extraction method includes using detergents present in the buffer it cannot be used to isolate intact mitochondria. Enzymatic extraction was performed as the following: adipose tissue samples were hand homogenized in PBS for 10 min in ice, then the homogenates were transferred into 1.5 ml tubes and centrifuged at 600g for 10 minutes at +4°C. Lipid was floating on the top of the supernatant while cellular organelles and components were precipitated at the bottom. The supernatant was collected and kept at -80 C.

3.5.2. Citrate Synthase Assay:

Citrate synthase is the first enzyme of the tricarboxylic acid (TCA) cycle. It catalyzes the reaction of 2 carbon acetyl CoA with 4 carbon oxaloacetate to form the 6 carbon citrate.

Citrate Synthase (CS) activity was measured using the colorimetric spectroscopic method. CS catalyzes the production of the citrate from the reaction between the oxaloacetate and acetyl-CoA, which releases as well sulphuryl acetyl-CoA (CoA-SH) that can by its sulphuryl group produce yellow product thiobis 2-nitrobenzoic acid (TNB) in the presence of 5,5'-Dithiobis 2- nitrobenzoic acid (DTNB). For the measurement, enzymatic adipose tissue extracts were added in a microplate well and mixed with an Assay Buffer composed of: TrisBase Buffer 200 mM pH 8.2, Acetyl CoA 0.25 mM, DTNB 0.025 mM, Triton solution X-100 10%. Oxaloacetate solution (Oxaloacetate 7.6 mM plus TrisBase Buffer 200 mM pH 8.2) was added before reading the reaction at 412 nm, 30 C, at intervals of 10 sec for 15 min. The absorbance values during the different time points generated a line whose slope represented the CS activity (figure 17).

3.5.3. Cytochrome C Oxidase:

Cytochrome c oxidase is located on the inner mitochondrial membrane dividing the mitochondrial matrix from the intermembrane space and has traditionally been used as a marker for mitochondrial function. Cytochrome c oxidase provides energy for the cell by coupling electron transport through the cytochrome chain with the process of oxidative phosphorylation (Michel et al., 1998).

COX activity was also measured using the colorimetric spectroscopic method. COX acts as a reduction reagent that reduces its substrate Cytochrome C from ferrous to ferric state, and this reaction can be measured by the spectrophotometer at 550 nm. Enzymatic adipose tissue extracts were added to a microplate well and mixed with the assay buffer (BSA 0.65 mM, $MgCl_2$ 10.3 mM, KPI Buffer 50 mM, and Cytochrome C 0.05 mM). The plate was read at 550 nm, 30 C, at intervals of 10 sec for 10 min. As CS measurement, the absorbance values during the different time points generated a line whose slope represented the COX activity (figure 18).

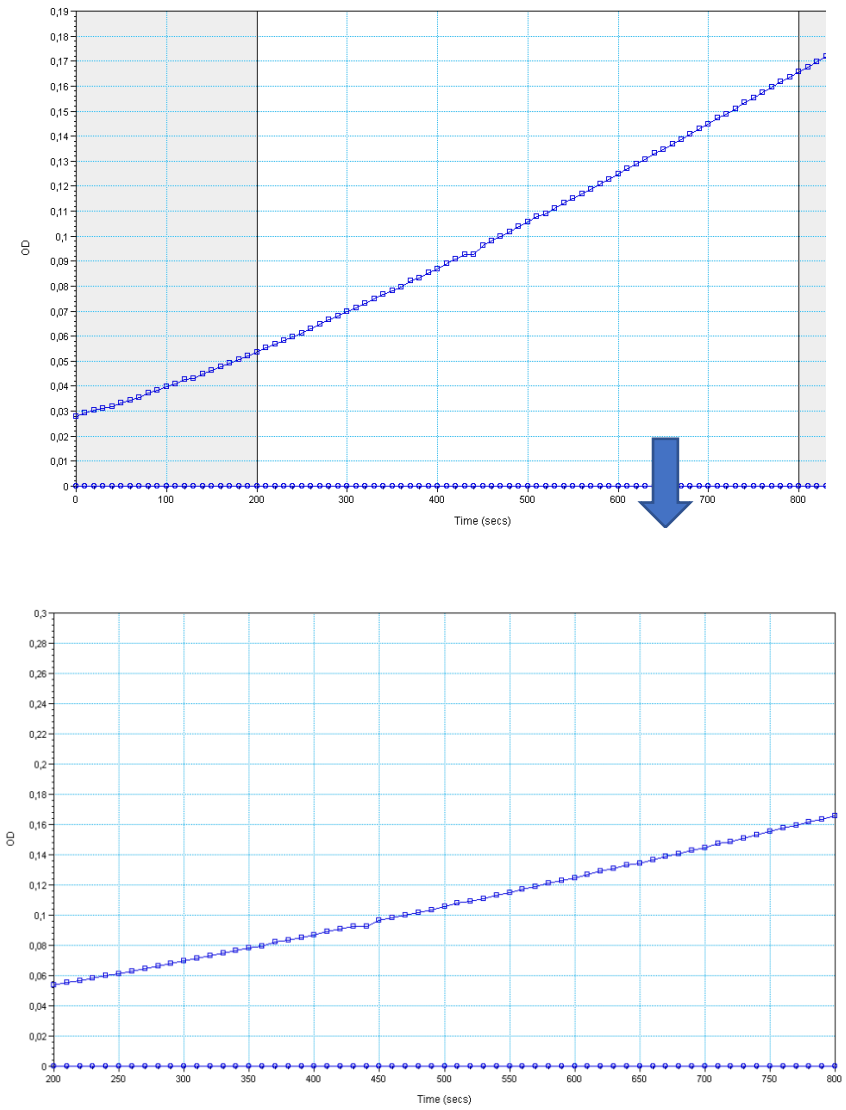

Figure (17): Calculating the slope of the generated line between X (Time) and Y(absorbance) to calculate CS content in the sample . An area with more linearity was selected to calculate the slope.

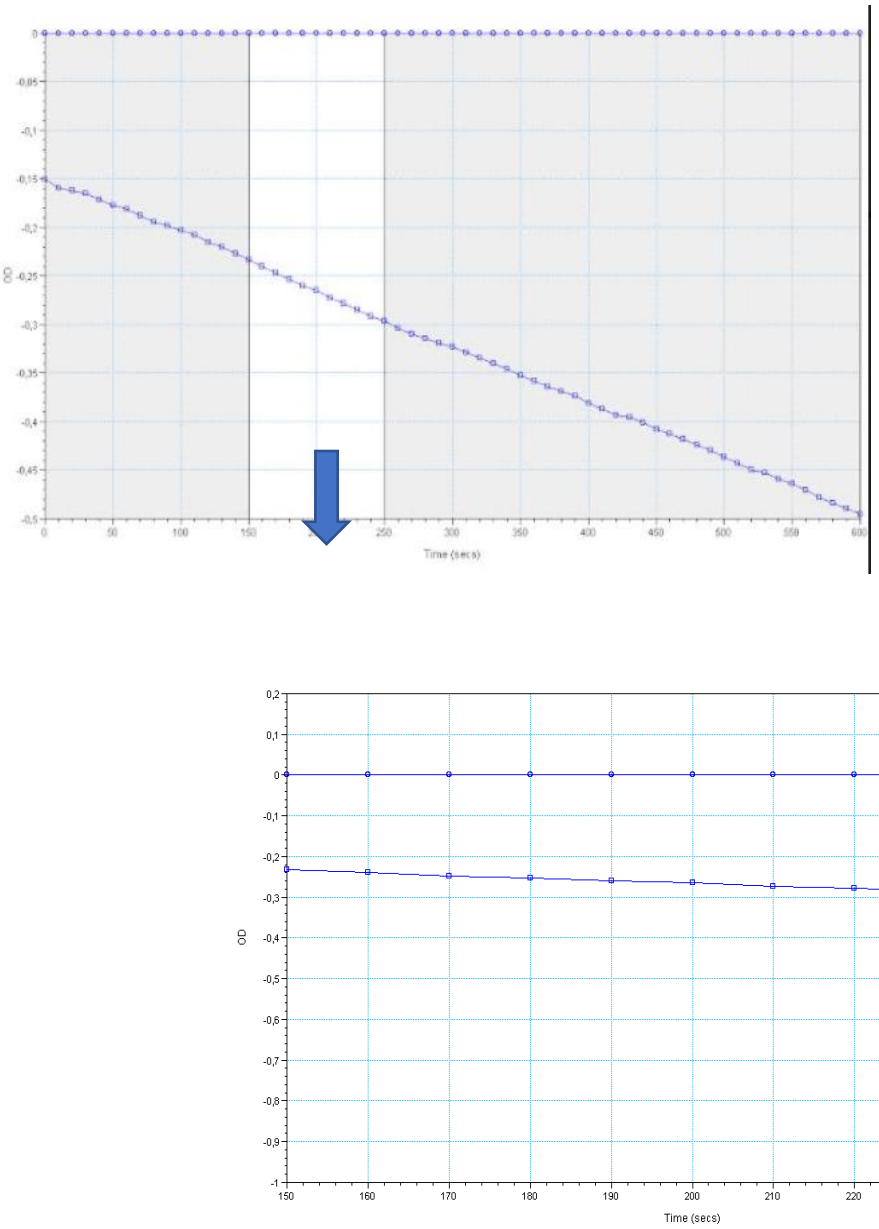

Figure (18): Calculating the slope for the generated line between X (Time) and Y(absorbance). An area with more linearity was selected to calculate the slope which will be used to calculate the COX content in the sample.

3.6. Statistical Analysis:

Comparisons between two groups was performed by Student T-test analysis for independent or dependent samples as appropriate. One-way ANOVA was used in case of multiple comparisons followed by appropriate post hoc tests. Bonferroni correction was applied for multiple comparisons. $P<0.05$ was considered significant. GraphPad software was used to generate the graphs presented in the study. Results were represented by the average and the standard error. Analyses in this study were performed using SPSS v.17 software (SPSS Inc., Chicago, IL).

4. Results:

4.1. Results from animal studies:

4.1.1. Exogenous Acylated Ghrelin Administration to Healthy Rats:

4.1.1.1. Animal Phenotype:

No statistical differences were observed among groups in cumulative food intake or body weight, suggesting that acylated ghrelin treatment (AGT) did not modify caloric intake and body weight, while the AG group had significantly higher glucose levels in agreement with other findings reported higher gluconeogenesis upon acylated ghrelin treatment (Barazzoni et al., 2007a) and higher glucagon secretion from beta-pancreatic cells (Chuang et al., 2011).

	Body weight (g)	**Body weight gain** (g)	**Caloric intake** (kcal/kg/day)	**Blood glucose** (mg/dL)
Ctrl	**319.6**±3.6	**14.0**±1.4	**73.5**±2.2	**118.6**±6.0
AGT	**320.8**±8.8	**16.1**±2.3	**72.9**±4.7	**133.8**±3.5 *

Table (2) Animal Charectiristics in the study: Exogenous Acylated Ghrelin Administration to Healthy Rats.
** P<0.05*

4.1.1.2. AG lowers the mitochondrial function in the white adipose tissue of healthy rats:

Citrate Synthase CS and Cytochrome Oxidase COX were analyzed as markers for the mitochondrial function, and AG was found to lower significantly the mitochondrial levels of these two enzymes.

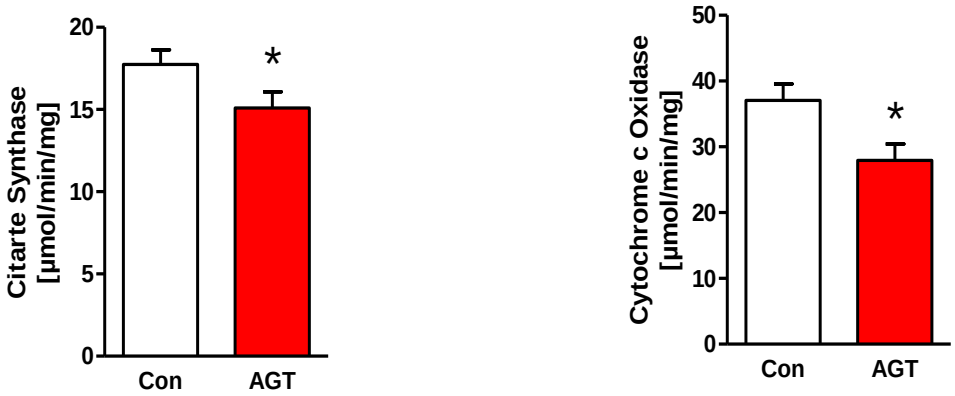

Figure (19) Mitochondrial function in adipose tissue of healthy rats is lowered by AG treatment. Right: Citrate Synthase, Left: Cytochrome c Oxidase.

4.1.1.3. AG treatment does not affect the cytokine profile in the white adipose tissue of healthy rats:

IL-1β, TNFα, IL-10 cytokines levels were measured using xMAP technology, and no differences were observed among the groups of the study.

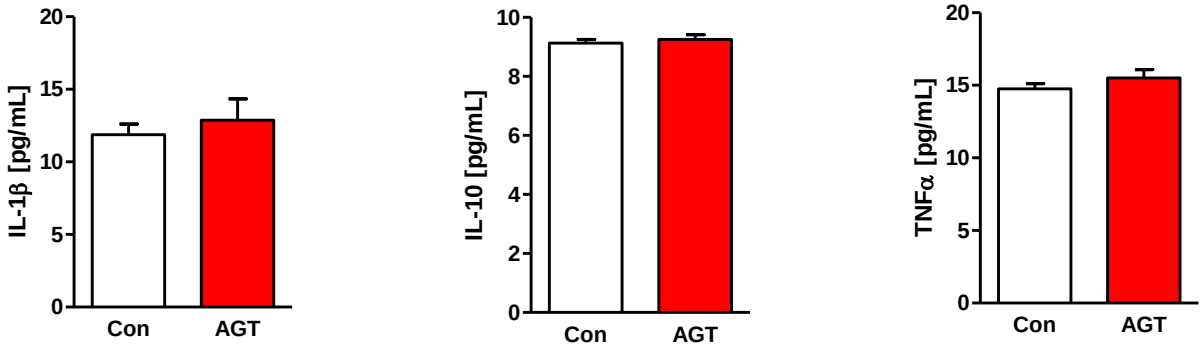

Figure (20) Cytokine Profile in adipose tissue of healthy rats treated and untreated by AG. Right:IL-1β, Middle: IL-10, Left: TNFα.

4.1.1.4. AG treatment does not affect the redox state in the white adipose tissue of healthy rats:

Total and oxidized glutathione levels were measured in the white adipose tissue and no differences were observed among the groups of the study.

Figure (21) Redox state in adipose tissue of healthy rats treated and untreated by AG. Right:Total Glutathione, Left: Oxidized/total Glutathione.

4.1.1.5. AG treatment lowers the insulin sensitivity in the white adipose tissue of healthy rats:

Insulin signaling was tested first by checking the phosphorylation of both AKT ^{S473} and GSK-3βS9 using western blot. AG lowered the phosphorylation ratio of these two proteins (AKT^{S473} P<0.05 with a similar trend at GSKβ P=0.08).

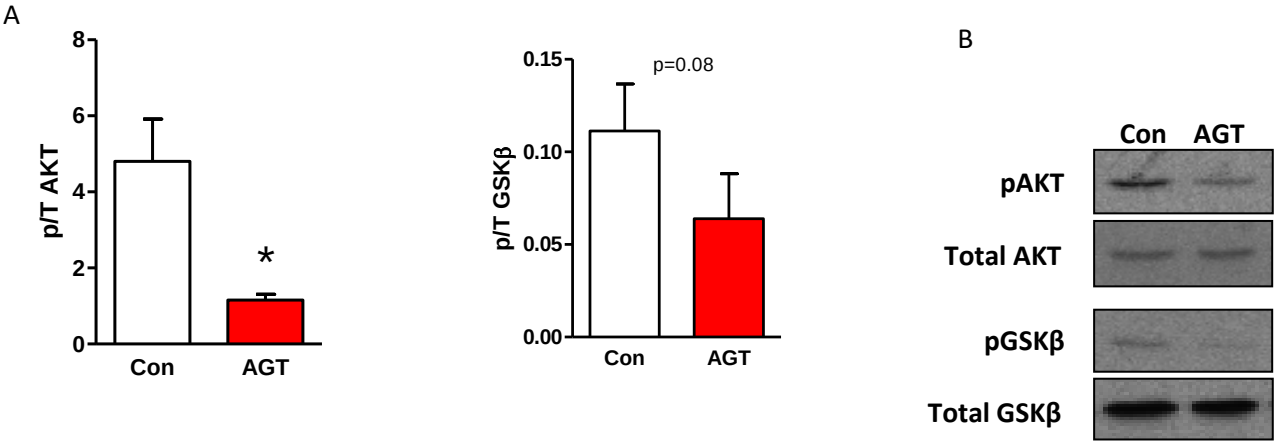

Figure (22) Insulin Sensitivity in white adipose tissue of healthy rats treated (AGT) and untreated by AG (Con). A)Densitometer Analysis: Right:p/tAKT, Left:p/t GSK3β. B) WB using protein extracts of white adipose tissue showing phosphorylated and total forms of AKT and GSK3β.

For further investigation of the insulin signaling, xMAP analysis was performed to test at the same time different targets in the insulin signaling pathway. The analysis included: Insulin Receptor (IR), Insulin Receptor Substrate 1 (IRS1 ^{S312}), AKT^{S473}, GSK-3β^{S9}, pTSC2^{S939}, mTOR^{S2448}, p70S6K^{T421}, GSK-3α^{S21}, PTEN^{380}.

As a result, AG lowered significantly the phosphorylation of insulin sensitivity at the levels of AKT^{S473}, GSK-3β^{S9}, GSK-3α^{S21} , pTSC2^{S939}, mTOR^{S2448}, with similar trend for PTEN^{380} and p70S6K^{T421}, while no effects were observed on IR. Importantly, AG treatment led to an increase in the phosphorylation of the IRS1^{S312} which exerts a negative feedback modulatory effect on the insulin signaling by inhibiting the binding of IRS1 to the IR thus disrupting the insulin signaling. This further supports the finding that AG lowers insulin sensitivity in the white adipose tissue of healthy rats.

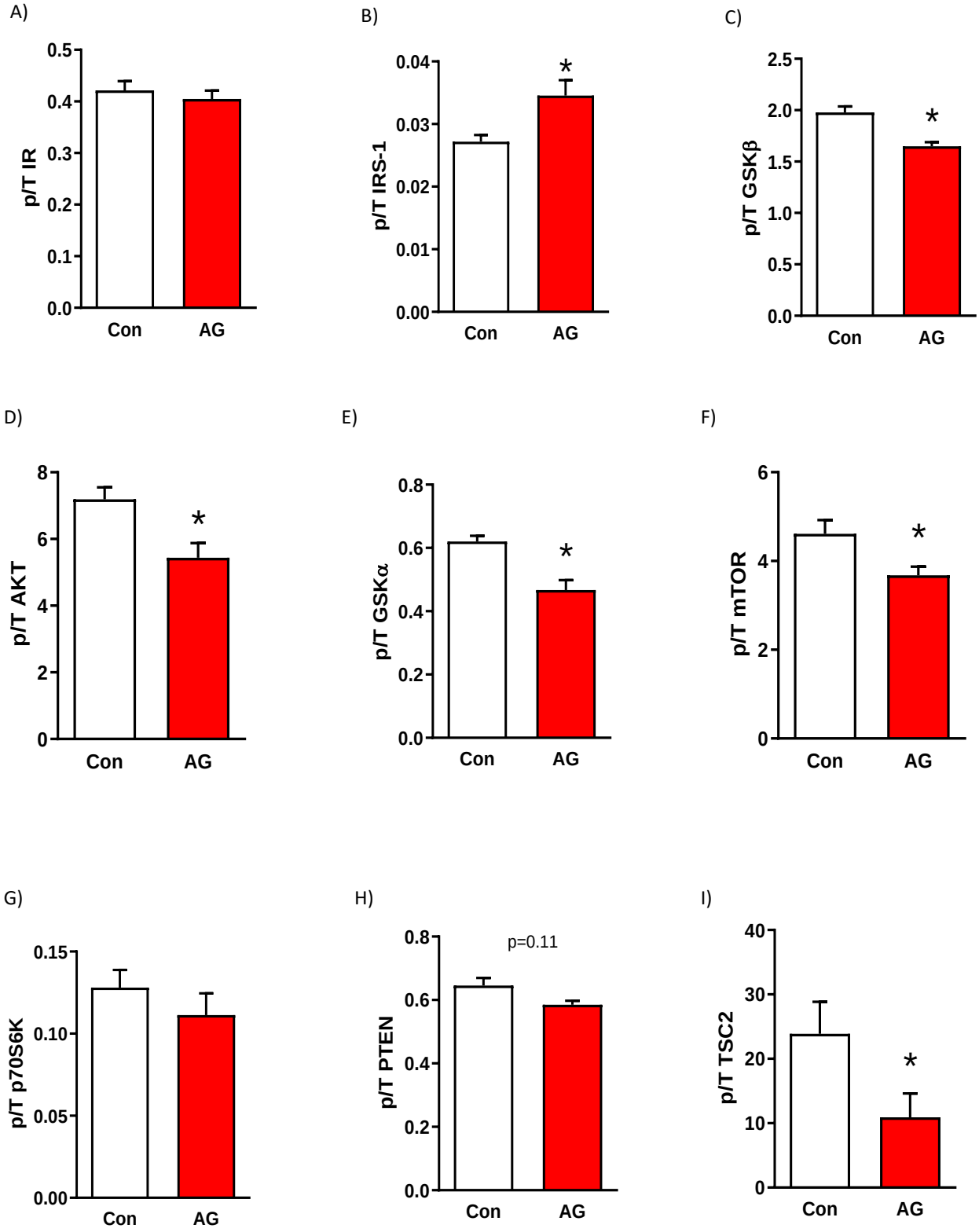

*Figure (23) Insulin Sensitivity in white adipose tissue of healthy rats treated (AG) and untreated by AG (Con) analysed by xMap technology. A) p/t IR, B) p/t IRS-1, C) p/t GSK3β, D) p/t AKT, E) p/t GSKα, F) p/t mTOR, G) p/t P70S6K, H) p/t PTEN, I) p/t TSC2. * P<0.05.*

4.1.1.6. AG upregulates the OGT levels in the white adipose tissue of healthy rats:

OGT levels were analyzed by WB. AG significantly increased the OGT levels in the white adipose tissue of healthy rats. The molecular weight of the detected band, 117 kDa, indicated the canonical nucleocytoplasmic OGT (nc OGT). Notably, no other isoforms were detected in the adipose tissue in this study.

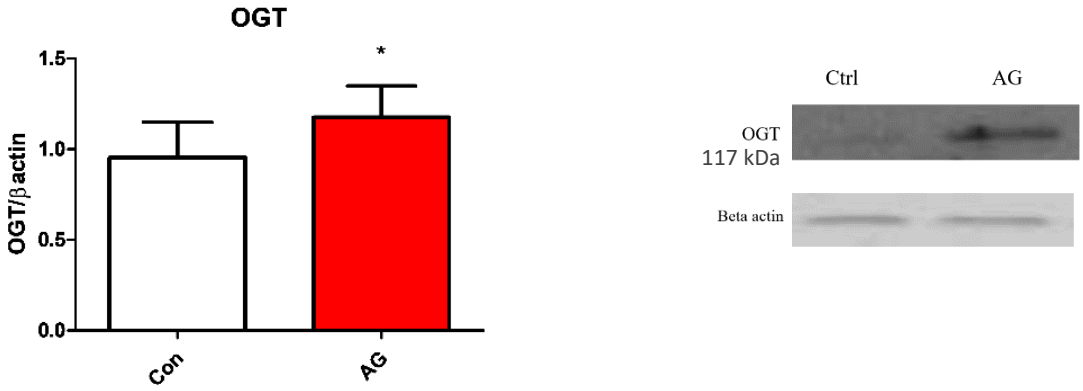

*Figure (24) OGT levels in white adipose tissue of healthy rats treated (AG) and untreated by AG (Con) analysed by WB on protein extracts of white adipose tissue. * P<0.05 vs. Con.*

4.1.1.7. AG upregulates the Short Cytosolic OGT isoform (sOGT) in the muscle tissue of healthy rats:

Interestingly, the molecular weight 75 kDa of the band, detected by WB on the muscle tissue of the healthy rats, indicated the Short form of the OGT, suggesting that OGT isoform expression and modulation by AG may be tissue specific.

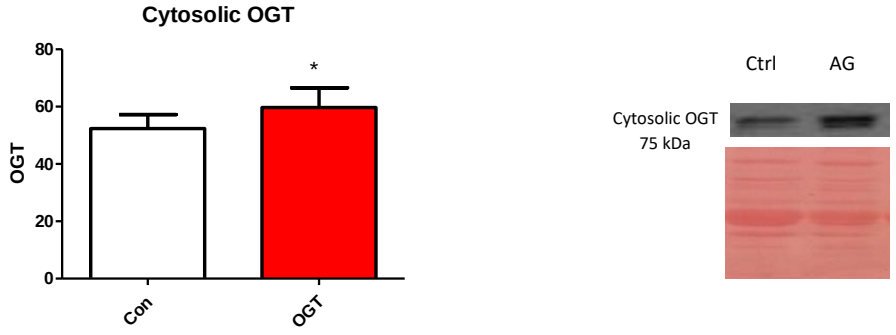

Figure (25) Cytosolic OGT levels in skeletal muscle tissue of healthy rats treated (AG) and untreated by AG (Con) analysed by WB on protein extracts of muscle tissue.

4.1.2. Exogenous Acylated Ghrelin Administration to 5/6 nephrectomized uremic rats:

4.1.2.1. Animal Phenotype:

	Body Weight		Average Caloric intake	Plasma Urea	Plasma Creatinine
	T0 g	T40 g	T0-T40 kcal/die	T40 mg/dL	T40 umol/L
Sham	362±7	454±7	63.9±1.9	18.5±3.0	16.7±1.2
Nx	368±5	421±8 *	62.0±2.7	30.3±1.0 *	26.8±1.9 *
NxAG	360±8	418±9 *	65.2±2.2	28.7±3.1 *	25,5±1.7 *

*Table (3) Animal Charectiristics in the study: Exogenous Acylated Ghrelin Administration to Uremic Rats. Measurement presented for T0 and T40. * P<0.05*

No significant differences were observed in the calorie intake. However, data shows important effects of surgically-induced CKD. Compared to the sham group, nephrectomized rats showed significantly lower body weights and elevated levels of plasma urea and plasma creatinine, which are direct consequences of CKD and developing chronic kidney disease; which is correlated with muscle wasting and reduced adipose tissue.

4.1.2.2. AG does not affect the mitochondrial function in the white adipose tissue of uremic rats:

As in the first study (4.1.1.2), CS and COX were measured as markers for mitochondrial function. Mitochondrial function was significantly lower in nephrectomized rats (Nx and NxAG) compared to the sham group, but there was no difference among the uremic rat groups.

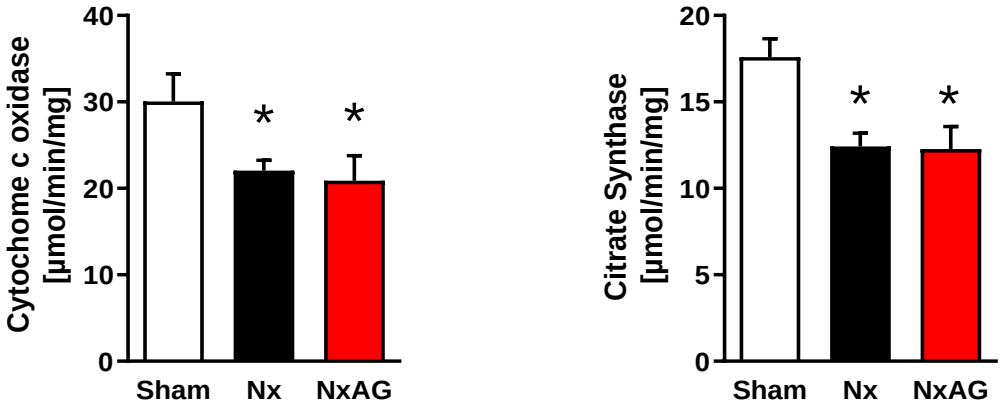

Figure (26) Mitochondrial function in the white adipose tissue of the animals groups in the study. Right: Cytochrome c Oxidase, Left: Citrate Synthase.

4.1.2.3. AG does not affect the redox state in the white adipose tissue of uremic rats:

Total and oxidized glutathione were measured as a marker of the redox state as in the first study. A higher redox state was observed in the uremic rats compared with the sham rats, which represents further validation of the model as an elevated general systemic model. However, AG did not exert a significant effect compared with Nx.

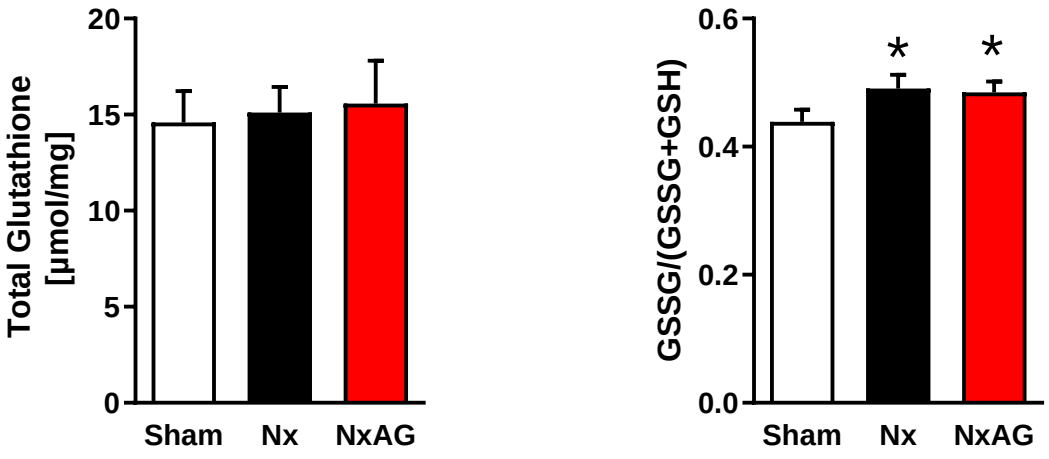

Figure (27) Redox state in adipose tissue of healthy rats treated and untreated by AG. Right: Total Glutathione, Left: Oxidized/total Glutathione.

4.1.2.4. AG lowers the TNFα in the adipose tissue of uremic rats:

TNFα levels in the groups of the study were analyzed by western blot. Uremic rats treated by AG showed significantly lower levels of TNFα compared with Nx. Compared with sham rats, Nx group showed strong significant higher levels of TNFα, while no differences were observed between the NxAG and Sham groups.

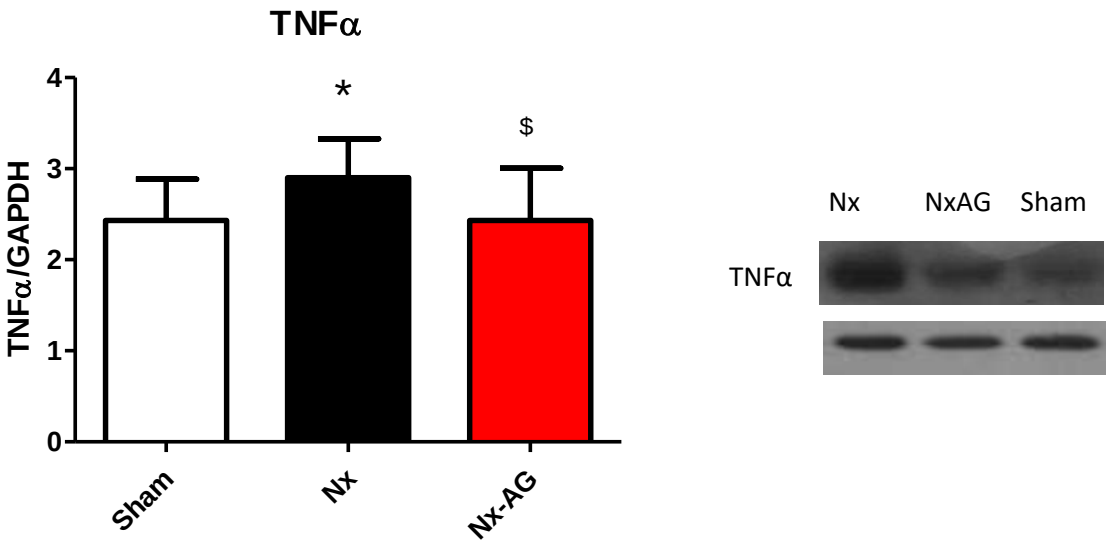

*Figure(28). TNFα levels in the white adipose tissue of the animals study by WB, densitometer analysis to the right, and blot image on the left). *P<0.05 vs. Sham, $ P<0.05 vs. Nx.*

4.1.2.5. AG lowers the insulin sensitivity in the white adipose tissue of uremic rats:

Insulin sensitivity was tested at the levels of AKT^{S473}, GSK-$3\beta^{S9}$. Uremic rats showed significantly lower insulin sensitivity compared with the sham rats. Interestingly, and in agreement with the findings from the first study AG treatment further lowered the insulin sensitivity significantly compared with Nx rats.

A)

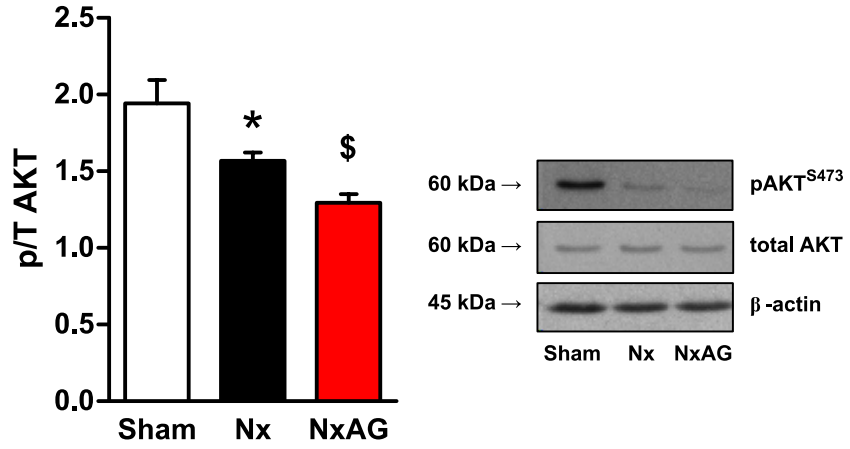

B)

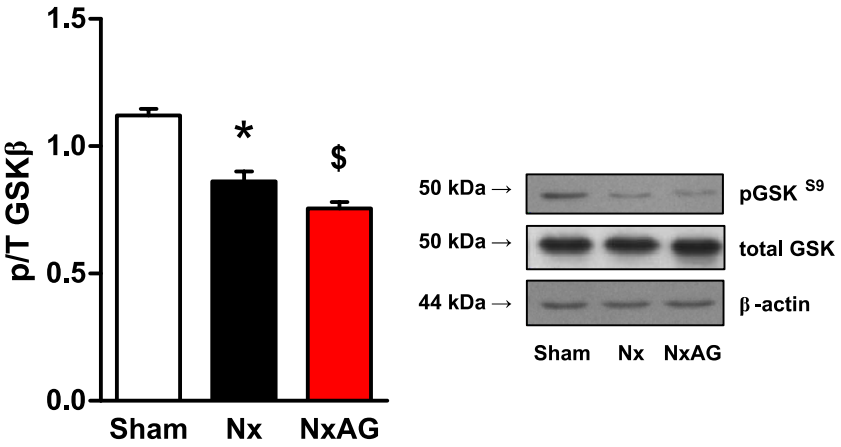

*Figure (29) Insulin Sensitivity in white adipose tissue of animals' groups in the study. A)Densitometer Analysis to the right and image blot to the left for p/tAKT. B) Densitometer Analysis to the right and image blot to the left for p/t GSK3β. WB was performed using protein extracts of white adipose tissue. * P<0.05 vs. sham, $ P<0.05 vs. Nx.*

4.1.2.6. AG upregulates the OGT levels in the white adipose tissue of uremic rats:

Compared with sham rats, Nx had unchanged levels of the OGT, however, AG was shown to upregulate the OGT level compared with Nx and sham rats suggesting, with the findings from the first study, the OGT as a target for the AG signaling in the white adipose tissue. As in the first study, the WB detected only the ncOGT isoform in the adipose tissue of the rats' study.

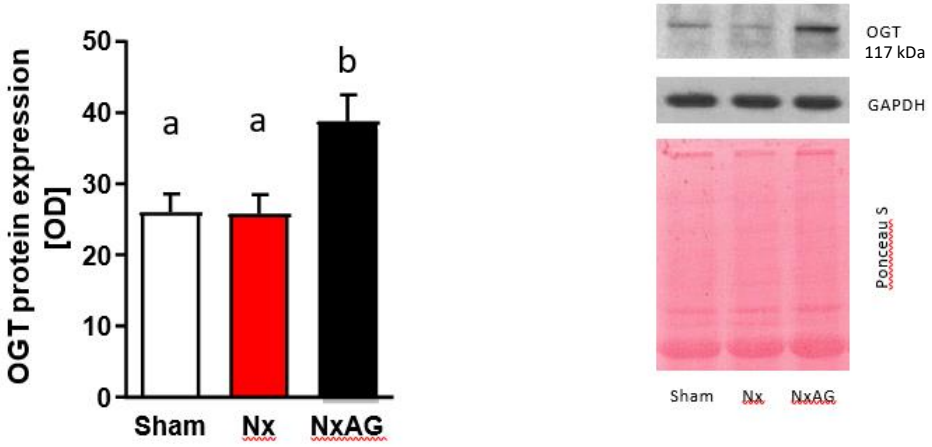

Figure (30) OGT levels in white adipose tissue of animals' groups in the study. Densitometer Analysis to the right and image blot to the left normalised for ponceau staining. P<0.05 between groups with different letters.

4.2. In Vitro Results:

4.2.1. 3T3L1 Cells

4.2.1.1. Identifying the effect of the Acylated Ghrelin on the insulin sensitivity in the differentiated adipocytes:

For the in vitro experiments, we focused on the effects of AG on the insulin sensitivity in the differentiated adipocytes as the in vivo findings suggested a direct effect of the AG on insulin sensitivity. Western blot analysis was applied to follow the insulin sensitivity at the level of AKT ^{S473} and GSK3β ^{S9}.

4.2.1.1.1. Normal Feeding Conditions FBS 10%:

AG was added to the maintenance adipocytes medium containing FBS10% for 72 h. AG administration to the adipocytes in all the followed doses resulted in lower ratios of the phosphorylation rates of both AKT ^{S473} and GSK3β ^{S9} compared to the control cells suggesting that

AG lowers insulin sensitivity in the adipocytes in consistence with our findings in the animals of the study. P values are reported in the following table.

	AKT ^{S473}	GSK3β ^{S9}
1000 ng vs con	0.092	0.131
100 ng vs con	0.024	0.068
10 ng vs con	0.059	0.116

Table (4): P values of T-test between the AG treatments and the control at the level of AKT ^{S473} and GSK3β ^{S9} phosphorylation.

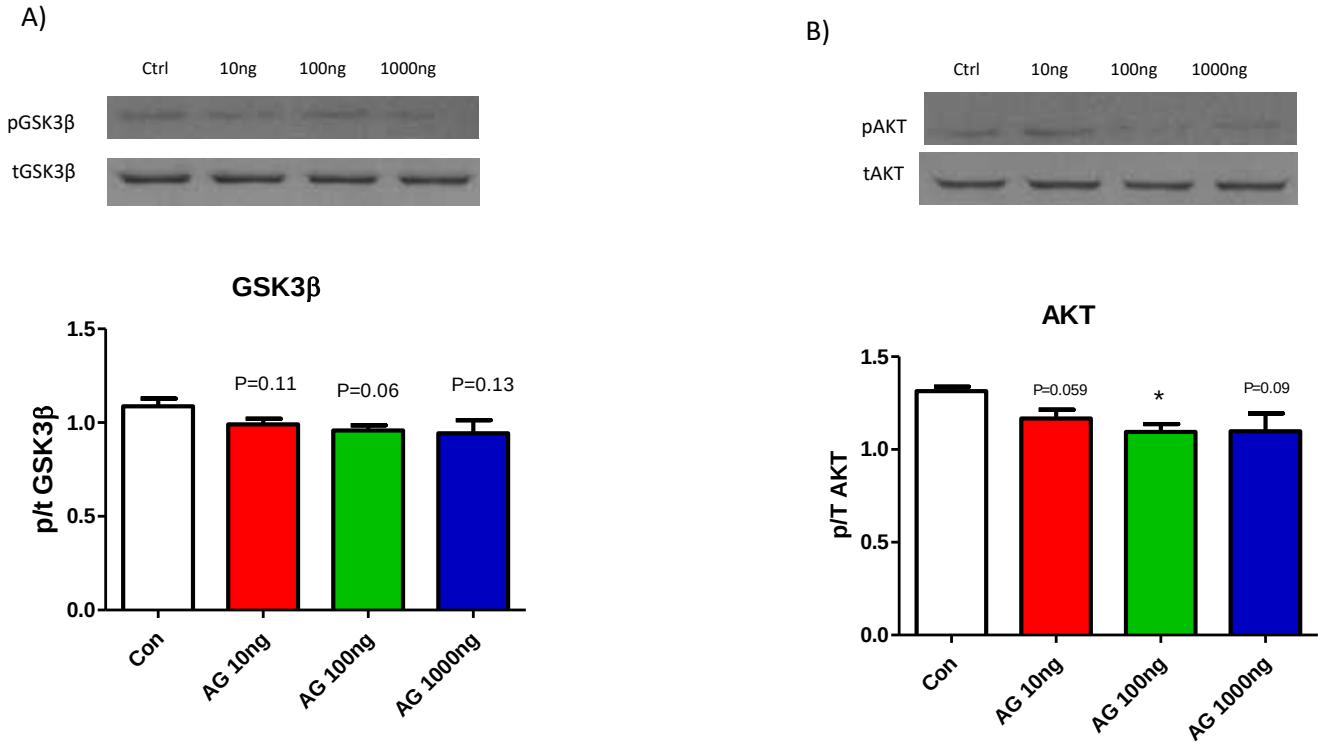

*Figure (31) Insulin sensitivity in 3T3L1 adipocytes treated by 10; 100; 1000 ng/ml AG for 72h in normal feeding conditions with 10% FBS at the level of GSK3β ^{S9} and AKT ^{S473} phosphorylation. **A)** GSK3β ^{S9} phosphorylation analysed by WB at the top, and represented by densitometer analysis at the bottom. **B)** AKT ^{S473} phosphorylation analysed by WB at the top, and represented by densitometer analysis at the bottom. * P<0.05 vs. Con*

4.2.1.1.2. Starvation conditions:

4.2.1.1.2.1. Partial Starvation (FBS 3%):

For this condition, FBS 3% medium was used. AG administration to the adipocytes in all the followed doses for 24 h did not show significant effects on the phosphorylation rates of the GSK3β ^{S9} and AKT ^{S473}, although there was a tendency to increase the insulin sensitivity at the GSK3β ^{S9} level.

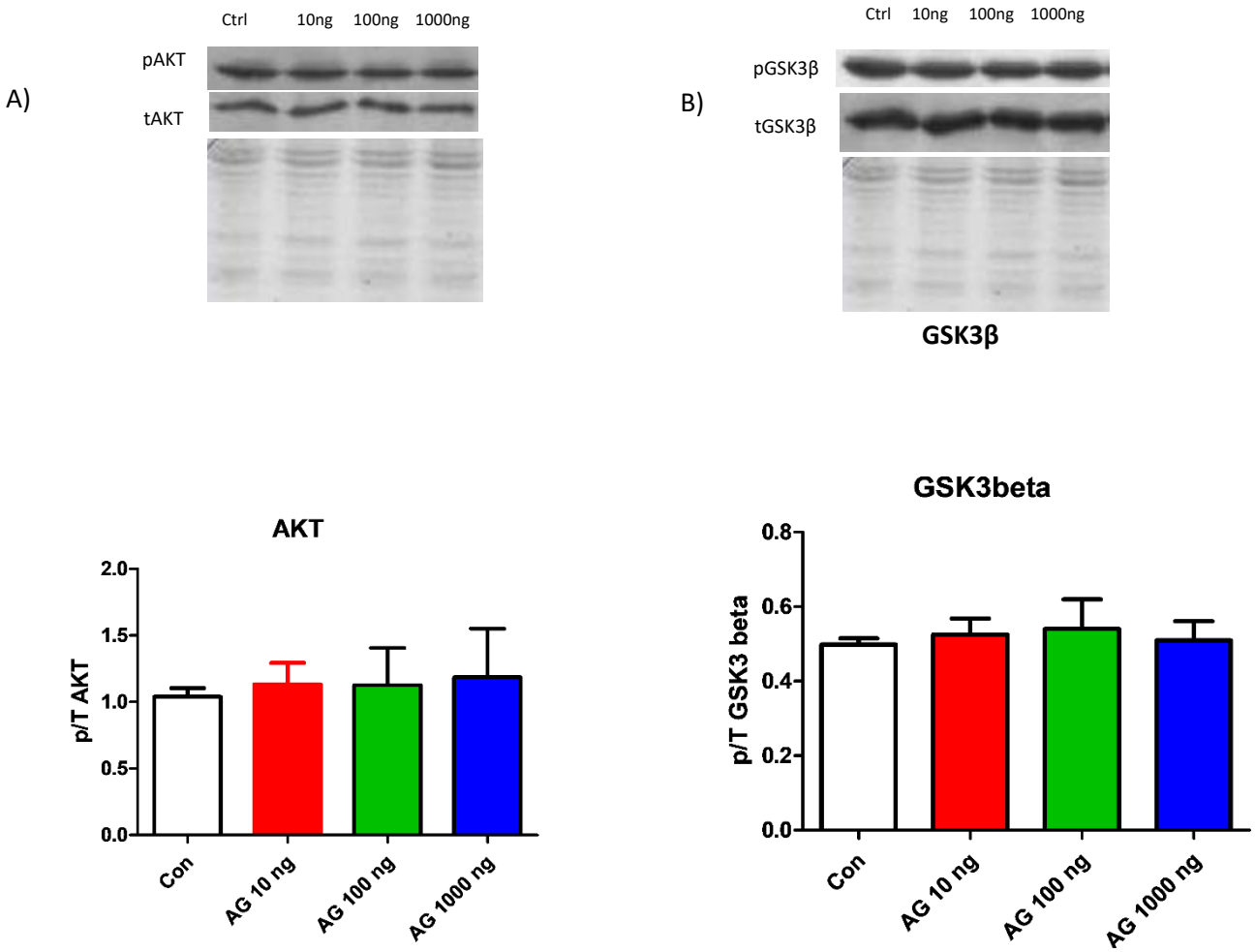

Figure (32) Insulin sensitivity in 3T3L1 adipocytes treated by 10; 100; 1000 ng/ml AG for 24h in partial starvation conditions with 3% FBS at the level of GSK3β ^{S9} and AKT ^{S473} phosphorylation. ***A)*** *AKT ^{S473} phosphorylation analysed by WB at the top, and represented by densitometer analysis at the bottom.* ***B)*** *GSK3β ^{S9} phosphorylation analysed by WB at the top, and represented by densitometer analysis at the bottom.*

4.2.1.1.2.2. Complete Starvation (FBS 0%):

AG treatment 24h combined by removing the serum from the medium did not result in a significant difference in the insulin sensitivity at the levels of AKT ^{S473} and GSK3β ^{S9} phosphorylation although it tended to decrease the insulin sensitivity at the AKT ^{S473} level but still without significant effect.

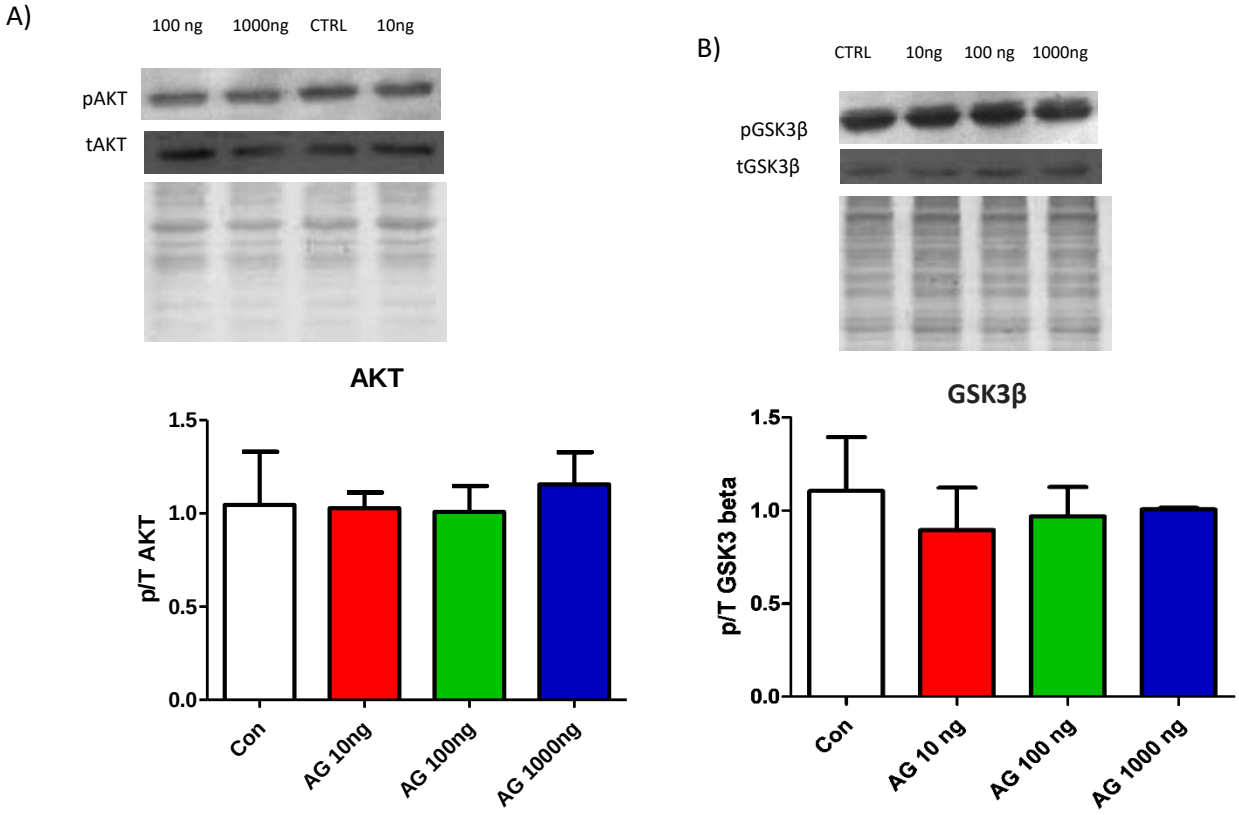

Figure (33) Insulin sensitivity in 3T3L1 adipocytes treated by 10; 100; 1000 ng/ml AG for 24h in complete serum starvation conditions with at the level of GSK3β ^{S9} and AKT ^{S473} phosphorylation. ***A)*** *AKT ^{S473} phosphorylation analysed by WB at the top, and represented by densitometer analysis at the bottom.* ***B)*** *GSK3β ^{S9} phosphorylation analysed by WB at the top, and represented by densitometer analysis at the bottom.*

Taking the results of the starvation conditions together suggests that the significant AG role in lowering insulin sensitivity in vitro might be impaired by reducing the nutrients in the medium.

4.2.1.2. Identifying the effect of the Acylated Ghrelin on OGT levels in the differentiated adipocytes:

In all the results obtained from 3T3L1 adipocytes, mitochondrial OGT, mOGT 103kDa, was the only detected isoform.

4.2.1.2.1. OGT levels in 3T3L1 adipocytes treated by AG in normal nutrient availability conditions FBS 10%:

OGT levels were not altered in adipocytes treated by the AG compared with the control cells.

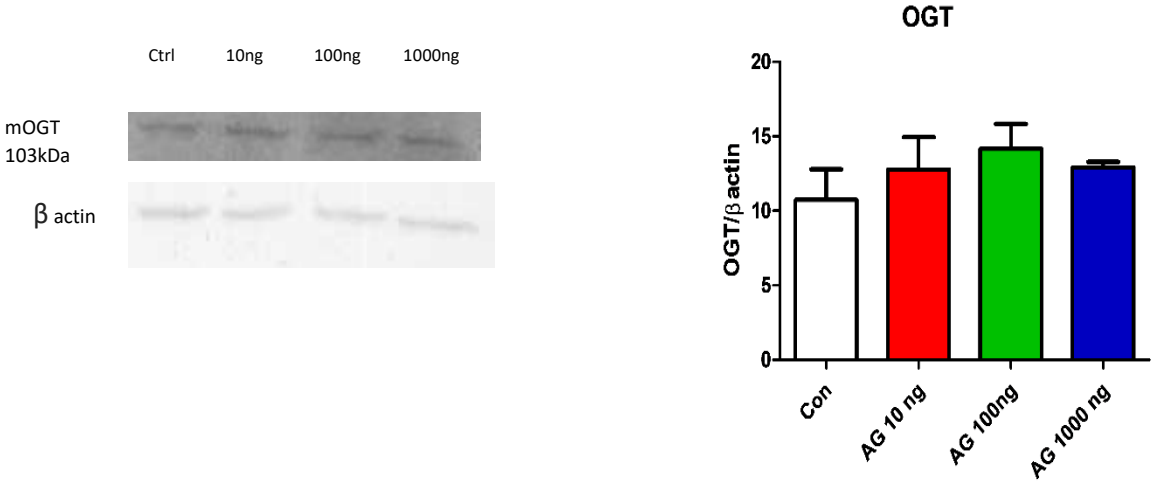

Figure (34) OGT levels in 3T3L1 adipocytes treated by 10; 100; 1000 ng/ml AG for 72h in normal feeding conditions with 10% FBS represented by image blot to the right and densitometer analysis to the left.

4.2.1.2.2. OGT levels in 3T3L1 adipocytes treated by AG in partial starvation conditions:

WB analysis did not unravel significant differences in the OGT levels in differentiated 3T3L1 adipocytes treated by AG compared with the control cells.

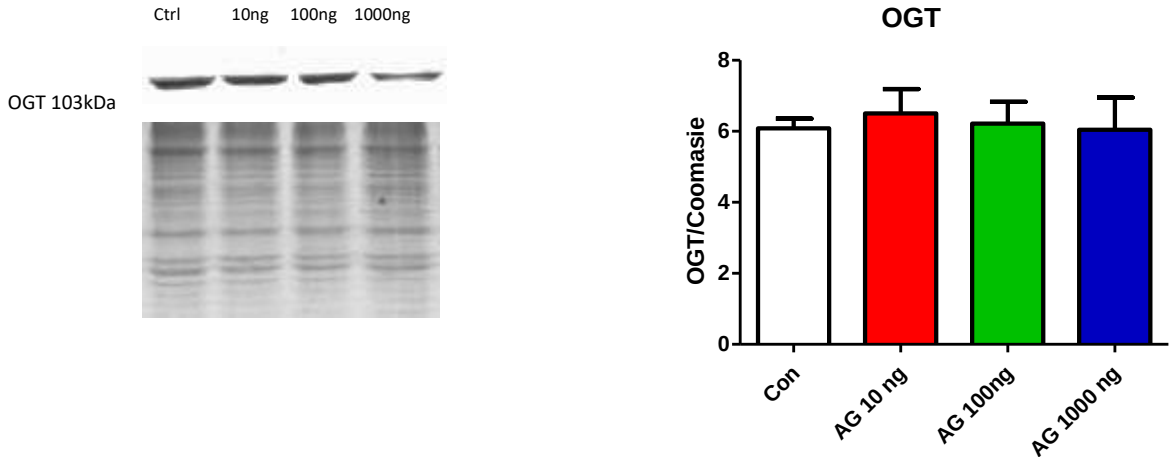

Figure (35) OGT levels in 3T3L1 adipocytes treated by 10; 100; 1000 ng/ml AG for 24h in partial starvation conditions with 3% FBS represented by image blot to the right and densitometer analysis to the left.

4.2.1.2.3. OGT levels in 3T3L1 adipocytes treated by AG in complete starvation conditions:

Even in complete starvation conditions, no differences were observed at the OGT levels in the adipocytes treated by AG compared to the control.

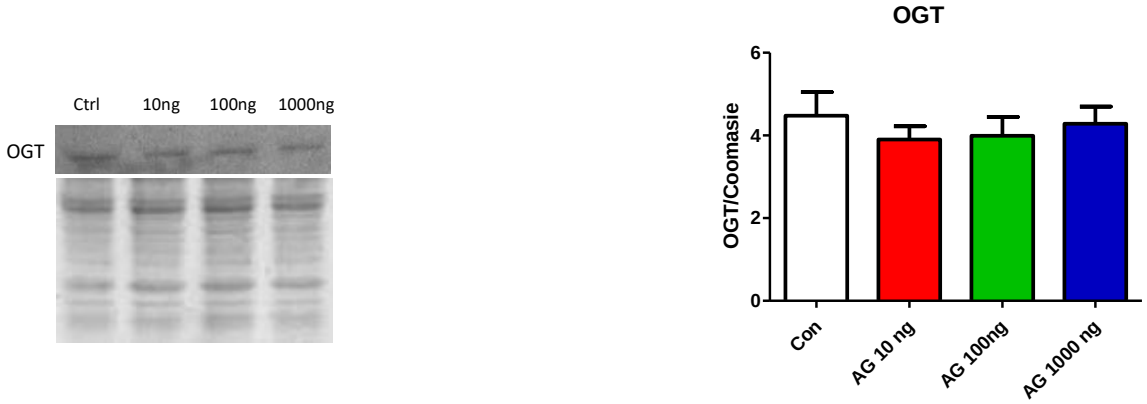

Figure (36) OGT levels in 3T3L1 adipocytes treated by 10; 100; 1000 ng/ml AG for 24h in complete serum starvation conditions represented by image blot to the right and densitometer analysis to the left.

Taken all together, AG treatment in vitro did not alter the OGT levels in the adipocytes which suggests that the increased OGT levels in the adipose tissue in the animal studies might be regulated by other organs rather than only in site regulation by adipose tissue.

4.2.1.3. Differentiated Adipocytes Knocked for OGT and Treated by AG

Based on the accumulated evidence in the previous animal studies, we wanted to confirm the link between the AG and the OGT by the siRNA knockdown methods. For this aim, adipocytes were transfected by the siRNA OGT and siRNA Control as described in the forward strategy, and after 48 h, AG 1000 ng was introduced to the cells for 24h in starvation conditions: partial starvation (FBS 3%) and complete starvation without FBS. The aim of using only starvation conditions was to investigate this link in the same conditions that AG physiological levels rise in the body.

4.2.1.3.1. Partial Starvation (Reduced FBS 3%):

ELISA was performed to test our hypothesis at the GSK3β and AKT levels. In control cells, AG treatment did not result in significant alterations in the phosphorylation ratios of GSK3β ^{S9} and AKT ^{S473}, but in knocked-down cells, AG increased the phosphorylation of GSK3β ^{S9} compared to control cells treated by AG and knocked OGT down cells not treated by AG, suggesting that knocking OGT

down affects the sensitivity of the adipocytes to the AG, which was represented by the significant increase in insulin sensitivity at the GSK3β ^{S9} level. Similar effects were found at AKT ^{S473} phosphorylation, where the AG treatment in knocked OGT down increased the insulin sensitivity compared to the knocked OGT down cells not treated by AG. These results provide the first evidence in this study about the link between the AG and the OGT in the adipose tissue.

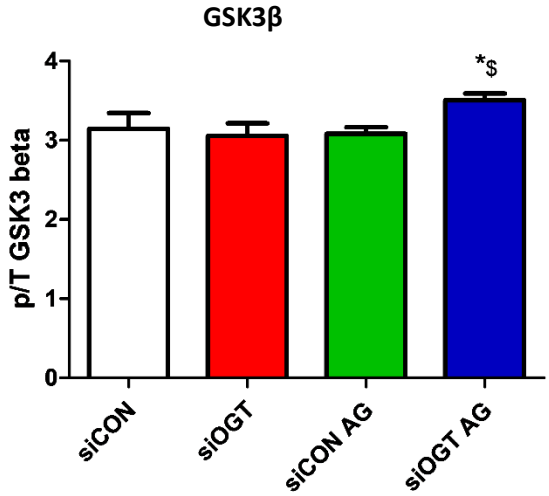

*Figure (39). Insulin sensitivity at GSK3β ^{S9} level in 3T3L1 adipocytes after knocking OGT expression and AG treatment for 24h in partial starvation. Data represented are from ELISA analysis using protein cellular extracts. * P<0.05 vs. siCON, $: P<0.05 vs. Other two groups.*

4.2.1.3.2. Starvation Conditions without FBS:

For further proof, we tested this link in complete starvation conditions. Interestingly, knocking the OGT down lowered the insulin sensitivity at the level of AKT ^{S473} phosphorylation both in the absence of AG significantly and in AG presence with a similar trend P=086, suggesting altered sensitivity of the cells to the AG when knocking OGT down. AG treatment showed a tendency to lower the insulin sensitivity when comparing controls treated and untreated by AG in agreement with the results obtained from the in vivo animal studies. Notably, AG treatment in knocked OGT cells did not show a difference compared to the knocked OGT cells without AG treatment, suggesting a dominant effect for the OGT knockdown reducing the sensitivity of the cells to the AG treatment when compared by knocked-down cells without AG treatment. To summarize, knocking OGT in complete starvation condition affects the sensitivity to the AG treatment, in addition to exerting a dominant effect in lowering insulin sensitivity.

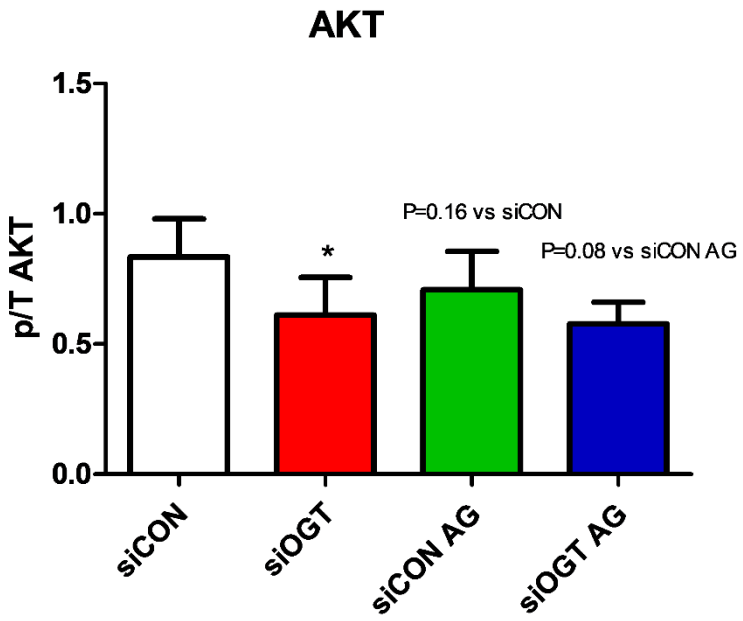

*Figure (40). Insulin sensitivity at AKT^{S473} level in 3T3L1 adipocytes after knocking OGT expression and AG treatment for 24h in complete serum starvation. Data represented are from ELISA analysis using protein cellular extracts. * P<0.05 vs. siCON.*

4.2.2. Results from Human Cells:

4.2.2.1. Effects of 5-days AG treatment on insulin sensitivity in human differentiated adipocytes:

AG was added to the differentiated cells starting from day-14 of the differentiation in three doses 10;100;1000 ng. No significant differences were observed between the treated cells and the control at the phosphorylation level of both AKT ^{S473} and GSK3β ^{S9}.

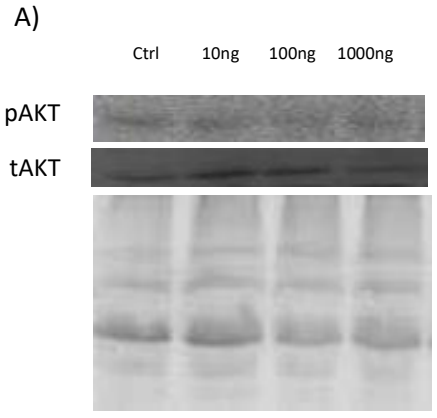

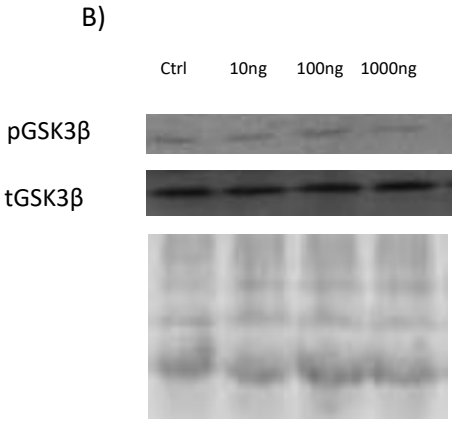

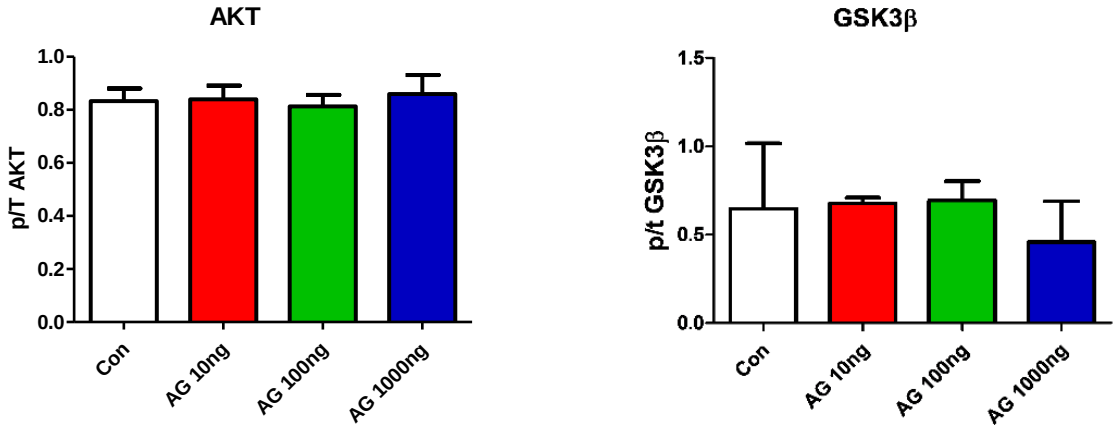

Figure (41) AKT^{S473} (A) and GSK3β^{S9} (B) phosphorylation levels in human differentiated adipocytes treated by 10; 100; 1000 ng/ml AG for five days in normal serum feeding conditions represented by image blot up and densitometer analysis down.

4.2.2.2. AG Effect on Insulin Sensitivity in Human Differentiated Adipocytes in Starvation Conditions:

Insulin sensitivity was investigated at the levels of GSK3β ^{S9} phosphorylation. AG was introduced at three doses 10; 100; 1000 ng/ml for 24h in starvation conditions using human adipocytes starvation medium. Notably, AG treatment showed a tendency to increase insulin sensitivity at the GSK3β ^{S9}.

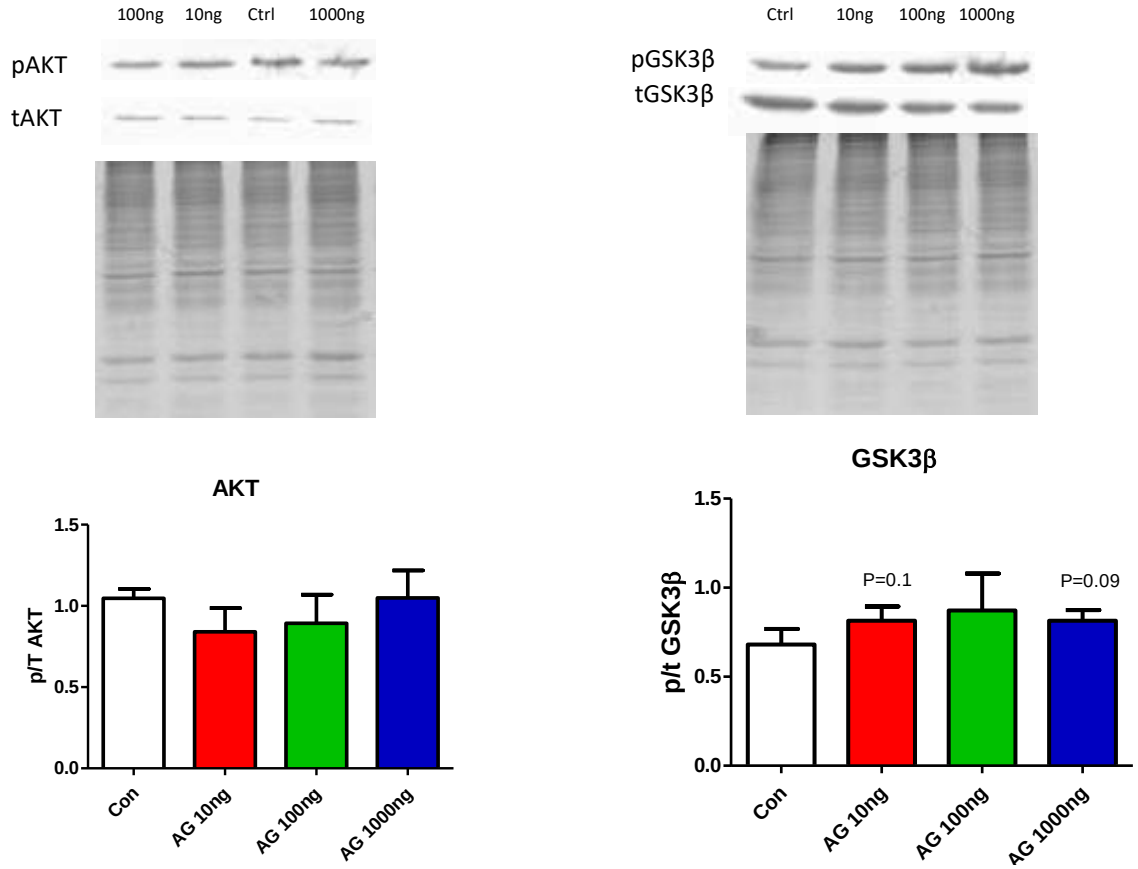

Figure (42) GSK3β phosphorylation levels in human differentiated adipocytes treated by 10; 100; 1000 ng/ml AG for 24h in starvation conditions represented by image blot to the right and densitometer analysis to the left. WB was performed using cellular protein extracts.

4.2.2.3. Knocking OGT in Human Adipocytes and Treating by AG:

Insulin sensitivity was tested at the phosphorylation levels of AKT ^{S473}. In human differentiated adipocytes, knocking OGT did not alter the insulin sensitivity at the level of AKT^{S473} phosphorylation when cells were not treated by the AG. However, introducing AG to knocked cells resulted in a significantly increased insulin sensitivity compared to all the other groups.

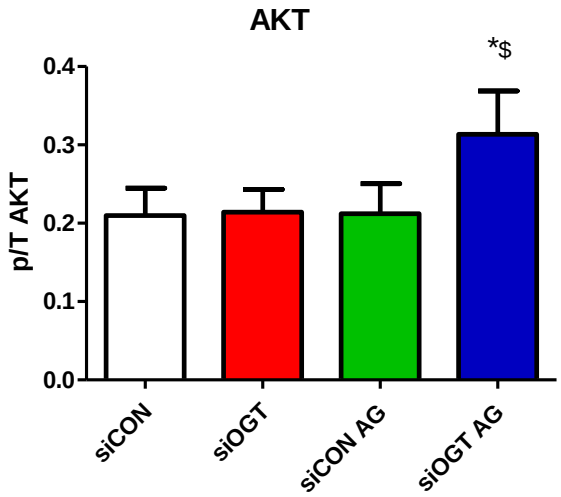

*Figure (43). Insulin sensitivity at AKT ^{S473} level in human differentiated adipocytes after knocking OGT expression and AG treatment for 24h in starvation conditions. Data represented are from ELISA analysis using protein cellular extracts. * P<0.05 vs. siCON. $: P<0.05 vs. siCON AG & siOGT*

5. Discussion:

In animal studies, AG lowered the insulin sensitivity in the adipose tissue of healthy rats, and in uremic rats compared even to untreated uremic rats. This result is in agreement with other findings that highlighted the adaptive role of ghrelin in starvation conditions where the the lipolysis response, counteracting the insulin effect, is activated (Vestergaard et al., 2008), and with the physiological role of the ghrelin as an inducement for the GH secretion which exerts anti-insulin effects in the adipose tissue (Kopchick et al., 2020). Lowered insulin sensitivity was correlated with lower mitochondrial function and unaltered redox state and cytokine profile in healthy rats. While adipocytes' mitochondrial function is linked to higher lipogenesis rates, the lowered mitochondrial function in adipose tissue reported by AG treatment can also be explained by the correlated inhibition of the lipogenesis mechanism in starvation conditions (Kersten et al., 2001) since mitochondrial function in the adipocytes is directly linked to the lipogenesis (Wilson-Fritch et al., 2003). In uremic rats, no significant effects for AG were observed at the level of mitochondrial function and redox state, which might be explained by the prevalent effect of the CKD-induced systemic inflammation. However, at cytokine profile, AG was found to modulate the proinflammatory status at the level of TNFα in agreement with previous findings reported reduced TNFα levels in omental adipocytes treated by both forms of ghrelin (Rodríguez et al., 2012) and with its role as an anti-inflammatory factor in adipose tissue (Liu et al., 2020) and in other tissues where ghrelin lowered inflammation-induced TNFα elevated levels like endothelial cells (Hedayati et al., 2009), human monocytes and T lymphocytes (Dixit et al., 2004), brain tissue (Qi et al., 2012) and cardiac tissue (Yuan et al., 2009). TNFα was extensively studied for its role in inducing insulin resistance (Ruan et al., 2002, Hube et al., 1999, da Costa et al., 2016, Gouranton et al., 2014), mainly by activating the NF-κB pathway mediated by TNFR and TRL as demonstrated in a recent proteomics-based study (Mohallem et al., 2020). While decreased TNFα levels by acylated ghrelin treatment were reported in uremic rats, this was not observed in healthy rats treated by AG although acylated ghrelin, not unacylated ghrelin, was reported to attenuate the basal and TNFα-induced autophagy in the omental differentiated human adipocytes. However, this was in vitro study, while our findings were reported in vivo. Our findings might be explained, at least in part, by the unaltered basal redox state reported in the healthy rats, while uremic rats experienced higher levels of redox state induced by the CKD complications. At this point, our results can give the conclusion that acylated ghrelin in visceral white adipose tissue did not alter basal cytokine profile

correlated with basal redox state, while it ameliorates this pro-inflammatory profile is positively induced redox state conditions. More experiments are needed to test this hypothesis that might involve autophagy pathways as well, and other adipose tissue depots in the body.

Regarding the findings of mitochondrial function in the adipose tissue of uremic rats, to our knowledge, this is the first study that investigates the mitochondrial function in the adipose tissue in the 5/6 nephrectomy CKD model, as well as the effects of AG on the mitochondrial function. Mitochondrial function was lowered in the adipose tiussue of uremic rats in association with the higher redox state and the systemic inflammation induced by the CKD which is in line with previous findings in skeletal muscle tissue showing lower mitochondrial function as a consequence of higher uremic toxins in CKD (Sun et al., 2017, Takemura et al., 2020, Thome et al., 2019); and AG did not alter the mitochondrial function in the adipose tissue of uremic rats. These results combined with findings from the first animal study suggested that AG exerts its role in lowering mitochondrial function at basal redox state, and this role might be impaired in elevated redox state conditions. Further experiments are needed to cover this important point that might include other aspects of the mitochondrial function including mitochondrial dynamics and mitophagy.

Altered in both animal studies, insulin sensitivity might be, among other mechanisms, the direct target for the AG physiological effects, which gave a rationale to investigate the effects of AG on insulin sensitivity in vitro in the following parts of the study.

AG treatment was found to lower the insulin sensitivity in 3T3L1 adipocytes, varying from significant to a strong tendency at the levels of AKT ^{S473} and GSK3β ^{S9} phosphorylation in all the used doses in the normal feeding conditions. In human differentiated adipocytes, AG treatment was not found to exert significant effects at the level of GSK3β^{s9} and AKT ^{S473} phosphorylation. Importantly, the lowered insulin sensitivity was observed from prolonged AG treatment, while the AG treatment for shorter periods did not show a dominant effect, except for a tendency to increase GSK3β^{s9} phosphorylation in human adipocytes treated by AG 24 h in starvation conditions. A previous study reported gradual increased AKT phosphorylation in terminally differentiated 3T3L1 adipocytes upon ghrelin treatment from 30 min to 24 h, but total AKT was not measured in this study, and the medium composition used for this experiment was not clarified whether it was starvation medium or not (Kim et al., 2004). Another study reported the anti-lipolytic role of the ghrelin forms in ex-vivo subcutaneous and visceral rats adipose tissue model, and this role was not exhibited in animals administered via intraperitoneal injection (Cervone et al., 2019). Although our study included

human adipocytes, they were differentiated in vitro differing from the ex vivo adipocytes model used in the aforementioned study. Additionally and importantly, this study did not test the insulin signaling in the primary adipocytes. While most of the in vitro literature focused on other sides in the adipocyte biology (Miao et al., 2019, Zhang et al., 2004, Liu et al,. 2009, Cervone et al., 2019), our in vitro study tested mainly the insulin signaling in the adipocytes in the absence of other hormonal responses presented in the in vivo studies.

The second part of the study included investigating the link between the OGT and AG. OGT was found to be elevated in mice adipose tissue during fasting conditions (Yang et al., 2020) that physiologically correlated with elevated AG levels. Previous studies reported that knocking OGT in white adipose tissue in the mice showed a similar effect of knocking AG receptor in the white adipose tissue; where both were correlated with improved insulin sensitivity in the visceral white adipose tissue (Yang et al., 2020, Lin et al., 2011, Ma et al., 2013). All together comprised a rationale for the hypothesis that OGT is mediating the AG effects in the visceral white adipose tissue. As a first step to test the hypothesis, we reported in vivo that OGT is upregulated upon AG treatment in the adipose tissue in its nucleocytoplasmic canonical isoform, which was reported to be sufficient to maintain the O-GlcNAc mitochondrial proteome (Trapannone et al., 2016). These results were confirmed in healthy rats and uremic rats which show a general systemic inflammation. Interestingly, cytosolic short OGT levels were upregulated in the muscle tissue of healthy rats treated by AG, suggesting that AG might directly target the OGT in vivo. However, to confirm this idea, further investigations in other organs are necessary to cover this interesting and important topic taking into consideration OGT is involved in a wide spectrum of cellular functions in different tissues.

As a second step, we aimed at investigating the OGT levels upon AG treatment in vitro. Importantly, no major alterations in OGT levels were reported in vitro when AG was introduced to the adipocytes, suggesting that the mechanisms responsible for OGT upregulation upon AG treatment are para-adipocytes regulated, and might involve other mechanisms mainly in the central nervous system, the hypothalamus. A previous study reported that OGT inhibition in the AgRP neurons in the arcuate nucleus (ARC) of the hypothalamus, which are activated by ghrelin in hunger conditions, induced the browning in the white adipose tissue, in correlation with starvation conditions and elevated ghrelin levels (Ruan et al., 2014).

Although the results did not show that OGT is directly mediating the AG effects in the white adipose tissue, the link between the two systems was shown and reported for the first time.

The last part of the study aimed at investigating whether OGT is at least involved in the AG network by silencing OGT in differentiated human and 3T3L1 adipocytes. Since both OGT (Yang et al., 2020) and AG (Toshinai et al., 2001) are upregulated in the fasting conditions, we tested the hypothesis in starvation medium conditions.

In 3T3L1 adipocytes, knocking OGT combined with AG treatment (siOGT AG) showed different responses according to the nutrients availability in the medium. In the partial starvation conditions, there was a strong significant increase in insulin sensitivity compared with the controls of both AG treatment (siCON AG) and silenced-OGT (siOGT) separately. In complete deprivation serum conditions, which in our study was used as complete starvation, knocking OGT combined with AG treatment (siOGT AG) showed a strong tendency to lower the insulin sensitivity compared to the control of AG treatment (siCON AG) and the control with basal OGT expression without AG treatment (siOGT). These results go in agreement, at least in part, with other findings that knocking OGT in the adipose tissue in starvation conditions led to increased lipolysis in mice (Yang et al., 2020). Although the results did not show that OGT is directly mediating the AG effects in the white adipose tissue, the link between the two systems was shown and reported for the first time. Putting all in one picture, AG lowered the insulin sensitivity in FBS 10% in basal OGT expression conditions, while for silenced-OGT expression, it increased the insulin sensitivity in partial starvation, then with complete serum deprivation it lowered the insulin sensitivity again. While lowering insulin sensitivity was reported in our in vivo animal studies, the increased insulin sensitivity needs to be explained. Reducing the nutrients available in the medium might be sensed by the cells, and activating an adaptive response to increase the energy storage by increasing the glucose uptake and insulin sensitivity, but in the complete absence of the FBS, adipocytes need to activate the lipolytic response to provide the energy to survive. This nutrients-dependent suggested mechanism was reported in the skeletal muscle tissue in the rodents where caloric overfeeding rapidly induced insulin resistance (Wang et al., 2001), while caloric restriction was found to contribute to higher insulin sensitivity in rodents (Cartee et al., 1994) and humans (Kelley et al., 1993). Interestingly, our results were reported in silenced-OGT conditions, not in the basal conditions, which suggested that OGT plays important role in the sensitivity of the cells to the AG treatment.

In human differentiated adipocytes, knocking OGT combined with AG treatment (siOGT AG) further increased the insulin sensitivity compared with both controls for the knocking down (siOGT) and AG treatment (siCON AG) separately, in agreement with the results obtained from the 3T3L1 adipocytes experiments performed in partial starvation conditions. These results suggest that silenced-OGT cells increased their sensitivity to the AG as compensation for the impaired OGT expression, which is a cellular stress sensor, to inhibit apoptosis induced by the starvation conditions, especially AG was reported to exert anti-apoptotic effects by increasing insulin sensitivity as an adaptive response to the starvation condition which induces the apoptosis (Rodríguez et al., 2012, Kim et al., 2004). This hypothesis is further supported by 1)the significant increase in the insulin sensitivity in OGT-silenced cells treated by AG compared with OGT-silenced cells without AG treatment, 2) the strong significant difference when compared to control cells without AG treatment, 3) the tendency to increased tendency in GSK3β ^{S9} phosphorylation reported in this study in human adipocytes treated by AG for 24h in starvation conditions. However, to test this hypothesis, more experiments are needed that mainly target the apoptosis pathway.

Taking all together, knocking OGT altered the sensitivity of both human and murine 3T3L1 adipocytes to the AG, which was reflected in the changes observed in the insulin sensitivity. These results from human and murine adipocytes demonstrated for the first time the link between the OGT and AG at the level of insulin sensitivity and suggested that lowering OGT levels by siRNA transfection increased the insulin sensitivity in starved humans adipocytes and 3T3L1 partially starved adipocytes. The findings introduced in this study gain their importance from linking two systems directly involved in energy storage and expenditure and open the door for further investigations for the interlinked connections between the two systems.

6. Conclusion:

In this study, we reported in the visceral white adipose tissue that sustained AG treatment lowers insulin sensitivity in vivo in healthy and uremic rats, lowers the mitochondrial function at physiological conditions, and ameliorates the high proinflammatory levels TNFα correlated with CKD conditions. Our in vivo results suggested that AG has effects on insulin sensitivity which are not mediated by changes in redox state or inflammation. The part of these findings of the insulin sensitivity was demonstrated by the prolonged AG treatment in 3T3L1 differentiated adipocytes. We also reported in vivo that AG treatment upregulates the levels of the ncOGT in the visceral white adipose tissue in healthy and uremic rats, and the sOGT levels in the muscle tissue of healthy rats suggesting a direct effect of the AG on the OGT system in vivo. The in vitro studies on the adipocytes suggested that the OGT upregulation by AG treatment, reported in vivo, is at least in part regulated by non-adipocytes mechanisms and might involve further regulation exerted by other tissues. Silencing OGT was shown to be altering the sensitivity of the adipocytes to the AG treatment, rather than directly mediating the directly the AG effects. Importantly, silencing OGT combined with AG improved insulin sensitivity in human and 3T3L1 adipocytes in non-complete starvation conditions.

In addition to characterizing metabolic roles of the AG in the visceral white adipose tissue, the findings introduced in this study gain their clinical importance from unraveling for the first time the link between two systems directly involved in adipose tissue homeostasis, AG and OGT. In particular, the improved insulin sensitivity in the adipocytes, induced by silencing OGT and AG treatment together, is of high interest and potential in the field of metabolic syndrome and type2 diabetes research since insulin resistance in the adipocytes is a major causative hallmark of these pathological conditions. Further studies using transgenic mice OGT-silenced specifically in adipose tissue are needed to confirm this finding in vivo.

7. References

Abel ED, Peroni O, Kim JK, Kim YB, Boss O, Hadro E, Minnemann T, Shulman GI, Kahn BB. Adipose-selective targeting of the GLUT4 gene impairs insulin action in muscle and liver. Nature. 2001 Feb 8;409(6821):729-33.

Alejandro EU, Bozadjieva N, Kumusoglu D, Abdulhamid S, Levine H, Haataja L, Vadrevu S, Satin LS, Arvan P, Bernal-Mizrachi E. Disruption of O-linked N-Acetylglucosamine Signaling Induces ER Stress and β Cell Failure. Cell Rep. 2015 Dec 22;13(11):2527-2538.

Altshuler-Keylin S, Kajimura S. Mitochondrial homeostasis in adipose tissue remodeling. *Sci Signal*. 2017;10(468):eaai9248.

American Diabetes Association. 2. Classification and Diagnosis of Diabetes: *Standards of Medical Care in Diabetes-2018*. Diabetes Care. 2018 Jan;41(Suppl 1):S13-S27.

Andralojc KM, Mercalli A, Nowak KW, Albarello L, Calcagno R, Luzi L, Bonifacio E, Doglioni C, Piemonti L. Ghrelin-producing epsilon cells in the developing and adult human pancreas. Diabetologia. 2009 Mar;52(3):486-93.

Aquino-Gil M, Pierce A, Perez-Cervera Y, Zenteno E, Lefebvre T. OGT: a short overview of an enzyme standing out from usual glycosyltransferases. Biochem Soc Trans. 2017 Apr 15;45(2):365-370.

Ashrafi G, Schwarz TL. The pathways of mitophagy for quality control and clearance of mitochondria. Cell Death Differ. 2013 Jan;20(1):31-42.

Bäckdahl J, Franzén L, Massier L, Li Q, Jalkanen J, Gao H, Andersson A, Bhalla N, Thorell A, Rydén M, Ståhl PL, Mejhert N. Spatial mapping reveals human adipocyte subpopulations with distinct sensitivities to insulin. Cell Metab. 2021 Sep 7;33(9):1869-1882.e6.

Barazzoni R, Gortan Cappellari G, Palus S, Vinci P, Ruozi G, Zanetti M, Semolic A, Ebner N, von Haehling S, Sinagra G, Giacca M, Springer J. Acylated ghrelin treatment normalizes skeletal muscle mitochondrial oxidative capacity and AKT phosphorylation in rat chronic heart failure. J Cachexia Sarcopenia Muscle. 2017 Dec;8(6):991-998.

Barazzoni R, Gortan Cappellari G, Semolic A, Ius M, Mamolo L, Dore F, Giacca M, Zanetti M, Vinci P, Guarnieri G. Plasma total and unacylated ghrelin predict 5-year changes in insulin resistance. Clin Nutr. 2016 Oct;35(5):1168-73.

Barazzoni R, Zanetti M, Bosutti A, Biolo G, Vitali-Serdoz L, Stebel M, Guarnieri G. Moderate caloric restriction, but not physiological hyperleptinemia per se, enhances mitochondrial oxidative capacity in rat liver and skeletal muscle--tissue-specific impact on tissue triglyceride content and AKT activation. Endocrinology. 2005 Apr;146(4):2098-106.

Barazzoni R, Zanetti M, Cattin MR, Visintin L, Vinci P, Cattin L, Stebel M, Guarnieri G. Ghrelin enhances in vivo skeletal muscle but not liver AKT signaling in rats. Obesity (Silver Spring). 2007 Nov;15(11):2614-23. A

Barazzoni R, Zanetti M, Ferreira C, Vinci P, Pirulli A, Mucci M, Dore F, Fonda M, Ciocchi B, Cattin L, Guarnieri G. Relationships between desacylated and acylated ghrelin and insulin sensitivity in the metabolic syndrome. J Clin Endocrinol Metab. 2007 Oct;92(10):3935-40. B

Barazzoni R, Zanetti M, Stulle M, Mucci MP, Pirulli A, Dore F, Panzetta G, Vasile A, Biolo G, Guarnieri G. Higher total ghrelin levels are associated with higher insulin-mediated glucose disposal in non-diabetic maintenance hemodialysis patients. Clin Nutr. 2008 Feb;27(1):142-9.

Barazzoni R, Zhu X, Deboer M, Datta R, Culler MD, Zanetti M, Guarnieri G, Marks DL. Combined effects of ghrelin and higher food intake enhance skeletal muscle mitochondrial oxidative capacity and AKT phosphorylation in rats with chronic kidney disease. Kidney Int. 2010 Jan;77(1):23-8.

Becker B, Kronenberg F, Kielstein JT, Haller H, Morath C, Ritz E, Fliser D; MMKD Study Group. Renal insulin resistance syndrome, adiponectin and cardiovascular events in patients with kidney disease: the mild and moderate kidney disease study. J Am Soc Nephrol. 2005 Apr;16(4):1091-8.

Benard G, Bellance N, James D, Parrone P, Fernandez H, Letellier T, Rossignol R. Mitochondrial bioenergetics and structural network organization. J Cell Sci. 2007 Mar 1;120(Pt 5):838-48.

Bergman RN. Non-esterified fatty acids and the liver: why is insulin secreted into the portal vein? Diabetologia. 2000 Jul;43(7):946-52.

Bloch-Damti A, Bashan N. Proposed mechanisms for the induction of insulin resistance by oxidative stress. Antioxid Redox Signal. 2005 Nov-Dec;7(11-12):1553-67.

Bond MR, Hanover JA. O-GlcNAc cycling: a link between metabolism and chronic disease. Annu Rev Nutr. 2013;33:205-29.

Bowen J, Noakes M, Clifton PM. Appetite regulatory hormone responses to various dietary proteins differ by body mass index status despite similar reductions in ad libitum energy intake. J Clin Endocrinol Metab. 2006 Aug;91(8):2913-9.

Broglio F, Gottero C, Van Koetsveld P, Prodam F, Destefanis S, Benso A, Gauna C, Hofland L, Arvat E, van der Lely AJ, Ghigo E. Acetylcholine regulates ghrelin secretion in humans. J Clin Endocrinol Metab. 2004 May;89(5):2429-33.

Bustin SA, Benes V, Garson JA, Hellemans J, Huggett J, Kubista M, Mueller R, Nolan T, Pfaffl MW, Shipley GL, Vandesompele J, Wittwer CT. The MIQE guidelines: minimum information for publication of quantitative real-time PCR experiments. Clin Chem. 2009 Apr;55(4):611-22.

Butkinaree C, Park K, Hart GW. O-linked beta-N-acetylglucosamine (O-GlcNAc): Extensive crosstalk with phosphorylation to regulate signaling and transcription in response to nutrients and stress. Biochim Biophys Acta. 2010 Feb;1800(2):96-106.

Canpolat N, Sever L, Agbas A, Tasdemir M, Oruc C, Ekmekci OB, Caliskan S. Leptin and ghrelin in chronic kidney disease: their associations with protein-energy wasting. Pediatr Nephrol. 2018 Nov;33(11):2113-2122.

Cartee GD, Dean DJ. Glucose transport with brief dietary restriction: heterogenous responses in muscles. Am J Physiol. 1994 Jun;266(6 Pt 1):E946-52.

Cervone DT, Sheremeta J, Kraft EN, Dyck DJ. Acylated and unacylated ghrelin directly regulate ß-3 stimulated lipid turnover in rodent subcutaneous and visceral adipose tissue ex vivo but not in vivo. Adipocyte. 2019 Dec;8(1):1-15.

Chang YH, Ho KT, Lu SH, Huang CN, Shiau MY. Regulation of glucose/lipid metabolism and insulin sensitivity by interleukin-4. Int J Obes (Lond). 2012 Jul;36(7):993-8.

Chmelar J, Chung KJ, Chavakis T. The role of innate immune cells in obese adipose tissue inflammation and development of insulin resistance. Thromb Haemost. 2013 Mar;109(3):399-406.

Cho CH, Koh YJ, Han J, Sung HK, Jong Lee H, Morisada T, Schwendener RA, Brekken RA, Kang G, Oike Y, Choi TS, Suda T, Yoo OJ, Koh GY. Angiogenic role of LYVE-1-positive macrophages in adipose tissue. Circ Res. 2007 Mar 2;100(4):e47-57.

Choi EW, Lee M, Song JW, Kim K, Lee J, Yang J, Lee SH, Kim IY, Choi JH, Seong JK. Fas mutation reduces obesity by increasing IL-4 and IL-10 expression and promoting white adipose tissue browning. Sci Rep. 2020 Jul 20;10(1):12001.

Choi K, Roh SG, Hong YH, Shrestha YB, Hishikawa D, Chen C, Kojima M, Kangawa K, Sasaki S. The role of ghrelin and growth hormone secretagogues receptor on rat adipogenesis. Endocrinology. 2003 Mar;144(3):754-9.

Choo HJ, Kim JH, Kwon OB, Lee CS, Mun JY, Han SS, Yoon YS, Yoon G, Choi KM, Ko YG. Mitochondria are impaired in the adipocytes of type 2 diabetic mice. Diabetologia. 2006 Apr;49(4):784-91.

Chouchani ET, Kazak L, Spiegelman BM. Mitochondrial reactive oxygen species and adipose tissue thermogenesis: Bridging physiology and mechanisms. J Biol Chem. 2017 Oct 13;292(41):16810-16816.

Chuang JC, Sakata I, Kohno D, Perello M, Osborne-Lawrence S, Repa JJ, Zigman JM. Ghrelin directly stimulates glucagon secretion from pancreatic alpha-cells. Mol Endocrinol. 2011 Sep;25(9):1600-11

Chung KJ, Nati M, Chavakis T, Chatzigeorgiou A. Innate immune cells in the adipose tissue. Rev Endocr Metab Disord. 2018 Dec;19(4):283-292.

Collins S. β-Adrenoceptor Signaling Networks in Adipocytes for Recruiting Stored Fat and Energy Expenditure. Front Endocrinol (Lausanne). 2012 Jan 3;2:102.

Comer FI, Hart GW. O-Glycosylation of nuclear and cytosolic proteins. Dynamic interplay between O-GlcNAc and O-phosphate. J Biol Chem. 2000 Sep 22;275(38):29179-82.

Cota D, Proulx K, Smith KA, Kozma SC, Thomas G, Woods SC, Seeley RJ. Hypothalamic mTOR signaling regulates food intake. Science. 2006 May 12;312(5775):927-30.

da Costa RM, Neves KB, Mestriner FL, Louzada-Junior P, Bruder-Nascimento T, Tostes RC. TNF-α induces vascular insulin resistance via positive modulation of PTEN and decreased Akt/eNOS/NO signaling in high fat diet-fed mice. Cardiovasc Diabetol. 2016 Aug 25;15(1):119.

De Vriese C, Gregoire F, Lema-Kisoka R, Waelbroeck M, Robberecht P, Delporte C. Ghrelin degradation by serum and tissue homogenates: identification of the cleavage sites. Endocrinology. 2004 Nov;145(11):4997-5005.

Deboer MD, Zhu X, Levasseur PR, Inui A, Hu Z, Han G, Mitch WE, Taylor JE, Halem HA, Dong JZ, Datta R, Culler MD, Marks DL. Ghrelin treatment of chronic kidney disease: improvements in lean body mass and cytokine profile. Endocrinology. 2008 Feb;149(2):827-35.

Dentin R, Hedrick S, Xie J, Yates J 3rd, Montminy M. Hepatic glucose sensing via the CREB coactivator CRTC2. Science. 2008 Mar 7;319(5868):1402-5.

Dietrich MO, Antunes C, Geliang G, Liu ZW, Borok E, Nie Y, Xu AW, Souza DO, Gao Q, Diano S, Gao XB, Horvath TL. Agrp neurons mediate Sirt1's action on the melanocortin system and energy balance: roles for Sirt1 in neuronal firing and synaptic plasticity. J Neurosci. 2010 Sep 1;30(35):11815-25.

Dixit VD, Schaffer EM, Pyle RS, Collins GD, Sakthivel SK, Palaniappan R, Lillard JW Jr, Taub DD. Ghrelin inhibits leptin- and activation-induced proinflammatory cytokine expression by human monocytes and T cells. J Clin Invest. 2004 Jul;114(1):57-66.

Dong MH, Kaunitz JD. Gastroduodenal mucosal defense. Curr Opin Gastroenterol. 2006 Nov;22(6):599-606.

Dufner A, Thomas G. Ribosomal S6 kinase signaling and the control of translation. Exp Cell Res. 1999 Nov 25;253(1):100-9.

Duquenne M, Folgueira C, Bourouh C, Millet M, Silva A, Clasadonte J, Imbernon M, Fernandois D, Martinez-Corral I, Kusumakshi S, Caron E, Rasika S, Deliglia E, Jouy N, Oishi A, Mazzone M, Trinquet E, Tavernier J, Kim YB, Ory S, Jockers R, Schwaninger M, Boehm U, Nogueiras R, Annicotte JS, Gasman S, Dam J, Prévot V. Leptin brain entry via a tanycytic LepR-EGFR shuttle controls lipid metabolism and pancreas function. Nat Metab. 2021 Aug;3(8):1071-1090.

Ebrahimi R, Bahiraee A, Jannat Alipour N, Toolabi K, Emamgholipour S. Evaluation of the Housekeeping Genes; β-Actin, Glyceraldehyde-3-Phosphate-Dehydrogenase, and 18S rRNA for Normalization in Real-Time Polymerase Chain Reaction Analysis of Gene Expression in Human Adipose Tissue. Arch Med Lab Sci [Internet]. 2020Feb.8 [cited 2021Nov.24];4(3).

Elgass K, Pakay J, Ryan MT, Palmer CS. Recent advances into the understanding of mitochondrial fission. Biochim Biophys Acta. 2013 Jan;1833(1):150-61.

Endemann G, Stanton LW, Madden KS, Bryant CM, White RT, Protter AA. CD36 is a receptor for oxidized low density lipoprotein. J Biol Chem. 1993 Jun 5;268(16):11811-6.

Ezquerro S, Mocha F, Frühbeck G, Guzmán-Ruiz R, Valentí V, Mugueta C, Becerril S, Catalán V, Gómez-Ambrosi J, Silva C, Salvador J, Colina I, Malagón MM, Rodríguez A. Ghrelin Reduces TNF-α-Induced Human Hepatocyte Apoptosis, Autophagy, and Pyroptosis: Role in Obesity-Associated NAFLD. J Clin Endocrinol Metab. 2019 Jan 1;104(1):21-37.

Fasshauer M, Blüher M. Adipokines in health and disease. Trends Pharmacol Sci. 2015 Jul;36(7):461-70.

Flatt JP, Ball EG. Studies on the metabolism of adipose tissue. XIX. An evaluation of the major pathways of glucose catabolism as influenced by acetate in the presence of insulin. J Biol Chem. 1966 Jun 25;241(12):2862-9.

François M, Barde S, Legrand R, Lucas N, Azhar S, El Dhaybi M, Guerin C, Hökfelt T, Déchelotte P, Coëffier M, Fetissov SO. High-fat diet increases ghrelin-expressing cells in stomach, contributing to obesity. Nutrition. 2016 Jun;32(6):709-15.

Fülöp N, Feng W, Xing D, He K, Nőt LG, Brocks CA, Marchase RB, Miller AP, Chatham JC. Aging leads to increased levels of protein O-linked N-acetylglucosamine in heart, aorta, brain and skeletal muscle in Brown-Norway rats. Biogerontology. 2008 Jun;9(3):139.

Fulton RJ, McDade RL, Smith PL, Kienker LJ, Kettman JR Jr. Advanced multiplexed analysis with the FlowMetrix system. Clin Chem. 1997 Sep;43(9):1749-56.

Funai K, Song H, Yin L, Lodhi IJ, Wei X, Yoshino J, Coleman T, Semenkovich CF. Muscle lipogenesis balances insulin sensitivity and strength through calcium signaling. J Clin Invest. 2013 Mar;123(3):1229-40.

Furuhashi M, Fucho R, Görgün CZ, Tuncman G, Cao H, Hotamisligil GS. Adipocyte/macrophage fatty acid-binding proteins contribute to metabolic deterioration through actions in both macrophages and adipocytes in mice. J Clin Invest. 2008 Jul;118(7):2640-50.

Furuhashi M, Tuncman G, Görgün CZ, Makowski L, Atsumi G, Vaillancourt E, Kono K, Babaev VR, Fazio S, Linton MF, Sulsky R, Robl JA, Parker RA, Hotamisligil GS. Treatment of diabetes and atherosclerosis by inhibiting fatty-acid-binding protein aP2. Nature. 2007 Jun 21;447(7147):959-65.

Gagnon J, Anini Y. Insulin and norepinephrine regulate ghrelin secretion from a rat primary stomach cell culture. Endocrinology. 2012 Aug;153(8):3646-56.

Gallardo-Montejano VI, Yang C, Hahner L, McAfee JL, Johnson JA, Holland WL, Fernandez-Valdivia R, Bickel PE. Perilipin 5 links mitochondrial uncoupled respiration in brown fat to healthy white fat remodeling and systemic glucose tolerance. Nat Commun. 2021 Jun 3;12(1):3320.

Giralt M, Villarroya F. White, brown, beige/brite: different adipose cells for different functions? Endocrinology. 2013 Sep;154(9):2992-3000.

Goldberg IJ, Eckel RH, Abumrad NA. Regulation of fatty acid uptake into tissues: lipoprotein lipase- and CD36-mediated pathways. J Lipid Res. 2009 Apr;50 Suppl(Suppl):S86-90.

Goossens GH. The role of adipose tissue dysfunction in the pathogenesis of obesity-related insulin resistance. Physiol Behav. 2008 May 23;94(2):206-18.

Gortan Cappellari G, Barazzoni R. Ghrelin forms in the modulation of energy balance and metabolism. Eat Weight Disord. 2019 Dec;24(6):997-1013.

Gortan Cappellari G, Semolic A, Ruozi G, Vinci P, Guarnieri G, Bortolotti F, Barbetta D, Zanetti M, Giacca M, Barazzoni R. Unacylated ghrelin normalizes skeletal muscle oxidative stress and prevents muscle catabolism by enhancing tissue mitophagy in experimental chronic kidney disease. FASEB J. 2017 Dec;31(12):5159-5171.

Gortan Cappellari G, Zanetti M, Semolic A, Vinci P, Ruozi G, Falcione A, Filigheddu N, Guarnieri G, Graziani A, Giacca M, Barazzoni R. Unacylated Ghrelin Reduces Skeletal Muscle Reactive Oxygen Species Generation and Inflammation and Prevents High-Fat Diet-Induced Hyperglycemia and Whole-Body Insulin Resistance in Rodents. Diabetes. 2016 Apr;65(4):874-86.

Gouranton E, Romier B, Marcotorchino J, Tourniaire F, Astier J, Peiretti F, Landrier JF. Visfatin is involved in TNFα-mediated insulin resistance via an NAD(+)/Sirt1/PTP1B pathway in 3T3-L1 adipocytes. Adipocyte. 2014 Jul 1;3(3):180-9.

Guebre-Egziabher F, Alix PM, Koppe L, Pelletier CC, Kalbacher E, Fouque D, Soulage CO. Ectopic lipid accumulation: A potential cause for metabolic disturbances and a contributor to the alteration of kidney function. Biochimie. 2013 Nov;95(11):1971-9.

Guilherme A, Henriques F, Bedard AH, Czech MP. Molecular pathways linking adipose innervation to insulin action in obesity and diabetes mellitus. Nat Rev Endocrinol. 2019 Apr;15(4):207-225.

Guilherme A, Virbasius JV, Puri V, Czech MP. Adipocyte dysfunctions linking obesity to insulin resistance and type 2 diabetes. Nat Rev Mol Cell Biol. 2008 May;9(5):367-77.

Guinez C, Lemoine J, Michalski JC, Lefebvre T. 70-kDa-heat shock protein presents an adjustable lectinic activity towards O-linked N-acetylglucosamine. Biochem Biophys Res Commun. 2004 Jun 18;319(1):21-6.

Guinez C, Losfeld ME, Cacan R, Michalski JC, Lefebvre T. Modulation of HSP70 GlcNAc-directed lectin activity by glucose availability and utilization. Glycobiology. 2006 Jan;16(1):22-8. doi: 10.

Guinez C, Mir AM, Leroy Y, Cacan R, Michalski JC, Lefebvre T. Hsp70-GlcNAc-binding activity is released by stress, proteasome inhibition, and protein misfolding. Biochem Biophys Res Commun. 2007 Sep 21;361(2):414-20.

Gunawardana SC, Piston DW. Insulin-independent reversal of type 1 diabetes in nonobese diabetic mice with brown adipose tissue transplant. Am J Physiol Endocrinol Metab. 2015 Jun 15;308(12):E1043-55.

Gunawardana SC, Piston DW. Reversal of type 1 diabetes in mice by brown adipose tissue transplant. Diabetes. 2012 Mar;61(3):674-82.

Gutierrez JA, Solenberg PJ, Perkins DR, Willency JA, Knierman MD, Jin Z, Witcher DR, Luo S, Onyia JE, Hale JE. Ghrelin octanoylation mediated by an orphan lipid transferase. Proc Natl Acad Sci U S A. 2008 Apr 29;105(17):6320-5.

Halberg N, Khan T, Trujillo ME, Wernstedt-Asterholm I, Attie AD, Sherwani S, Wang ZV, Landskroner-Eiger S, Dineen S, Magalang UJ, Brekken RA, Scherer PE. Hypoxia-inducible factor 1alpha induces fibrosis and insulin resistance in white adipose tissue. Mol Cell Biol. 2009 Aug;29(16):4467-83.

Hammond E, McKinnon E, Nolan D. Human immunodeficiency virus treatment-induced adipose tissue pathology and lipoatrophy: prevalence and metabolic consequences. Clin Infect Dis. 2010 Sep 1;51(5):591-9.

Hammoud SH, AlZaim I, Al-Dhaheri Y, Eid AH, El-Yazbi AF. Perirenal Adipose Tissue Inflammation: Novel Insights Linking Metabolic Dysfunction to Renal Diseases. Front Endocrinol (Lausanne). 2021 Aug 2;12:707126.

Han MS, White A, Perry RJ, Camporez JP, Hidalgo J, Shulman GI, Davis RJ. Regulation of adipose tissue inflammation by interleukin 6. Proc Natl Acad Sci U S A. 2020 Feb 11;117(6):2751-2760.

Hanover JA, Krause MW, Love DC. Bittersweet memories: linking metabolism to epigenetics through O-GlcNAcylation. Nat Rev Mol Cell Biol. 2012 Apr 23;13(5):312-21.

Hanover JA, Krause MW, Love DC. The hexosamine signaling pathway: O-GlcNAc cycling in feast or famine. Biochim Biophys Acta. 2010 Feb;1800(2):80-95.

Hardivillé S, Hart GW. Nutrient regulation of signaling, transcription, and cell physiology by O-GlcNAcylation. Cell Metab. 2014 Aug 5;20(2):208-13.

Hart GW, Slawson C, Ramirez-Correa G, Lagerlof O. Cross talk between O-GlcNAcylation and phosphorylation: roles in signaling, transcription, and chronic disease. Annu Rev Biochem. 2011;80:825-58.

Haus JM, Kashyap SR, Kasumov T, Zhang R, Kelly KR, Defronzo RA, Kirwan JP. Plasma ceramides are elevated in obese subjects with type 2 diabetes and correlate with the severity of insulin resistance. Diabetes. 2009 Feb;58(2):337-43.

Hedayati N, Annambhotla S, Jiang J, Wang X, Chai H, Lin PH, Yao Q, Chen C. Growth hormone-releasing peptide ghrelin inhibits homocysteine-induced endothelial dysfunction in porcine coronary arteries and human endothelial cells. J Vasc Surg. 2009 Jan;49(1):199-207.

Hill AA, Reid Bolus W, Hasty AH. A decade of progress in adipose tissue macrophage biology. Immunol Rev. 2014;262(1):134–52.

Hong EG, Ko HJ, Cho YR, Kim HJ, Ma Z, Yu TY, Friedline RH, Kurt-Jones E, Finberg R, Fischer MA, Granger EL, Norbury CC, Hauschka SD, Philbrick WM, Lee CG, Elias JA, Kim JK. Interleukin-10 prevents diet-induced insulin resistance by attenuating macrophage and cytokine response in skeletal muscle. Diabetes. 2009 Nov;58(11):2525-35.

Hopkins AL, Nelson TA, Guschina IA, Parsons LC, Lewis CL, Brown RC, Christian HC, Davies JS, Wells T. Unacylated ghrelin promotes adipogenesis in rodent bone marrow via ghrelin O-acyl transferase and GHS-R1a activity: evidence for target cell-induced acylation. Sci Rep. 2017 Mar 31;7:45541.

Hotamisligil GS, Johnson RS, Distel RJ, Ellis R, Papaioannou VE, Spiegelman BM. Uncoupling of obesity from insulin resistance through a targeted mutation in aP2, the adipocyte fatty acid binding protein. Science. 1996 Nov 22;274(5291):1377-9.

Hotamisligil GS. Foundations of Immunometabolism and Implications for Metabolic Health and Disease. Immunity. 2017 Sep 19;47(3):406-420.

Housley MP, Rodgers JT, Udeshi ND, Kelly TJ, Shabanowitz J, Hunt DF, Puigserver P, Hart GW. O-GlcNAc regulates FoxO activation in response to glucose. J Biol Chem. 2008 Jun 13;283(24):16283-92.

Huang PL. A comprehensive definition for metabolic syndrome. Dis Model Mech. 2009 May-Jun;2(5-6):231-7.

Hube F, Hauner H. The role of TNF-alpha in human adipose tissue: prevention of weight gain at the expense of insulin resistance? Horm Metab Res. 1999 Dec;31(12):626-31.

Hui X, Gu P, Zhang J, Nie T, Pan Y, Wu D, Feng T, Zhong C, Wang Y, Lam KS, Xu A. Adiponectin Enhances Cold-Induced Browning of Subcutaneous Adipose Tissue via Promoting M2 Macrophage Proliferation. Cell Metab. 2015 Aug 4;22(2):279-90.

Ibrahim MM. Subcutaneous and visceral adipose tissue: structural and functional differences. Obes Rev. 2010 Jan;11(1):11-8. doi: 10.1111/j.1467-789X.2009.00623.x. Epub 2009 Jul 28. PMID: 19656312

Ida S, Morino K, Sekine O, Ohashi N, Kume S, Chano T, Iwasaki K, Harada N, Inagaki N, Ugi S, Maegawa H. Diverse metabolic effects of O-GlcNAcylation in the pancreas but limited effects in insulin-sensitive organs in mice. Diabetologia. 2017 Sep;60(9):1761-1769.

Ikenoya C, Takemi S, Kaminoda A, Aizawa S, Ojima S, Gong Z, Chacrabati R, Kondo D, Wada R, Tanaka T, Tsuda S, Sakai T, Sakata I. β-Oxidation in ghrelin-producing cells is important for ghrelin acyl-modification. Sci Rep. 2018 Jun 15;8(1):9176.

Jager J, Grémeaux T, Cormont M, Le Marchand-Brustel Y, Tanti JF. Interleukin-1beta-induced insulin resistance in adipocytes through down-regulation of insulin receptor substrate-1 expression. Endocrinology. 2007 Jan;148(1):241-51.

Jang HS, Noh MR, Kim J, Padanilam BJ. Defective Mitochondrial Fatty Acid Oxidation and Lipotoxicity in Kidney Diseases. Front Med (Lausanne). 2020 Mar 12;7:65.

Jarkovská Z, Rosická M, Krsek M, Sulková S, Haluzík M, Justová V, Lacinová Z, Marek J. Plasma ghrelin levels in patients with end-stage renal disease. Physiol Res. 2005;54(4):403-8.

Jensen PN, Fretts AM, Yu C, Hoofnagle AN, Umans JG, Howard BV, Sitlani CM, Siscovick DS, King IB, Sotoodehnia N, McKnight B, Lemaitre RN. Circulating sphingolipids, fasting glucose, and impaired fasting glucose: The Strong Heart Family Study. EBioMedicine. 2019 Mar;41:44-49.

Kajimura S. Adipose tissue in 2016: Advances in the understanding of adipose tissue biology. Nat Rev Endocrinol. 2017 Feb;13(2):69-70.

Kelley DE, Wing R, Buonocore C, Sturis J, Polonsky K, Fitzsimmons M. Relative effects of calorie restriction and weight loss in noninsulin-dependent diabetes mellitus. J Clin Endocrinol Metab. 1993 Nov;77(5):1287-93.

Kersten S. Mechanisms of nutritional and hormonal regulation of lipogenesis. EMBO Rep. 2001 Apr;2(4):282-6.

Khatib MN, Gaidhane S, Gaidhane AM, Simkhada P, Zahiruddin QS. Ghrelin O Acyl Transferase (GOAT) as a Novel Metabolic Regulatory Enzyme. J Clin Diagn Res. 2015 Feb;9(2):LE01-5.

Kim J, Kundu M, Viollet B, Guan KL. AMPK and mTOR regulate autophagy through direct phosphorylation of Ulk1. Nat Cell Biol. 2011 Feb;13(2):132-41.

Kim JK. Fat uses a TOLL-road to connect inflammation and diabetes. Cell Metab. 2006 Dec;4(6):417-9.

Kim JY, van de Wall E, Laplante M, Azzara A, Trujillo ME, Hofmann SM, Schraw T, Durand JL, Li H, Li G, Jelicks LA, Mehler MF, Hui DY, Deshaies Y, Shulman GI, Schwartz GJ, Scherer PE. Obesity-associated improvements in metabolic profile through expansion of adipose tissue. J Clin Invest. 2007 Sep;117(9):2621-37.

Kim MS, Yoon CY, Jang PG, Park YJ, Shin CS, Park HS, Ryu JW, Pak YK, Park JY, Lee KU, Kim SY, Lee HK, Kim YB, Park KS. The mitogenic and antiapoptotic actions of ghrelin in 3T3-L1 adipocytes. Mol Endocrinol. 2004 Sep;18(9):2291-301.

Kim YS, Lee JS, Lee TH, Cho JY, Kim JO, Kim WJ, Kim HG, Jeon SR, Jeong HS. Plasma levels of acylated ghrelin in patients with functional dyspepsia. World J Gastroenterol. 2012 May 14;18(18):2231-7.

Klok MD, Jakobsdottir S, Drent ML. The role of leptin and ghrelin in the regulation of food intake and body weight in humans: a review. Obes Rev. 2007 Jan;8(1):21-34.

Kojima M, Hamamoto A, Sato T. Ghrelin O-acyltransferase (GOAT), a specific enzyme that modifies ghrelin with a medium-chain fatty acid. J Biochem. 2016 Oct;160(4):189-194.

Kojima M, Hosoda H, Date Y, Nakazato M, Matsuo H, Kangawa K. Ghrelin is a growth-hormone-releasing acylated peptide from stomach. Nature. 1999 Dec 9;402(6762):656-60.

Kojima M, Kangawa K. Ghrelin: structure and function. Physiol Rev. 2005 Apr;85(2):495-522.

Koliaki C, Kokkinos A, Tentolouris N, Katsilambros N. The effect of ingested macronutrients on postprandial ghrelin response: a critical review of existing literature data. Int J Pept. 2010;2010:710852.

Kopchick JJ, Berryman DE, Puri V, Lee KY, Jorgensen JOL. The effects of growth hormone on adipose tissue: old observations, new mechanisms. Nat Rev Endocrinol. 2020 Mar;16(3):135-146.

Koshiba T, Detmer SA, Kaiser JT, Chen H, McCaffery JM, Chan DC. Structural basis of mitochondrial tethering by mitofusin complexes. Science. 2004 Aug 6;305(5685):858-62.

Krahmer N, Farese RV Jr, Walther TC. Balancing the fat: lipid droplets and human disease. EMBO Mol Med. 2013 Jul;5(7):973-83.

Kujoth GC, Bradshaw PC, Haroon S, Prolla TA. The role of mitochondrial DNA mutations in mammalian aging. PLoS Genet. 2007 Feb 23;3(2):e24.

Kusminski CM, Bickel PE, Scherer PE. Targeting adipose tissue in the treatment of obesity-associated diabetes. Nat Rev Drug Discov. 2016 Sep;15(9):639-660.

Laclaustra M, Corella D, Ordovas JM. Metabolic syndrome pathophysiology: the role of adipose tissue. Nutr Metab Cardiovasc Dis. 2007 Feb;17(2):125-39.

Lagarde D, Jeanson Y, Barreau C, Moro C, Peyriga L, Cahoreau E, Guissard C, Arnaud E, Galinier A, Bouzier-Sore AK, Pellerin L, Chouchani ET, Pénicaud L, Ader I, Portais JC, Casteilla L, Carrière A. Lactate fluxes mediated by the monocarboxylate transporter-1 are key determinants of the metabolic activity of beige adipocytes. J Biol Chem. 2021 Jan-Jun;296:100137.

Lauritzen ES, Jørgensen JOL, Møller N, Nielsen S, Vestergaard ET. Increased lipolysis after infusion of acylated ghrelin: a randomized, double-blinded placebo-controlled trial in hypopituitary patients. Clin Endocrinol (Oxf). 2020 Dec;93(6):672-677.

Lazarus BD, Love DC, Hanover JA. Recombinant O-GlcNAc transferase isoforms: identification of O-GlcNAcase, yes tyrosine kinase, and tau as isoform-specific substrates. Glycobiology. 2006 May;16(5):415-21.

Lee HH, Kang SK, Yoon YE, Huh KH, Kim MS, Kim SI, Kim YS, Han WK. Impact of the Ratio of Visceral to Subcutaneous Adipose Tissue in Donor Nephrectomy Patients. Transplant Proc. 2017 Jun;49(5):940-943.

Lee K, Kuo CK. Extracellular matrix remodeling and mechanical stresses as modulators of adipose tissue metabolism and inflammation. The mechanobiology of obesity and related diseases. 2013. p. 105–22.

Lee MW, Odegaard JI, Mukundan L, Qiu Y, Molofsky AB, Nussbaum JC, Yun K, Locksley RM, Chawla A. Activated type 2 innate lymphoid cells regulate beige fat biogenesis. Cell. 2015 Jan 15;160(1-2):74-87.

Lemarié F, Beauchamp E, Drouin G, Legrand P, Rioux V. Dietary caprylic acid and ghrelin O-acyltransferase activity to modulate octanoylated ghrelin functions: What is new in this nutritional field? Prostaglandins Leukot Essent Fatty Acids. 2018 Aug;135:121-127.

Lenz M, Arts ICW, Peeters RLM, de Kok TM, Ertaylan G. Adipose tissue in health and disease through the lens of its building blocks. Sci Rep. 2020 Jun 26;10(1):10433.

Li MD, Ruan HB, Hughes ME, Lee JS, Singh JP, Jones SP, Nitabach MN, Yang X. O-GlcNAc signaling entrains the circadian clock by inhibiting BMAL1/CLOCK ubiquitination. Cell Metab. 2013 Feb 5;17(2):303-10.

Li MD, Vera NB, Yang Y, Zhang B, Ni W, Ziso-Qejvanaj E, Ding S, Zhang K, Yin R, Wang S, Zhou X, Fang EX, Xu T, Erion DM, Yang X. Adipocyte OGT governs diet-induced hyperphagia and obesity. Nat Commun. 2018 Nov 30;9(1):5103.

Li P, Liu S, Lu M, Bandyopadhyay G, Oh D, Imamura T, Johnson AMF, Sears D, Shen Z, Cui B, Kong L, Hou S, Liang X, Iovino S, Watkins SM, Ying W, Osborn O, Wollam J, Brenner M, Olefsky JM. Hematopoietic-Derived Galectin-3 Causes Cellular and Systemic Insulin Resistance. Cell. 2016 Nov 3;167(4):973-984.e12.

Li RY, Li XS, Shao L, Wu ZY, Du WH, Li SX, Zhao SX, Chen KM, Chen MD, Song HD. Influence of visceral adiposity on ghrelin secretion and expression in rats during fasting. J Mol Endocrinol. 2009 Jan;42(1):67-74.

Li Y, Xu S, Mihaylova MM, Zheng B, Hou X, Jiang B, Park O, Luo Z, Lefai E, Shyy JY, Gao B, Wierzbicki M, Verbeuren TJ, Shaw RJ, Cohen RA, Zang M. AMPK phosphorylates and inhibits SREBP activity to attenuate hepatic steatosis and atherosclerosis in diet-induced insulin-resistant mice. Cell Metab. 2011 Apr 6;13(4):376-388.

Liao P, Yang D, Liu D, Zheng Y. GLP-1 and Ghrelin Attenuate High Glucose/High Lipid-Induced Apoptosis and Senescence of Human Microvascular Endothelial Cells. Cell Physiol Biochem. 2017;44(5):1842-1855.

Liesa M, Shirihai OS. Mitochondrial dynamics in the regulation of nutrient utilization and energy expenditure. Cell Metab. 2013 Apr 2;17(4):491-506.

Lim CT, Korbonits M. Paediatric endocrine aspects of ghrelin. Pediatr Endocrinol Rev. 2012 Mar;9(3):628-38.

Lin L, Lee JH, Buras ED, Yu K, Wang R, Smith CW, Wu H, Sheikh-Hamad D, Sun Y. Ghrelin receptor regulates adipose tissue inflammation in aging. Aging (Albany NY). 2016 Jan;8(1):178-91.

Lin L, Saha PK, Ma X, Henshaw IO, Shao L, Chang BH, Buras ED, Tong Q, Chan L, McGuinness OP, Sun Y. Ablation of ghrelin receptor reduces adiposity and improves insulin sensitivity during aging by regulating fat metabolism in white and brown adipose tissues. Aging Cell. 2011 Dec;10(6):996-1010.

Liu H, Luo J, Guillory B, Chen JA, Zang P, Yoeli JK, Hernandez Y, Lee II, Anderson B, Storie M, Tewnion A, Garcia JM. Ghrelin ameliorates tumor-induced adipose tissue atrophy and

inflammation *via* Ghrelin receptor-dependent and -independent pathways. Oncotarget. 2020 Sep 1;11(35):3286-3302.

Liu J, Lin H, Cheng P, Hu X, Lu H. Effects of ghrelin on the proliferation and differentiation of 3T3-L1 preadipocytes. J Huazhong Univ Sci Technolog Med Sci. 2009 Apr;29(2):227-30.

Liu Y, Ren Y, Cao Y, Huang H, Wu Q, Li W, Wu S, Zhang J. Discovery of a Low Toxicity O-GlcNAc Transferase (OGT) Inhibitor by Structure-based Virtual Screening of Natural Products. Sci Rep. 2017 Sep 26;7(1):12334.

Liu Y, Yao RZ, Lian S, Liu P, Hu YJ, Shi HZ, Lv HM, Yang YY, Xu B, Li SZ. O-GlcNAcylation: the "stress and nutrition receptor" in cell stress response. Cell Stress Chaperones. 2021 Mar;26(2):297-309.

Loh K, Deng H, Fukushima A, Cai X, Boivin B, Galic S, Bruce C, Shields BJ, Skiba B, Ooms LM, Stepto N, Wu B, Mitchell CA, Tonks NK, Watt MJ, Febbraio MA, Crack PJ, Andrikopoulos S, Tiganis T. Reactive oxygen species enhance insulin sensitivity. Cell Metab. 2009 Oct;10(4):260-72.

Lomenick JP, Melguizo MS, Mitchell SL, Summar ML, Anderson JW. Effects of meals high in carbohydrate, protein, and fat on ghrelin and peptide YY secretion in prepubertal children. J Clin Endocrinol Metab. 2009 Nov;94(11):4463-71.

Lumeng CN, Deyoung SM, Saltiel AR. Macrophages block insulin action in adipocytes by altering expression of signaling and glucose transport proteins. Am J Physiol Endocrinol Metab. 2007 Jan;292(1):E166-74.

Ma X, Lin L, Yue J, Pradhan G, Qin G, Minze LJ, Wu H, Sheikh-Hamad D, Smith CW, Sun Y. Ghrelin receptor regulates HFCS-induced adipose inflammation and insulin resistance. Nutr Diabetes. 2013 Dec 23;3(12):e99.

Mak RH, Cheung W, Purnell J. Ghrelin in chronic kidney disease: too much or too little? Perit Dial Int. 2007 Jan-Feb;27(1):51-5.

Mancini G, Pirruccio K, Yang X, Blüher M, Rodeheffer M, Horvath TL. Mitofusin 2 in Mature Adipocytes Controls Adiposity and Body Weight. Cell Rep. 2019 Mar 12;26(11):2849-2858.e4.

Manning BD, Tee AR, Logsdon MN, Blenis J, Cantley LC. Identification of the tuberous sclerosis complex-2 tumor suppressor gene product tuberin as a target of the phosphoinositide 3-kinase/akt pathway. Mol Cell. 2002 Jul;10(1):151-62.

Mansuy-Aubert V, Zhou QL, Xie X, Gong Z, Huang JY, Khan AR, Aubert G, Candelaria K, Thomas S, Shin DJ, Booth S, Baig SM, Bilal A, Hwang D, Zhang H, Lovell-Badge R, Smith SR, Awan FR, Jiang ZY. Imbalance between neutrophil elastase and its inhibitor α1-antitrypsin in obesity alters insulin sensitivity, inflammation, and energy expenditure. Cell Metab. 2013 Apr 2;17(4):534-48.

Martin-Taboada M, Vila-Bedmar R, Medina-Gómez G. From Obesity to Chronic Kidney Disease: How Can Adipose Tissue Affect Renal Function? Nephron. 2021;145(6):609-613.

Martos-Rus C, Katz-Greenberg G, Lin Z, Serrano E, Whitaker-Menezes D, Domingo-Vidal M, Roche M, Ramaswamy K, Hooper DC, Falkner B, Martinez Cantarin MP. Macrophage and adipocyte interaction as a source of inflammation in kidney disease. Sci Rep. 2021 Feb 3;11(1):2974.

Martyniak K, Masternak MM. Changes in adipose tissue cellular composition during obesity and aging as a cause of metabolic dysregulation. Exp Gerontol. 2017 Aug;94:59-63.

Matsuo K, Nakano M, Nakashima M, Watanuki T, Egashira K, Matsubara T, Watanabe Y. Neural correlates of plasma acylated ghrelin level in individuals with major depressive disorder. Brain Res. 2012 Sep 14;1473:185-92.

Miao H, Pan H, Wang L, Yang H, Zhu H, Gong F. Ghrelin Promotes Proliferation and Inhibits Differentiation of 3T3-L1 and Human Primary Preadipocytes. Front Physiol. 2019 Oct 11;10:1296.

Michailidou Z, Turban S, Miller E, Zou X, Schrader J, Ratcliffe PJ, et al. Increased angiogenesis protects against adipose hypoxia and fibrosis in metabolic disease-resistant 11beta-hydroxysteroid dehydrogenase type 1 (HSD1)-deficient mice. J Biol Chem. 2012;287(6):4188–97.

Michel H, Behr J, Harrenga A, Kannt A. Cytochrome c oxidase: structure and spectroscopy. Annu Rev Biophys Biomol Struct. 1998;27:329-56.

Mihalache L, Gherasim A, Niţă O, Ungureanu MC, Pădureanu SS, Gavril RS, Arhire LI. Effects of ghrelin in energy balance and body weight homeostasis. Hormones (Athens). 2016 Feb;15(2):186-196.

Minakuchi H, Wakino S, Hosoya K, Sueyasu K, Hasegawa K, Shinozuka K, Yoshifuji A, Futatsugi K, Komatsu M, Kanda T, Tokuyama H, Hayashi K, Itoh H. The role of adipose tissue asymmetric dimethylarginine/dimethylarginine dimethylaminohydrolase pathway in adipose tissue phenotype and metabolic abnormalities in subtotally nephrectomized rats. Nephrol Dial Transplant. 2016 Mar;31(3):413-23.

Minokoshi Y, Alquier T, Furukawa N, Kim YB, Lee A, Xue B, Mu J, Foufelle F, Ferré P, Birnbaum MJ, Stuck BJ, Kahn BB. AMP-kinase regulates food intake by responding to hormonal and nutrient signals in the hypothalamus. Nature. 2004 Apr 1;428(6982):569-74.

Mohallem R, Aryal UK. Regulators of TNFα mediated insulin resistance elucidated by quantitative proteomics. Sci Rep. 2020 Nov 30;10(1):20878.

Moller DE, Flier JS. Insulin resistance--mechanisms, syndromes, and implications. N Engl J Med. 1991 Sep 26;325(13):938-48.

Mu Y, Yu H, Wu T, Zhang J, Evans SM, Chen J. O-linked β-N-acetylglucosamine transferase plays an essential role in heart development through regulating angiopoietin-1. PLoS Genet. 2020 Apr 6;16(4):e1008730.

Mueckler M, Thorens B. The SLC2 (GLUT) family of membrane transporters. Mol Aspects Med. 2013 Apr-Jun;34(2-3):121-38.

Mueller, T., Ouyang, X., Johnson, M. S., Qian, W.-J., Chatham, J. C., Darley-Usmar, V., & Zhang, J. (2021). New Insights Into the Biology of Protein O-GlcNAcylation: Approaches and Observations. *Frontiers in Aging*, *1*.

Murashima M, Nishimoto M, Kokubu M, Hamano T, Matsui M, Eriguchi M, Samejima KI, Akai Y, Tsuruya K. Inflammation as a predictor of acute kidney injury and mediator of higher mortality after acute kidney injury in non-cardiac surgery. Sci Rep. 2019 Dec 30;9(1):20260.

Murata K, Morino K, Ida S, Ohashi N, Lemecha M, Park SY, Ishikado A, Kume S, Choi CS, Sekine O, Ugi S, Maegawa H. Lack of O-GlcNAcylation enhances exercise-dependent glucose utilization potentially through AMP-activated protein kinase activation in skeletal muscle. Biochem Biophys Res Commun. 2018 Jan 8;495(2):2098-2104.

Nakai Y, Hosoda H, Nin K, Ooya C, Hayashi H, Akamizu T, Kangawa K. Plasma levels of active form of ghrelin during oral glucose tolerance test in patients with anorexia nervosa. Eur J Endocrinol. 2003 Jul;149(1):R1-3.

Navé BT, Ouwens M, Withers DJ, Alessi DR, Shepherd PR. Mammalian target of rapamycin is a direct target for protein kinase B: identification of a convergence point for opposing effects of insulin and amino-acid deficiency on protein translation. Biochem J. 1999 Dec 1;344 Pt 2(Pt 2):427-31.

NCD Risk Factor Collaboration (NCD-RisC). Worldwide trends in diabetes since 1980: a pooled analysis of 751 population-based studies with 4.4 million participants. Lancet. 2016 Apr 9;387(10027):1513-1530. doi: 10.1016/S0140-6736(16)00618-8. Epub 2016 Apr 6. Erratum in: Lancet. 2017 Feb 4;389(10068):e2. PMID: 27061677; PMCID: PMC5081106.

Ngoh GA, Facundo HT, Zafir A, Jones SP. O-GlcNAc signaling in the cardiovascular system. Circ Res. 2010 Jul 23;107(2):171-85.

Ohashi N, Morino K, Ida S, Sekine O, Lemecha M, Kume S, Park SY, Choi CS, Ugi S, Maegawa H. Pivotal Role of *O*-GlcNAc Modification in Cold-Induced Thermogenesis by Brown Adipose Tissue Through Mitochondrial Biogenesis. Diabetes. 2017 Sep;66(9):2351-2362.

Okura T, Koda M, Ando F, Niino N, Tanaka M, Shimokata H. Association of the mitochondrial DNA 15497G/A polymorphism with obesity in a middle-aged and elderly Japanese population. Hum Genet. 2003 Oct;113(5):432-6.

Olivero A, Basso L, Barabino E, Milintenda P, Testino N, Chierigo F, Dell'oglio P, Neumaier CE, Suardi N, Terrone C. The impact of visceral adipose tissue on post -operative renal Function after Radical Nephrectomy for renal cell carcinoma. Minerva Urol Nephrol. 2021 Mar 26.

O'Rourke RW. Adipose tissue and the physiologic underpinnings of metabolic disease. Surg Obes Relat Dis. 2018 Nov;14(11):1755-1763.

Ortiz-Meoz RF, Jiang J, Lazarus MB, Orman M, Janetzko J, Fan C, Duveau DY, Tan ZW, Thomas CJ, Walker S. A small molecule that inhibits OGT activity in cells. ACS Chem Biol. 2015 Jun 19;10(6):1392-7.

Park A, Kim WK, Bae KH. Distinction of white, beige and brown adipocytes derived from mesenchymal stem cells. World J Stem Cells. 2014 Jan 26;6(1):33-42.

Pelletier CC, Koppe L, Croze ML, Kalbacher E, Vella RE, Guebre-Egziabher F, Géloën A, Badet L, Fouque D, Soulage CO. White adipose tissue overproduces the lipid-mobilizing factor zinc α2-glycoprotein in chronic kidney disease. Kidney Int. 2013 May;83(5):878-86.

Pengcheng Zhang, Daniels Konja, Yu Wang. Adipose tissue secretory profile and cardiometabolic risk in obesity, Endocrine and Metabolic Science, Volume 1, Issues 3–4, 2020, 100061, ISSN 2666-3961.

Perry RJ, Camporez JG, Kursawe R, Titchenell PM, Zhang D, Perry CJ, Jurczak MJ, Abudukadier A, Han MS, Zhang XM, Ruan HB, Yang X, Caprio S, Kaech SM, Sul HS, Birnbaum MJ, Davis RJ, Cline

GW, Petersen KF, Shulman GI. Hepatic acetyl CoA links adipose tissue inflammation to hepatic insulin resistance and type 2 diabetes. Cell. 2015 Feb 12;160(4):745-758.

Perry RJ, Lyu K, Rabin-Court A, Dong J, Li X, Yang Y, Qing H, Wang A, Yang X, Shulman GI. Leptin mediates postprandial increases in body temperature through hypothalamus-adrenal medulla-adipose tissue crosstalk. J Clin Invest. 2020 Apr 1;130(4):2001-2016.

Peterson RT, Beal PA, Comb MJ, Schreiber SL. FKBP12-rapamycin-associated protein (FRAP) autophosphorylates at serine 2481 under translationally repressive conditions. J Biol Chem. 2000 Mar 10;275(10):7416-23.

Pradhan G, Samson SL, Sun Y. Ghrelin: much more than a hunger hormone. Curr Opin Clin Nutr Metab Care. 2013 Nov;16(6):619-24.

Pullen N, Thomas G. The modular phosphorylation and activation of p70s6k. FEBS Lett. 1997 Jun 23;410(1):78-82.

Qi L, Cui X, Dong W, Barrera R, Nicastro J, Coppa GF, Wang P, Wu R. Ghrelin attenuates brain injury after traumatic brain injury and uncontrolled hemorrhagic shock in rats. Mol Med. 2012 Mar 27;18(1):186-93.

Rahman I, Kode A, Biswas SK. Assay for quantitative determination of glutathione and glutathione disulfide levels using enzymatic recycling method. Nat Protoc. 2006;1(6):3159-65.

Rindi G, Necchi V, Savio A, Torsello A, Zoli M, Locatelli V, Raimondo F, Cocchi D, Solcia E. Characterisation of gastric ghrelin cells in man and other mammals: studies in adult and fetal tissues. Histochem Cell Biol. 2002 Jun;117(6):511-9.

Rodríguez A, Gómez-Ambrosi J, Catalán V, Gil MJ, Becerril S, Sáinz N, Silva C, Salvador J, Colina I, Frühbeck G. Acylated and desacyl ghrelin stimulate lipid accumulation in human visceral adipocytes. Int J Obes (Lond). 2009 May;33(5):541-52.

Rodríguez A, Gómez-Ambrosi J, Catalán V, Rotellar F, Valentí V, Silva C, Mugueta C, Pulido MR, Vázquez R, Salvador J, Malagón MM, Colina I, Frühbeck G. The ghrelin O-acyltransferase-ghrelin system reduces TNF-α-induced apoptosis and autophagy in human visceral adipocytes.

Rong JX, Qiu Y, Hansen MK, Zhu L, Zhang V, Xie M, Okamoto Y, Mattie MD, Higashiyama H, Asano S, Strum JC, Ryan TE. Adipose mitochondrial biogenesis is suppressed in db/db and high-fat diet-fed mice and improved by rosiglitazone. Diabetes. 2007 Jul;56(7):1751-60.

Ruan H, Hacohen N, Golub TR, Van Parijs L, Lodish HF. Tumor necrosis factor-alpha suppresses adipocyte-specific genes and activates expression of preadipocyte genes in 3T3-L1 adipocytes: nuclear factor-kappaB activation by TNF-alpha is obligatory. Diabetes. 2002 May;51(5):1319-36.

Ruan HB, Dietrich MO, Liu ZW, Zimmer MR, Li MD, Singh JP, Zhang K, Yin R, Wu J, Horvath TL, Yang X. O-GlcNAc transferase enables AgRP neurons to suppress browning of white fat. Cell. 2014 Oct 9;159(2):306-17.

Ruan HB, Han X, Li MD, Singh JP, Qian K, Azarhoush S, Zhao L, Bennett AM, Samuel VT, Wu J, Yates JR 3rd, Yang X. O-GlcNAc transferase/host cell factor C1 complex regulates gluconeogenesis by modulating PGC-1α stability. Cell Metab. 2012 Aug 8;16(2):226-37.

Ruan HB, Nie Y, Yang X. Regulation of protein degradation by O-GlcNAcylation: crosstalk with ubiquitination. Mol Cell Proteomics. 2013 Dec;12(12):3489-97.

Ruby MA, Massart J, Hunerdosse DM, Schönke M, Correia JC, Louie SM, Ruas JL, Näslund E, Nomura DK, Zierath JR. Human Carboxylesterase 2 Reverses Obesity-Induced Diacylglycerol Accumulation and Glucose Intolerance. Cell Rep. 2017 Jan 17;18(3):636-646.

Ruozi G, Bortolotti F, Recchia F.A. , Chapter 6 - Gut-Derived Hormones—Cardiac Effects of Ghrelin and Glucagon-Like Peptide-1, Editor(s): Jonathan C. Schisler, Charles H. Lang, Monte S. Willis, Endocrinology of the Heart in Health and Disease, Academic Press, 2017, Pages 139-166, ISBN 9780128031117.

Saito N, Furuhashi M, Koyama M, Higashiura Y, Akasaka H, Tanaka M, Moniwa N, Ohnishi H, Saitoh S, Ura N, Shimamoto K, Miura T. Elevated circulating FABP4 concentration predicts cardiovascular death in a general population: a 12-year prospective study. Sci Rep. 2021 Feb 17;11(1):4008.

Sanchez-Gurmaches J, Tang Y, Jespersen NZ, Wallace M, Martinez Calejman C, Gujja S, Li H, Edwards YJK, Wolfrum C, Metallo CM, Nielsen S, Scheele C, Guertin DA. Brown Fat AKT2 Is a Cold-Induced Kinase that Stimulates ChREBP-Mediated De Novo Lipogenesis to Optimize Fuel Storage and Thermogenesis. Cell Metab. 2018 Jan 9;27(1):195-209.e6.

Sangiao-Alvarellos S, Vázquez MJ, Varela L, Nogueiras R, Saha AK, Cordido F, López M, Diéguez C. Central ghrelin regulates peripheral lipid metabolism in a growth hormone-independent fashion. Endocrinology. 2009 Oct;150(10):4562-74.

Santoro A, McGraw TE, Kahn BB. Insulin action in adipocytes, adipose remodeling, and systemic effects. Cell Metab. 2021 Apr 6;33(4):748-757.

Saponaro C, Gaggini M, Carli F, Gastaldelli A. The Subtle Balance between Lipolysis and Lipogenesis: A Critical Point in Metabolic Homeostasis. Nutrients. 2015 Nov 13;7(11):9453-74.

Sato T, Nakamura Y, Shiimura Y, Ohgusu H, Kangawa K, Kojima M. Structure, regulation and function of ghrelin. J Biochem. 2012 Feb;151(2):119-28.

Schalla MA, Stengel A. The Role of Ghrelin in Anorexia Nervosa. Int J Mol Sci. 2018 Jul 20;19(7):2117.

Shafi R, Iyer SP, Ellies LG, O'Donnell N, Marek KW, Chui D, Hart GW, Marth JD. The O-GlcNAc transferase gene resides on the X chromosome and is essential for embryonic stem cell viability and mouse ontogeny. Proc Natl Acad Sci U S A. 2000 May 23;97(11):5735-9.

Shapiro H, Pecht T, Shaco-Levy R, Harman-Boehm I, Kirshtein B, Kuperman Y, Chen A, Blüher M, Shai I, Rudich A. Adipose tissue foam cells are present in human obesity. J Clin Endocrinol Metab. 2013 Mar;98(3):1173-81.

Shepherd PR, Gnudi L, Tozzo E, Yang H, Leach F, Kahn BB. Adipose cell hyperplasia and enhanced glucose disposal in transgenic mice overexpressing GLUT4 selectively in adipose tissue. J Biol Chem. 1993 Oct 25;268(30):22243-6.

Shi H, Munk A, Nielsen TS, Daughtry MR, Larsson L, Li S, Høyer KF, Geisler HW, Sulek K, Kjøbsted R, Fisher T, Andersen MM, Shen Z, Hansen UK, England EM, Cheng Z, Højlund K, Wojtaszewski JFP, Yang X, Hulver MW, Helm RF, Treebak JT, Gerrard DE. Skeletal muscle O-GlcNAc transferase is important for muscle energy homeostasis and whole-body insulin sensitivity. Mol Metab. 2018 May;11:160-177.

Silva JE, Larsen PR. Potential of brown adipose tissue type II thyroxine 5'-deiodinase as a local and systemic source of triiodothyronine in rats. J Clin Invest. 1985 Dec;76(6):2296-305.

Silverio R, Gonçalves DC, Andrade MF, Seelaender M. Coronavirus Disease 2019 (COVID-19) and Nutritional Status: The Missing Link? Adv Nutr. 2021 Jun 1;12(3):682-692.

Smith PK, Krohn RI, Hermanson GT, Mallia AK, Gartner FH, Provenzano MD, Fujimoto EK, Goeke NM, Olson BJ, Klenk DC. Measurement of protein using bicinchoninic acid. Anal Biochem. 1985 Oct;150(1):76-85. H, Kehinde O. An established preadipose cell line and its differentiation in culture. II. Factors affecting the adipose conversion. Cell. 1975 May;5(1):19-27.

Smith U, Kahn BB. Adipose tissue regulates insulin sensitivity: role of adipogenesis, de novo lipogenesis and novel lipids. J Intern Med. 2016 Nov;280(5):465-475. doi: 10.1111/joim.12540. Epub 2016 Oct 3.

Song Z, Xiaoli AM, Yang F. Regulation and Metabolic Significance of De Novo Lipogenesis in Adipose Tissues. Nutrients. 2018 Sep 29;10(10):1383.

Stahl A, Evans JG, Pattel S, Hirsch D, Lodish HF. Insulin causes fatty acid transport protein translocation and enhanced fatty acid uptake in adipocytes. Dev Cell. 2002 Apr;2(4):477-88.

Sun CY, Cheng ML, Pan HC, Lee JH, Lee CC. Protein-bound uremic toxins impaired mitochondrial dynamics and functions. Oncotarget. 2017 Sep 8;8(44):77722-77733.

Sun Y. Ghrelin receptor controls obesity by fat burning. Oncotarget. 2015 Mar 30;6(9):6470-1.

Swarup S, Goyal A, Grigorova Y, et al. Metabolic Syndrome. [Updated 2021 Aug 1]. In: StatPearls [Internet]. Treasure Island (FL): StatPearls Publishing; 2021 Jan-. Available from: https://www.ncbi.nlm.nih.gov/books/NBK459248/

Syed I, Rubin de Celis MF, Mohan JF, Moraes-Vieira PM, Vijayakumar A, Nelson AT, Siegel D, Saghatelian A, Mathis D, Kahn BB. PAHSAs attenuate immune responses and promote β cell survival in autoimmune diabetic mice. J Clin Invest. 2019 Aug 5;129(9):3717-3731.

Sztalryd C, Brasaemle DL. The perilipin family of lipid droplet proteins: Gatekeepers of intracellular lipolysis. Biochim Biophys Acta Mol Cell Biol Lipids. 2017 Oct;1862(10 Pt B):1221-1232.

Taati M, Moghadasi M, Dezfoulian O, Asadian P, Zendehdel M. Effects of Ghrelin on germ cell apoptosis and proinflammatory cytokines production in Ischemia-reperfusion of the rat testis. Iran J Reprod Med. 2015 Feb;13(2):85-92.

Takemura K, Nishi H, Inagi R. Mitochondrial Dysfunction in Kidney Disease and Uremic Sarcopenia. Front Physiol. 2020 Sep 4;11:565023.

Talukdar S, Oh DY, Bandyopadhyay G, Li D, Xu J, McNelis J, Lu M, Li P, Yan Q, Zhu Y, Ofrecio J, Lin M, Brenner MB, Olefsky JM. Neutrophils mediate insulin resistance in mice fed a high-fat diet through secreted elastase. Nat Med. 2012 Sep;18(9):1407-12.

Tamaki M, Hagiwara A, Miyashita K, Wakino S, Inoue H, Fujii K, Fujii C, Sato M, Mitsuishi M, Muraki A, Hayashi K, Doi T, Itoh H. Improvement of Physical Decline Through Combined Effects of Muscle Enhancement and Mitochondrial Activation by a Gastric Hormone Ghrelin in Male 5/6Nx CKD Model Mice. Endocrinology. 2015 Oct;156(10):3638-48.

Tang Y, Wallace M, Sanchez-Gurmaches J, Hsiao WY, Li H, Lee PL, Vernia S, Metallo CM, Guertin DA. Adipose tissue mTORC2 regulates ChREBP-driven de novo lipogenesis and hepatic glucose metabolism. Nat Commun. 2016 Apr 21;7:11365.

Taylor RP, Geisler TS, Chambers JH, McClain DA. Up-regulation of O-GlcNAc transferase with glucose deprivation in HepG2 cells is mediated by decreased hexosamine pathway flux. J Biol Chem. 2009 Feb 6;284(6):3425-32.

Thome T, Salyers ZR, Kumar RA, Hahn D, Berru FN, Ferreira LF, Scali ST, Ryan TE. Uremic metabolites impair skeletal muscle mitochondrial energetics through disruption of the electron transport system and matrix dehydrogenase activity. Am J Physiol Cell Physiol. 2019 Oct 1;317(4):C701-C713.

Tormos KV, Anso E, Hamanaka RB, Eisenbart J, Joseph J, Kalyanaraman B, Chandel NS. Mitochondrial complex III ROS regulate adipocyte differentiation. Cell Metab. 2011 Oct 5;14(4):537-44.

Torres J, Pulido R. The tumor suppressor PTEN is phosphorylated by the protein kinase CK2 at its C terminus. Implications for PTEN stability to proteasome-mediated degradation. J Biol Chem. 2001 Jan 12;276(2):993-8.

Toshinai K, Mondal MS, Nakazato M, Date Y, Murakami N, Kojima M, Kangawa K, Matsukura S. Upregulation of Ghrelin expression in the stomach upon fasting, insulin-induced hypoglycemia, and leptin administration. Biochem Biophys Res Commun. 2001 Mar;281(5):1220-5.

Trapannone R, Mariappa D, Ferenbach AT, van Aalten DM. Nucleocytoplasmic human O-GlcNAc transferase is sufficient for O-GlcNAcylation of mitochondrial proteins. Biochem J. 2016 Jun 15;473(12):1693-702.

Trojnar M, Patro-Małysza J, Kimber-Trojnar Ż, Leszczyńska-Gorzelak B, Mosiewicz J. Associations between Fatty Acid-Binding Protein 4–A Proinflammatory Adipokine and Insulin Resistance, Gestational and Type 2 Diabetes Mellitus. Cells. 2019 Mar 8;8(3):227.

Tschöp M, Smiley DL, Heiman ML. Ghrelin induces adiposity in rodents. Nature. 2000 Oct 19;407(6806):908-13.

Tschöp M, Weyer C, Tataranni PA, Devanarayan V, Ravussin E, Heiman ML. Circulating ghrelin levels are decreased in human obesity. Diabetes. 2001 Apr;50(4):707-9.

Vazirani RP, Verma A, Sadacca LA, Buckman MS, Picatoste B, Beg M, Torsitano C, Bruno JH, Patel RT, Simonyte K, Camporez JP, Moreira G, Falcone DJ, Accili D, Elemento O, Shulman GI, Kahn BB, McGraw TE. Disruption of Adipose Rab10-Dependent Insulin Signaling Causes Hepatic Insulin Resistance. Diabetes. 2016 Jun;65(6):1577-89.

Vazquez F, Ramaswamy S, Nakamura N, Sellers WR. Phosphorylation of the PTEN tail regulates protein stability and function. Mol Cell Biol. 2000 Jul;20(14):5010-8.

Vestergaard ET, Djurhuus CB, Gjedsted J, Nielsen S, Møller N, Holst JJ, Jørgensen JO, Schmitz O. Acute effects of ghrelin administration on glucose and lipid metabolism. J Clin Endocrinol Metab. 2008 Feb;93(2):438-44.

Vijayakumar A, Aryal P, Wen J, Syed I, Vazirani RP, Moraes-Vieira PM, Camporez JP, Gallop MR, Perry RJ, Peroni OD, Shulman GI, Saghatelian A, McGraw TE, Kahn BB. Absence of Carbohydrate

Response Element Binding Protein in Adipocytes Causes Systemic Insulin Resistance and Impairs Glucose Transport. Cell Rep. 2017 Oct 24;21(4):1021-1035.

Wada J, Nakatsuka A. Mitochondrial Dynamics and Mitochondrial Dysfunction in Diabetes. Acta Med Okayama. 2016 Jun;70(3):151-8.

Wang CH, Wang CC, Huang HC, Wei YH. Mitochondrial dysfunction leads to impairment of insulin sensitivity and adiponectin secretion in adipocytes. FEBS J. 2013 Feb;280(4):1039-50.

Wang J, Obici S, Morgan K, Barzilai N, Feng Z, Rossetti L. Overfeeding rapidly induces leptin and insulin resistance. Diabetes. 2001 Dec;50(12):2786-91.

Wang Q, Xie Z, Zhang W, Zhou J, Wu Y, Zhang M, Zhu H, Zou MH. Myeloperoxidase deletion prevents high-fat diet-induced obesity and insulin resistance. Diabetes. 2014 Dec;63(12):4172-85.

Wang W, Bansal S, Falk S, Ljubanovic D, Schrier R. Ghrelin protects mice against endotoxemia-induced acute kidney injury. Am J Physiol Renal Physiol. 2009 Oct;297(4):F1032-7.

Wang Y, Zhu J, Zhang L. Discovery of Cell-Permeable O-GlcNAc Transferase Inhibitors via Tethering in Situ Click Chemistry. J Med Chem. 2017 Jan 12;60(1):263-272.

Westermann B. Mitochondrial fusion and fission in cell life and death. Nat Rev Mol Cell Biol. 2010 Dec;11(12):872-84.

Wigger L, Cruciani-Guglielmacci C, Nicolas A, Denom J, Fernandez N, Fumeron F, Marques-Vidal P, Ktorza A, Kramer W, Schulte A, Le Stunff H, Liechti R, Xenarios I, Vollenweider P, Waeber G, Uphues I, Roussel R, Magnan C, Ibberson M, Thorens B. Plasma Dihydroceramides Are Diabetes Susceptibility Biomarker Candidates in Mice and Humans. Cell Rep. 2017 Feb 28;18(9):2269-2279.

Wilson-Fritch L, Burkart A, Bell G, Mendelson K, Leszyk J, Nicoloro S, Czech M, Corvera S. Mitochondrial biogenesis and remodeling during adipogenesis and in response to the insulin sensitizer rosiglitazone. Mol Cell Biol. 2003 Feb;23(3):1085-94.

Wilson-Fritch L, Nicoloro S, Chouinard M, Lazar MA, Chui PC, Leszyk J, Straubhaar J, Czech MP, Corvera S. Mitochondrial remodeling in adipose tissue associated with obesity and treatment with rosiglitazone. J Clin Invest. 2004 Nov;114(9):1281-9.

Wong RH, Sul HS. Insulin signaling in fatty acid and fat synthesis: a transcriptional perspective. Curr Opin Pharmacol. 2010 Dec;10(6):684-91.

Wren AM, Seal LJ, Cohen MA, Brynes AE, Frost GS, Murphy KG, Dhillo WS, Ghatei MA, Bloom SR. Ghrelin enhances appetite and increases food intake in humans. J Clin Endocrinol Metab. 2001 Dec;86(12):5992.

Wren AM, Small CJ, Ward HL, Murphy KG, Dakin CL, Taheri S, Kennedy AR, Roberts GH, Morgan DG, Ghatei MA, Bloom SR. The novel hypothalamic peptide ghrelin stimulates food intake and growth hormone secretion. Endocrinology. 2000 Nov;141(11):4325-8.

Wu D, Molofsky AB, Liang HE, Ricardo-Gonzalez RR, Jouihan HA, Bando JK, Chawla A, Locksley RM. Eosinophils sustain adipose alternatively activated macrophages associated with glucose homeostasis. Science. 2011 Apr 8;332(6026):243-7.

Wu HY, Li NS, Song YL, Bai CM, Wang Q, Zhao YP, Xiao Y, Yu S, Li M, Chen YJ. Plasma levels of acylated ghrelin in patients with insulinoma and expression of ghrelin and its receptor in insulinomas. Endocrine. 2020 May;68(2):448-457.

Wulff-Fuentes E, Berendt RR, Massman L, Danner L, Malard F, Vora J, Kahsay R, Olivier-Van Stichelen S. The human O-GlcNAcome database and meta-analysis. Sci Data. 2021 Jan 21;8(1):25.

Xiang DM, Song XZ, Zhou ZM, Liu Y, Dai XY, Huang XL, Hou FF, Zhou QG. Chronic kidney disease promotes chronic inflammation in visceral white adipose tissue. Am J Physiol Renal Physiol. 2017 Apr 1;312(4):F689-F701.

Xu A, Tso AW, Cheung BM, Wang Y, Wat NM, Fong CH, Yeung DC, Janus ED, Sham PC, Lam KS. Circulating adipocyte-fatty acid binding protein levels predict the development of the metabolic syndrome: a 5-year prospective study. Circulation. 2007 Mar 27;115(12):1537-43.

Yamauchi T, Kamon J, Waki H, Murakami K, Motojima K, Komeda K, Ide T, Kubota N, Terauchi Y, Tobe K, Miki H, Tsuchida A, Akanuma Y, Nagai R, Kimura S, Kadowaki T. The mechanisms by which both heterozygous peroxisome proliferator-activated receptor gamma (PPARgamma) deficiency and PPARgamma agonist improve insulin resistance. J Biol Chem. 2001 Nov 2;276(44):41245-54.

Yang D, Liu Z, Luo Q. Plasma ghrelin and pro-inflammatory markers in patients with obstructive sleep apnea and stable coronary heart disease. Med Sci Monit. 2013 Apr 8;19:251-6.

Yang J, Brown MS, Liang G, Grishin NV, Goldstein JL. Identification of the acyltransferase that octanoylates ghrelin, an appetite-stimulating peptide hormone. Cell. 2008 Feb 8;132(3):387-96.

Yang Q, Vijayakumar A, Kahn BB. Metabolites as regulators of insulin sensitivity and metabolism. *Nat Rev Mol Cell Biol*. 2018;19(10):654-672.

Yang X, Qian K. Protein O-GlcNAcylation: emerging mechanisms and functions. Nat Rev Mol Cell Biol. 2017 Jul;18(7):452-465.

Yang Y, Fu M, Li MD, Zhang K, Zhang B, Wang S, Liu Y, Ni W, Ong Q, Mi J, Yang X. O-GlcNAc transferase inhibits visceral fat lipolysis and promotes diet-induced obesity. Nat Commun. 2020 Jan 10;11(1):181.

Yasuda T, Masaki T, Kakuma T, Yoshimatsu H. Centrally administered ghrelin suppresses sympathetic nerve activity in brown adipose tissue of rats. Neurosci Lett. 2003 Oct 2;349(2):75-8.

Yokokawa H, Fukuda H, Saita M, Goto K, Kaku T, Miyagami T, Takahashi Y, Hamada C, Hisaoka T, Naito T. An association between visceral or subcutaneous fat accumulation and diabetes mellitus among Japanese subjects. Diabetol Metab Syndr. 2021 Apr 14;13(1):44.

Yoshimoto A, Mori K, Sugawara A, Mukoyama M, Yahata K, Suganami T, Takaya K, Hosoda H, Kojima M, Kangawa K, Nakao K. Plasma ghrelin and desacyl ghrelin concentrations in renal failure. J Am Soc Nephrol. 2002 Nov;13(11):2748-52.

Yuan MJ, Huang CX, Tang YH, Wang X, Huang H, Chen YJ, Wang T. A novel peptide ghrelin inhibits neural remodeling after myocardial infarction in rats. Eur J Pharmacol. 2009 Sep 15;618(1-3):52-7.

Zachara NE, O'Donnell N, Cheung WD, Mercer JJ, Marth JD, Hart GW. Dynamic O-GlcNAc modification of nucleocytoplasmic proteins in response to stress. A survival response of mammalian cells. J Biol Chem. 2004 Jul 16;279(29):30133-42.

Zenitani M, Hosoda H, Nose S, Kangawa K, Kawahara H, Oue T. Importance of plasma ghrelin levels with special reference to nutritional metabolism and energy expenditure in pediatric patients with severe motor and intellectual disabilities. Clin Nutr ESPEN. 2021 Apr;42:180-187.

Zhang F, Su K, Yang X, Bowe DB, Paterson AJ, Kudlow JE. O-GlcNAc modification is an endogenous inhibitor of the proteasome. Cell. 2003 Dec 12;115(6):715-25.

Zhang W, Lin TR, Hu Y, Fan Y, Zhao L, Stuenkel EL, Mulholland MW. Ghrelin stimulates neurogenesis in the dorsal motor nucleus of the vagus. J Physiol. 2004 Sep 15;559(Pt 3):729-37.

Zhang WX, Fan J, Ma J, Rao YS, Zhang L, Yan YE. Selection of Suitable Reference Genes for Quantitative Real-Time PCR Normalization in Three Types of Rat Adipose Tissue. Int J Mol Sci. 2016 Jun 22;17(6):968.

Zhang Y, Goldman S, Baerga R, Zhao Y, Komatsu M, Jin S. Adipose-specific deletion of autophagy-related gene 7 (atg7) in mice reveals a role in adipogenesis. Proc Natl Acad Sci U S A. 2009 Nov 24;106(47):19860-5.

Zhao L, Feng Z, Yang X, Liu J. The regulatory roles of O-GlcNAcylation in mitochondrial homeostasis and metabolic syndrome. Free Radic Res. 2016 Oct;50(10):1080-1088.

Zhao M, Ren K, Xiong X, Cheng M, Zhang Z, Huang Z, Han X, Yang X, Alejandro EU, Ruan HB. Protein O-GlcNAc Modification Links Dietary and Gut Microbial Cues to the Differentiation of Enteroendocrine L Cells. Cell Rep. 2020 Aug 11;32(6):108013.

Zhao T, Hou M, Xia M, Wang Q, Zhu H, Xiao Y, Tang Z, Ma J, Ling W. Globular adiponectin decreases leptin-induced tumor necrosis factor-alpha expression by murine macrophages: involvement of cAMP-PKA and MAPK pathways. Cell Immunol. 2005 Nov;238(1):19-30.

Zhao TJ, Liang G, Li RL, Xie X, Sleeman MW, Murphy AJ, Valenzuela DM, Yancopoulos GD, Goldstein JL, Brown MS. Ghrelin O-acyltransferase (GOAT) is essential for growth hormone-mediated survival of calorie-restricted mice. Proc Natl Acad Sci U S A. 2010 Apr 20;107(16):7467-72.

Zhou P, Santoro A, Peroni OD, Nelson AT, Saghatelian A, Siegel D, Kahn BB. PAHSAs enhance hepatic and systemic insulin sensitivity through direct and indirect mechanisms. J Clin Invest. 2019 Oct 1;129(10):4138-4150.

Zhu Y, Liu TW, Cecioni S, Eskandari R, Zandberg WF, Vocadlo DJ. O-GlcNAc occurs cotranslationally to stabilize nascent polypeptide chains. Nat Chem Biol. 2015 May;11(5):319-25.

Zwick RK, Guerrero-Juarez CF, Horsley V, Plikus MV. Anatomical, Physiological, and Functional Diversity of Adipose Tissue. Cell Metab. 2018 Jan 9;27(1):68-83.

Appendix A:

A.1. 3T3L1 Cells:

A.1.1 Differentiation of 3T3L1 cells:

Different doses of insulin were used to set the protocol of the differentiation. The insulin concentrations were 10;5;1; ug/ml during all the differentiation, and 1 ug/ml for the first 4 days of the differentiation. FBS medium was also used without hormones as a control in addition to the preadipocytes cultured in normal proliferation medium with calf bovine serum. The differentiation of 3T3L1 cells in all the different sets was demonstrated at protein, gene expression, and lipid staining levels.

A.1.1.1. At the protein level:

Western blot was used to test the adiponectin and FABP4 which were used as markers for the differentiation of the cells. Insulin sensitivity at the IRS1 level was tested, and importantly OGT levels were measured aiming at identifying the dose that gives the highest expression of the OGT to be applied in the siRNA knockdown experiments.

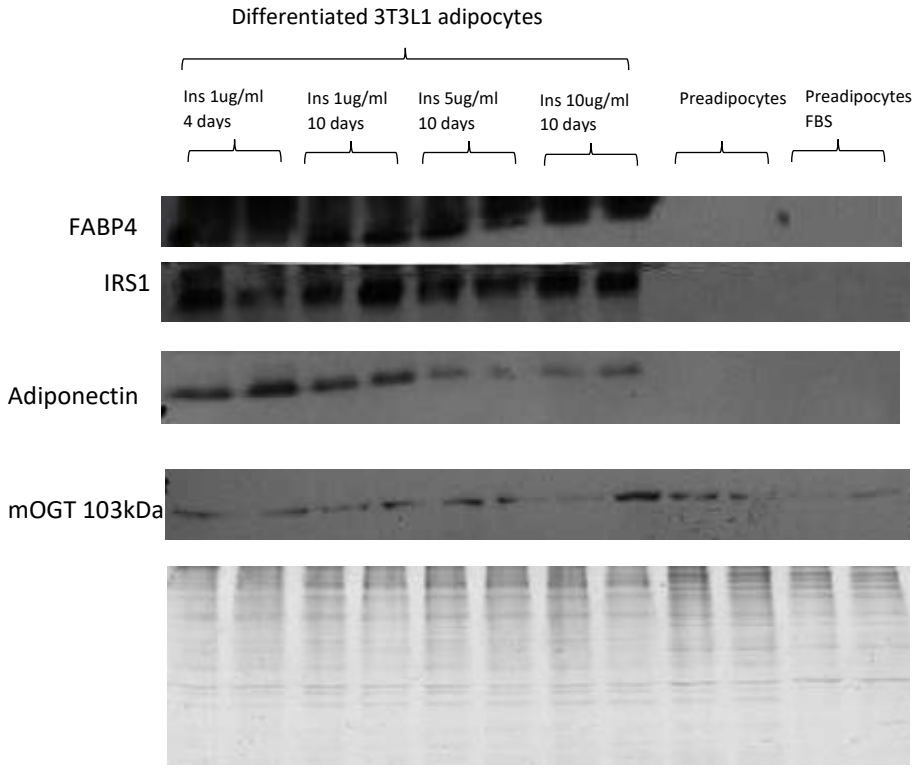

Figure (1) Differentiation validation of 3T3L1 cells. Protein cellular extracts was used for WB analysis of: FABP4, IRS1, Adiponectin, OGT.

A.1.1.2. : Quantitative Real-time PCR

Real-time PCR analysis was performed to test the gene expression of OGT, adiponectin, and FABP4 in the differentiated 3T3L1 adipocytes compared to the preadipocytes. Results were normalized for two reference genes according to the MIQE guidelines (Bustin et al., 2009): GAPDH (Zhang et al., 2016) and 18S rRNA (Ebrahimi et al., 2020). Table (1) summarizes the final results tested by the T student test.

Results normalized to 18S

	FABP4	Adiponectin	OGT
	T-test (related to preadipocytes)	T-test (related to preadipocytes)	T-test (related to preadipocytes)
INS 1 ug/ml	0.079223071	0.355917654	0.272228401
INS 10 ug/ml	0.100141606	0.028236539 *	0.040352189 *
INS 5 ug/ml	0.181054223	0.113220769	0.25321495
INS 1 ug/ml 4 days	0.017921303 *	0.042300855 *	0.021488699

Results normalized to GAPDH:

	FABP4	adiponectin	OGT
	T test (related to preadipocytes)	T test (related to preadipocytes)	T test (related to preadipocytes)
INS 1 ug/ml	0.30060474	0.001222225 *	0.396150123
INS 10 ug/ml	0.104829613	0.028790922 *	0.060520974
INS 5 ug/ml	0.200883542	0.210132632	0.904301497
INS 1 ug/ml	0.00165188 *	0.001376986 *	0.453840032

*Table (1) Differentiation validation of 3T3L1 cells by measuring FABP4 and Adiponectin expression levels, and measuring OGT expression in the differentiated adipocytes. Quantitative PCR method was used. * P<0.05 vs preadipocytes.*

A.1.1.3. Staining Method: Oil Red O Staining

Oil red O staining was performed to quantify the lipid contents in the adipocytes. Differentiated cells accumulated lipids in droplets that appeared in red, while the preadipocytes showed very

few differentiated cells when FBS was used. Below are images acquired for the different treatments (figure 3).

1)

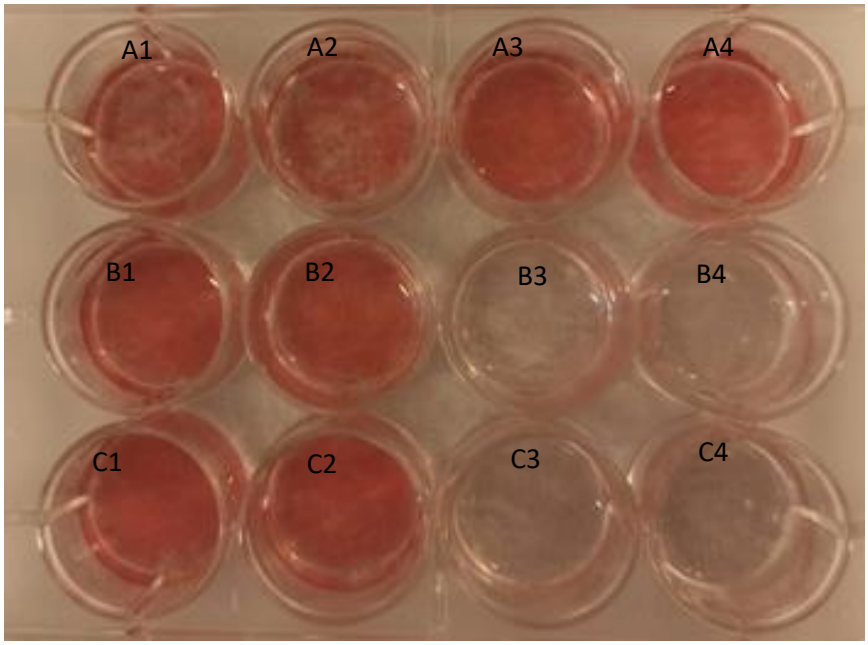

2)

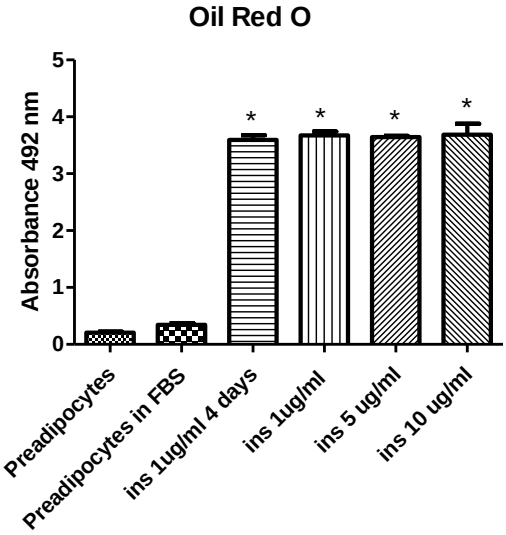

Oil Red O Quantification for Differentiated 3T3L1 Adipocytes

* P<0.05 vs both groups of preadipocytes

Figure (2) Oil Red O staining for 3T3L1 cells. ***1)*** *3T3L1 cells in different treatments in multiwell plate: A1,A2 differentiated adipocytes using 1 ug/ml insulin for 4 days. A3, A4 differentiated adipocytes using 1 ug/ml insulin for 10 days. B1,C1 differentiated adipocytes using 5 ug/ml insulin. B2, C2 differentiated adipocytes using 10 ug/ml insulin. B3, C3 Preadipocytes in FBS without hormonal inducement. B4, C4 Preadipocytes in proliferation medium with calf bovine serum without hormonal inducement.* ***2)*** *Quantification of the lipid contents spectrphotometrly at 492nm.*

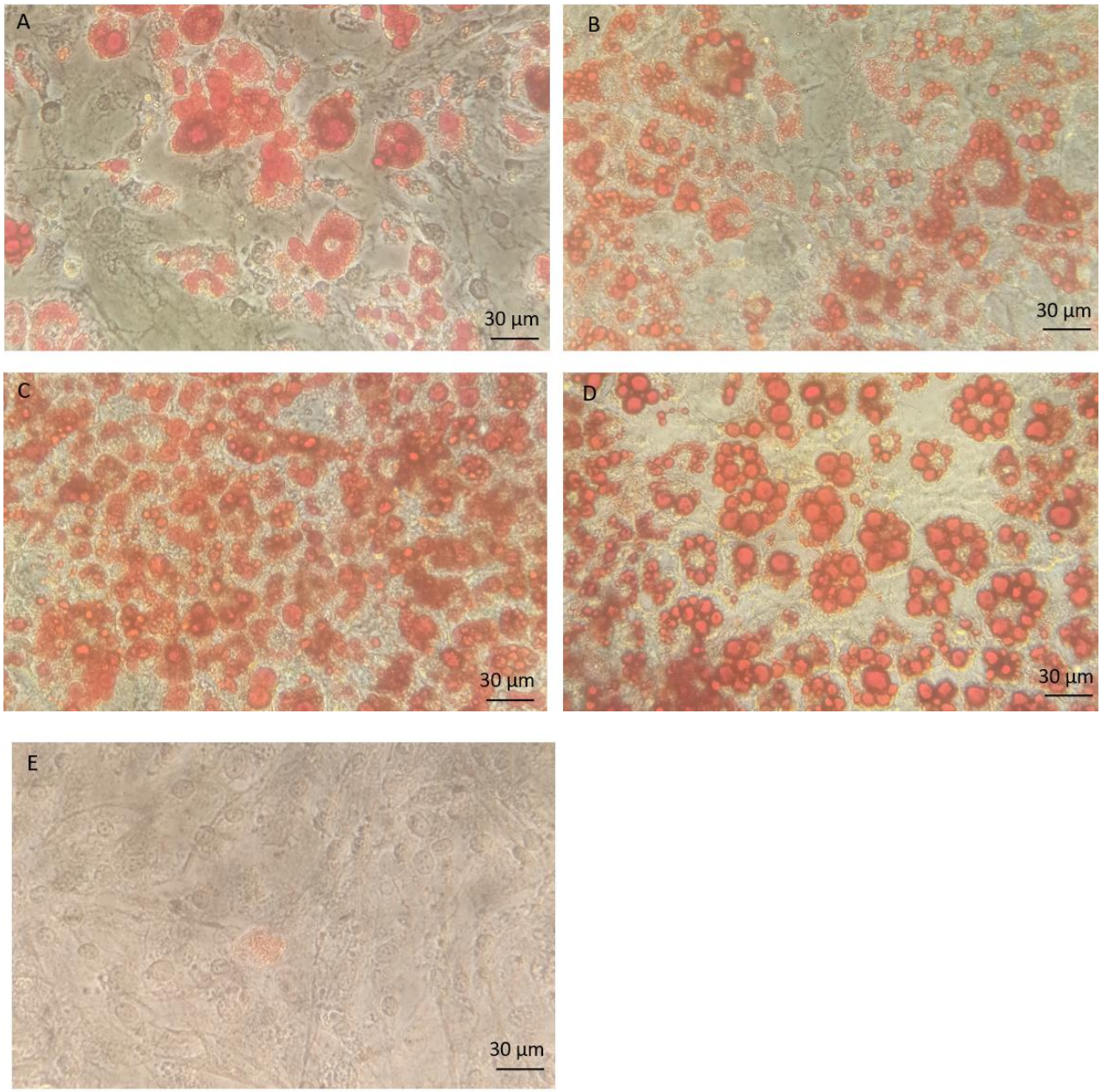

Figure (3). Oil Red O staining for the different followed treatments. A) Insulin 1 ug/ml for 4 days, B) Insulin 1 ug/ml for 10 days, C) Insulin 5 ug/ml , D) Insulin 10 ug/ml, and E) Preadipocytes.

A.1.2. Set of the siRNA transfection protocol:

Different siRNA concentrations: 25; 50; 100 ng were to identify the concentration to be applied for the following experiments with AG administration. Two different transfection strategies were used: In Suspension transfection and Forward transfection to test the transfection efficacy,

especially the transfection was planned to be performed on terminally differentiated cells. Transfection efficacy was estimated by the analysis of the gene expression and the protein levels.

A.1.2.1. In suspension strategy:

In suspension, transfection is known to be an efficient transfection method used widely in high-throughput sets. The differentiated adipocytes were suspended with the siRNA/lipid and re-plated in multi-well plates and analyzed at two different time points for the gene expression: 48 h; 96 h and at 120 h for the protein measurement. The concentration of 50 nM was selected to be applied for further experiments. Although pretty good efficacy was obtained, the protein yield was low which is the major drawback of this strategy. These findings forced to move to the other strategy.

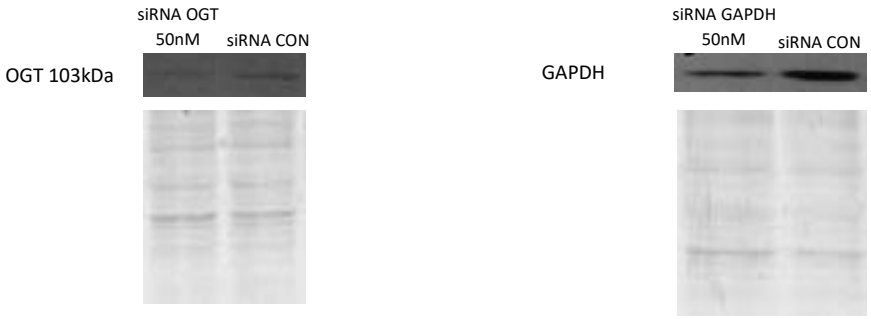

Figure (4) Knocking OGT expression in 3T3L1 adipocytes using siRNA transfection. WB analysis was performed using the cellular protein extracts. Right) 50nM siRNA OGT compared to siRNA control. Left) siRNA GAPDH as a positive control for the transfection.

Quantitative PCR showed that 50nM siRNA OGT reduced the expression of the OGT by 62% and 57% at 48 h, 96 h respectively normalized to GAPDH levels, and by 48% at 48 h normalized by 18S. These results confirmed that the dose 50 nM gave sufficient reduction at both protein and gene expression levels, so it was applied to check in forwarding strategy.

A.1.2.2. Forward Strategy:

siRNA/lipid complexes were added to starved cells. The concentration 50 nM was also selected to be used for further experiments. Protein analysis by WB showed a reduction by 50% at 72 h after transfection. Taking into consideration the high protein yield from this strategy and the lower siRNA needed amounts, this strategy was selected to proceed with in the following experiments.

Importantly, the reduction ratios obtained from the two strategies indicate the possibility to transfect differentiated adipocytes with a good transfection efficency.

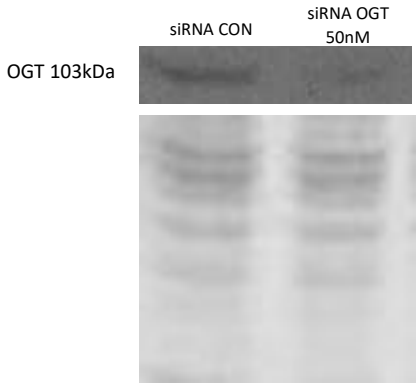

Figure (5) OGT protein levels in siRNA transfected 3T3L1 cells estimated by WB analysis at 72h post-transfection.

A.2. Differentiation of the human cells:

Oil Red O staining was used to test the differentiation ratio of the human adipocytes. Lipid droplets appeared clearly on days 5-6 from the differentiation and get larger during the differentiation. Following are images for the differentiation steps (Figure 6).

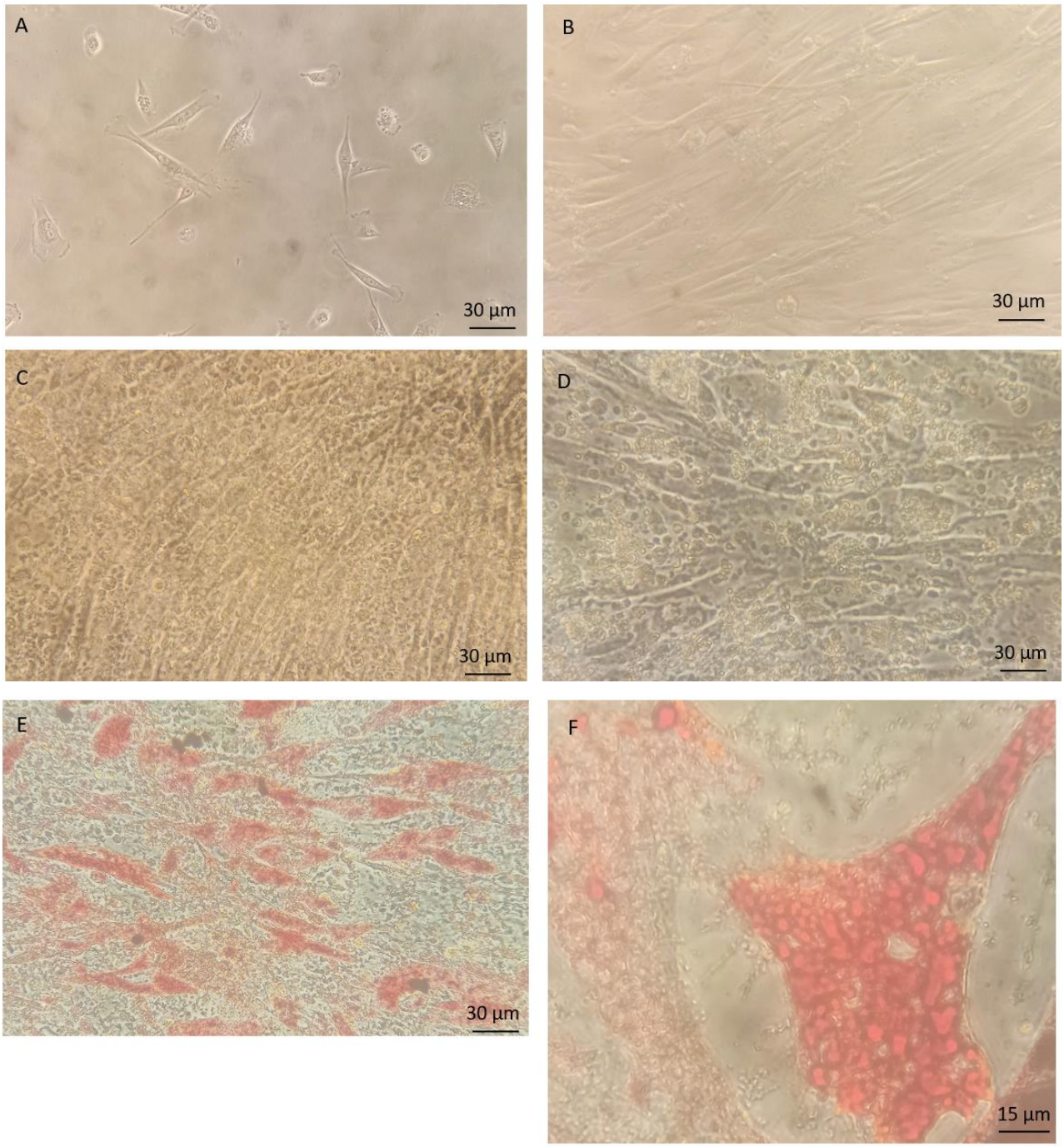

Figure (6). Differentiation of human preadipocytes into mature adipocytes. A) Preadipocytes P2, B) 4 days differentiation, C) 7 days differentiation, D) 14 days differentiation, E) human adipocytes stained by Oil Red O on day 14 of differentiation, and F) human mature adipocyte with accumulated lipid droplets.